Filtration in granular materials with non-spherical particle shapes

Ali Abdallah

N° d'ordre : 2023ECDL0047 Année 2023

THÈSE

présentée pour l'obtention du titre de

DOCTEUR DE L'ECOLE CENTRALE DE LYON

École doctorale : MEGA
Spécialité : Génie Civil

par

Ali ABDALLAH

FILTRATION IN GRANULAR MATERIALS WITH NON-SPHERICAL PARTICLE SHAPES

Soutenue à l'École Centrale de Lyon, le 8 Décembre 2023

devant le jury composé de

Mme Catherine O'SULLIVAN	Professeur, Imperial College London	Rapporteur
M. Luc SIBILLE	Maître de conférences, Université de Grenoble-Alpes	Rapporteur
M. Didier MAROT	Professeur, Université de Nantes	Président
M. Antoine WAUTIER	Chercheur, INRAE	Examinateur
M. Christophe PICAULT	Ingénieur, Compagnie Nationale du Rhône	Invité
M. Eric VINCENS	Professeur, École Centrale de Lyon	Directeur de thèse
Mme. Hélène MAGOARIEC	Maître de conférences, École Centrale de Lyon	Co-directeur de thèse

Thèse préparée au Laboratoire de Tribologie et Dynamique des Systèmes (CNRS-UMR 5513)
de l'École Centrale de Lyon, Ecully, France

Acknowledgements

First and foremost, I sincerely thank my supervisors, Prof. Eric Vincens and Dr. Helene Magoariec, for their invaluable guidance, leadership, and support throughout my PhD journey. Their patience and encouragement afforded me the freedom to deeply explore, fostering a rich environment for learning and discovery. I consider myself exceptionally fortunate to have had supervisors who played a major role in my achievements over the past three years.

I gratefully acknowledge the Compagnie Nationale du Rhône for funding this project. Special thanks to Mr. Christophe Picault, whose time and enlightening discussions were instrumental to my research. Additionally, I extend my appreciation to the dedicated team members there who assisted me in preparing the experiments, contributing significantly to the progress of my research.

My appreciation extends to Prof. Didier Marot, Prof. Catherine O'Sullivan, Dr. Luc Sibille, and Dr. Antoine Wautier for their presence on my jury, enriching this journey with their expertise and insights.

I am grateful to all members and staff of École Centrale and Centrale Innovation for ensuring all the prerequisites for my work were met during these three years.

My gratitude extends to all my colleagues and friends. Our interactions and exchanges profoundly influenced my thinking, behaviour, and actions throughout my PhD. Your direct or indirect contributions to this work have been invaluable.

A special acknowledgement goes to all my family, whose dedicated support has strengthened me during challenging times. I am especially thankful to my brother, who has been an immense help throughout my career. Additionally, heartfelt gratitude is extended to my uncle Ali and his family, who not only hosted me in France but were always there for me, providing consistent support and a home away from home.

Lastly, but most importantly, I express my profound gratitude to my parents. Their support, patience, and sacrifices have been the foundation of my accomplishments. Without them, none of this would have been possible.

Table of Contents

List of Figures

List of Tables

Abstract

Hydraulic structures are vulnerable to erosion, particularly from seepage flows, which pose a threat to the preservation of the initial properties of the granular materials they were built with. Granular filters, commonly used as protective layers, play a critical role in controlling or preventing the washout of fine material out of the structure.

Although factors such as grading, porosity, and particle shape influence their filtration properties, the significance of particle shape and its inherent anisotropy have not been sufficiently explored. This knowledge gap results in granular filter design criteria that underestimate the role of particle shape.

This study extensively investigated the impact of particle shape and seepage direction on filtration mechanisms within granular filters made of particles with rounded and anisotropic shapes. Using the discrete element method (DEM), directional filtration tests were conducted both vertically (aligned with the direction of gravity) and horizontally (perpendicular to the direction of gravity) on numerical samples with diverse particle shapes. A novel numerical filtration model was specifically designed for this purpose, capable of conducting filtration tests within samples consisting of non-spherical particles without the need for fluid-solid coupling and with an affordable computation time. These tests revealed direct insights into how particle shape and its intrinsic anisotropy affect retention capability. Subsequently, a comprehensive analysis of the pore space within the samples was performed using a pore extraction algorithm that effectively identified the pore structures and constrictions within the numerical samples. The obtained results provide quantitative insights that explain the observations from the filtration tests.

Ultimately, this research offers valuable insights that provide the basis for enhancing existing design criteria for granular filters, with a particular emphasis on constraint-based criteria.

Key words: Particle shape - granular filters - DEM - void space extraction - pore - constriction - Directional filtration - controlling constriction size

Résumé

Les ouvrages hydrauliques sont particulièrement vulnérables à l'érosion interne, rendue possible par des écoulements parasites, menaçant leur intégrité. Aussi des filtres composés de matériaux granulaires, sont-ils classiquement utilisés comme couches protectrices, permettant de prévenir ou de contrôler cet aléa.

Si des paramètres tels que la granulométrie, la porosité et la forme des particules sont réputés influencer les propriétés de filtration de ces filtres, le rôle joué par la forme des particules dans ces propriétés n'ont pas encore pleinement retenu l'attention de la communauté scientifique. Ce manque de connaissances se traduit par des critères de conception de filtres granulaires qui ne tient pas compte de la possible influence de la forme des particules.

Cette étude a eu pour but d'approfondir la connaissance autour de l'impact de la forme des particules et de la direction d'infiltration sur les mécanismes de filtration, au sein de filtres granulaires constitués de particules de formes arrondies et anisotropes. À l'aide de la méthode des éléments discrets (DEM), des tests de filtration multi-directionnelle ont été effectués à la fois verticalement (dans le sens de la gravité) et horizontalement sur des échantillons numériques présentant diverses formes de particules. Un nouveau modèle de filtration numérique a été spécialement conçu à cet effet, capable de réaliser des tests de filtration au sein d'échantillons constitués de particules non sphériques sans nécessiter de couplage fluide-solide et avec un temps de calcul abordable. Ces tests ont révélé des informations directes sur la façon dont la forme des particules et l'anisotropie inhérente des échantillons affectent la capacité de rétention. Par la suite, une analyse complète de l'espace poral pour ces échantillons a été réalisée à l'aide d'un algorithme d'extraction de pores qui a identifié efficacement les structures et les constrictions des pores. Les résultats obtenus fournissent des informations quantitatives qui expliquent les observations des tests de filtration.

En fin de compte, cette recherche offre des informations importantes nécessaires à l'amélioration des critères de filtre fondés sur l'exclusion géométrique.

Mots clés: Forme des particules - filtres granulaires - DEM - extraction de l'espace vide - pore - constriction - Filtration directionnelle - diamètre d'ouverture de contrôle

Introduction

1. Background

The migration of fine particles under seepage flow is a critical phenomenon across various industrial sectors including chemical (Khilar and Fogler, 1987; Xie et al., 2021), petroleum (Huang et al., 2008; Jung et al., 2018), environmental (Sen and Khilar, 2006; Li et al., 2021a), and civil engineering (Abdelhamid and El Shamy, 2016; Kamalov et al., 2017). Controlling particles migration in seepage flow is essential as it can lead to severe consequences.

In civil engineering, seepage flow can initiate erosion and scouring of the base soil within various structures such as embankments, dams, dikes, water turbine foundations, and retaining walls (Den Boon et al., 2004; Novak et al., 2017; Gao et al., 2023). Under the influence of hydraulic loading, unstable soils may lose a portion of their materials, potentially resulting in critical problems and ultimately leading to structural failure.

Fig. 1. Failure by piping, Tunbridge dam, Australia in 2005 (available from Geoengineer.org website)

For instance, when internal erosion occurs within hydraulic earth embankments, excessive migration of fine particles from the base soil can create voids in the core of the structure (Fell and Fry, 2007; Deangeli et al., 2009). This can facilitate the formation of a continuous pipe, leading to an increase in flow. As the flow rate increases, the erosion rate increases, culminating in the eventual loss of structural stability and ultimate failure. Figure 1 illustrates the failure of Tunbridge Dam

(2005) caused by internal erosion. Considering the substantial threat this phenomenon poses to both structural stability and the safety of individuals, it is imperative to block the migration of fine particles effectively.

One widely used solution to prevent this phenomenon is installing protective filter layers made of granular materials for the base soil (Fig. 2). These filters have two main roles: Firstly, they effectively block the transportation of suspended particles carried by the seepage flow (BERTRAM, 1940; Sherard et al., 1984; Terzaghi et al., 1996). Secondly, as these granular filters are permeable, they permit the passage of the flow, preventing the buildup of excessive hydraulic pressure that could lead to structural instability (Delgado-Ramos et al., 2016).

As filters play a pivotal role in ensuring the security of such hydraulic structures, their design should be thoroughly executed. The pore space of the filter is the key parameter controlling the successful retention of fine particles and an open gate for the flow to pass (Kenney et al., 1985; Khilar and Fogler, 1998). This pore/void space can be divided into two main components: pores, which refer to the large local void spaces situated between particles, and constrictions, which are the narrower passages connecting adjacent pores. To achieve effective retention, the constriction sizes should be smaller than those of fine particles (Kenney et al., 1985; Locke et al., 2001; Indraratna et al., 2007). Otherwise, the filter fails to capture the migrating fines, potentially leading to significant issues. Nonetheless, it is essential to ensure that the constriction sizes are not excessively small to permit the passage of the flow. Simultaneously, it is crucial to consider the internal stability of the filter, as it must possess adequate resistance to seepage flow (Kenney and Lau, 1985).

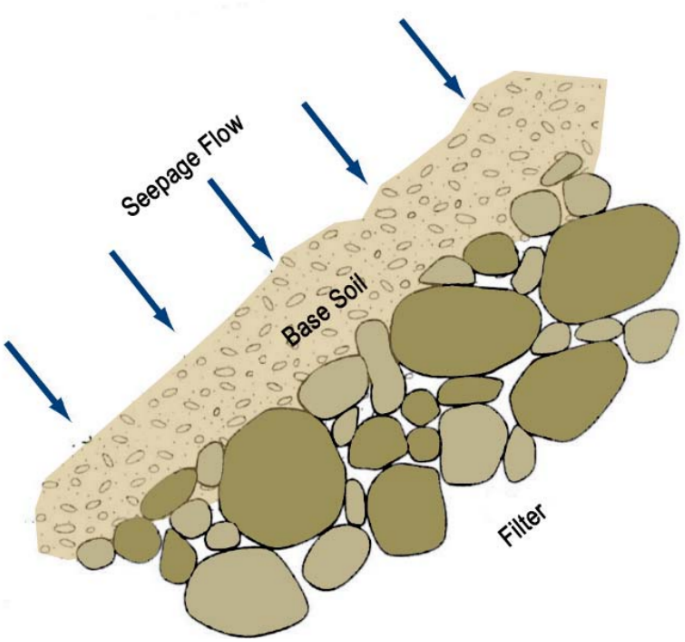

Fig. 2. Schematic of seepage flow through a base soil and filter material. (available from Montana.gov website)

Therefore, the design of an effective filter necessitates adherence to various criteria, encompassing retention ability, permeability, and internal stability. Granular filters exhibit significant variability due to factors such as particle grading, shape, preparation method, and installation position. Thus, understanding the filtration mechanism is a highly complex undertaking (Khilar and Fogler, 1998),

making the design of an efficient filter equally challenging. Hence, numerous studies have been conducted, addressing each of the filter criteria individually or collectively. However, there are still numerous unresolved aspects that necessitate further research to establish more effective criteria.

2. Statement of the problem

One of the earliest and most commonly used criteria for assessing the retention capacity of a granular filter is based on characteristic particle sizes found in both filter and base soil materials. Originally proposed by Terzaghi (1922), this geometric criterion indirectly defines the controlling constriction size, representing the equivalent opening size of the filter, in function of the size of the filter particles. Several studies have shown that this original criterion was overly conservative, as it includes a high margin of safety, and was partially improved (BERTRAM, 1940; Sherard et al., 1984). While these criteria are widely applied in different domains, they possess certain limitations. The chosen characteristic sizes representing the filter and granular materials lack physical significance, thereby restricting the use of these criteria to uniform cohesionless materials exclusively (Kenney et al., 1985).

In response, Kenney et al. (1985) introduced a novel concept for filter design based directly on their constriction sizes. This parameter carries greater physical significance as it primarily governs particle blockage. Building upon this concept, various filter criteria based on constriction size have been introduced (Locke et al., 2001; Indraratna et al., 2007; Seblany et al., 2021). Several experimental, image-based, and numerical triangulation-based methods have been proposed to calculate constriction sizes. However, due to the demanding and complex procedures of such methods, the quantification of the controlling constriction size has primarily relied on analytical approaches developed under the assumption that the particle shapes are spherical. These methods are well documented in the literature review.

Despite the extensive body of research on these particle size and constriction based retention criteria, there are still significant features that have not been thoroughly investigated or considered quantitatively:

Firstly, the impact of particle shape remains inadequately represented in current research. In reality, particle shapes can vary widely, ranging from elongated to flat and from rounded to angular. However, particle size based criteria typically consider only the particle size (along with a statement of a filter in a dense state), typically obtained from a sieve analysis. This parameter does not incorporate particle shape considerations, resulting in its exclusion from these criteria. Similarly, constriction-based criteria, relying on constriction sizes derived from spherical particles, overlook the influence of particle shapes. Despite the extensive studies conducted to calculate the constriction size, there remains a lack of quantitative research into the effect of particle shape on constriction sizes and its consequent impact on retention capacity.

Secondly, the direction of seepage flow with respect to the principal stresses has not been considered. In practice, the filtration direction can vary depending on the filter's position within hydraulic structures. However, the experimental filtration tests used to develop particle-size-based criteria were typically conducted in the direction of gravity (vertically). Consequently, these criteria are primarily applicable to vertical filtration. Furthermore, the method used to calculate the controlling constriction size did not account for the orientation of the constrictions. It is widely

recognised that granular materials can exhibit fabric anisotropy due to factors such as particle shape, preparation method, and loading type, which can influence their mechanical and hydraulic properties. Nevertheless, the impact of such anisotropy on retention capacity has not been extensively investigated.

3. Research objectives

The primary objective of this study, conducted in collaboration with the French stakeholder Compagnie Nationale du Rhône (CNR), is to perform a comprehensive quantitative analysis to assess the influence of particle shape (case of rounded particles) and seepage direction on the filtration mechanism of granular filters. The current design criteria for granular filters overlook these crucial parameters, potentially raising efficacy concerns. This study seeks to bridge these gaps by supplying the essential knowledge needed for adjusting existing criteria to incorporate the impacts of these parameters. Previous research conducted at the Laboratoire de Tribologie et Dynamique des Systèmes (LTDS) has been dedicated to the development of tools and the execution of filtration tests to establish a new criterion based on constriction size (Reboul et al., 2008, 2010; Wu et al., 2012; Sjah and Vincens, 2013; Li et al., 2014; Seblany et al., 2018a, 2021). Building upon their studies and with a specific focus on the objectives of this work, the chosen methodology which is mainly based on numerical experiments (using the Discrete Element Method) consists of the following sequential tasks:

- Generate numerical samples with diverse non-spherical shapes, varying in grading and porosity, for conducting filtration tests and extracting their pore space.
- Develop an efficient numerical filtration model capable of efficiently conducting filtration tests on samples consisting of non-spherical shapes skipping coupled fluid-solid approaches.
- Identify effective tools for extracting and analysing the pore space components (pores and constrictions) derived from numerical samples.

By adhering to this methodology, the influence of particle shape and seepage direction on the filtration mechanism will be examined through two interconnected approaches. Firstly, performing directional filtration tests in both vertical and horizontal orientations on numerical samples with diversified particle shapes will allow for a comprehensive analysis of how these parameters impact the directional retention capacity of the granular filter. Subsequently, analyzing the pore space from these identical numerical samples will provide insights into the influence of particle shape on the size, number, and orientation of the constrictions. Given the intricate connection between filtration results and the geometric characteristics of the pore space, the findings from both approaches will corroborate each other, yielding a more profound comprehension of the filtration mechanism.

4. Thesis outline

This manuscript is structured in a paper-based format and consists of four chapters:

- **Chapter I** explores a comprehensive literature review of laboratory and numerical experiments that investigated the main mechanisms at stake in filtration processes in granular materials. If a lot of studies were based on samples made of spheres, some authors explored the case of non-spherical or angular materials. A specific focus was made on the quantification of the void space in terms of pores and constrictions and the methods developed to achieve them since they are intimately connected to the capacity for fines to cross a granular material. Finally, two main geometric filter criteria are presented together with their limitations.

- **Chapter II** consists of an article that examines the filtration mechanism in granular materials under both dry and wet filtration models using numerical samples generated by the Discrete Element Method. Furthermore, an enhanced dry filtration model that is capable of replicating the filtration results obtained from the wet filtration model, particularly in terms of the retention coefficient, was introduced. This filtration model serves as an alternative efficient tool that significantly reduces computational time and is applicable to particles of all shapes.

  This paper was submitted to *International Journal for Numerical and Analytical Methods in Geomechanics*.

- **Chapter III** comprises an article that explores how particle shape affects the structure of the void space in granular materials. Using an extraction algorithm, the void space of the numerical samples consisting of different particle shapes was extracted and analysed. Filtration tests were conducted on these numerical samples to validate the obtained void space results. This study highlights the importance of considering particle shape when designing filters, as it can significantly influence the void space characteristics and the filtration performance.

  This paper will be submitted to *Granular Matter* Journal.

- **Chapter IV** presents an article that investigates the impact of fabric anisotropy on directional filtration mechanisms in granular materials. This study considers the effects of particle shape and preparation methods used to generate the numerical samples. Filtration tests were conducted vertically and horizontally, and the pore space from these samples was extracted, considering the orientation of normals to constriction planes. This study provides valuable insights into the role of anisotropy in granular materials with respect to directional filtration mechanisms.

  This paper will be submitted to *Granular Matter* Journal.

Finally, the conclusion integrates the findings from all the papers and engages in a discussion about the necessary future perspectives required to enhance existing filter criteria.

Chapter I

Filtration Mechanisms and Design Criteria for Granular Materials

1. Introduction

Filtration is a process that involves separating solid particles from a given flow. This separation is achieved by passing the flow through a porous medium that is capable of blocking the movement of solid particles while allowing the flow to pass through. The choice of the porous medium able to filtrate transported solid particles depends on their size. To effectively remove solid particles smaller than μm, such as algae and bacteria, filter membranes with nano- or micro-openings are required (Song et al., 2023). Conversely, for particles larger than 10 μm, filters constructed from granular materials serve as effective barriers. In the civil engineering sector, granular filters are commonly employed to protect base soils in hydraulic structures from erosion induced by seepage flow (Terzaghi et al., 1996). For example, granular filters are used to prevent the washout of fine particles within the core of zoned dams (Fig.I.1).

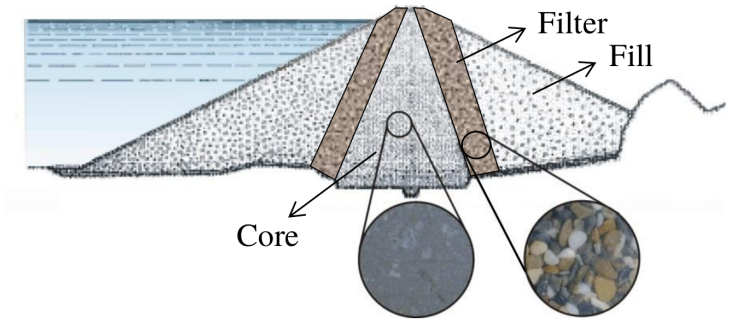

Fig. I.1. Sketch of a zoned core dam (Seblany, 2018).

However, filters can also be installed downstream of fluvial dykes in order to control active processes of internal erosion that has developed throughout the service life of these structures. This pathology is related to the excessive migration of particles under seepage through and out of hydraulic structures or their foundation.

To design an effective granular filter, it is crucial to understand the mechanisms at stake throughout the process of filtration. At the pore scale, the filtration mechanisms are primarily governed by two fundamental components: fluid dynamics and pore space geometry. Adopting this study approach provides a deep understanding of the phenomenon, which can then be extrapolated to the flow region scale, streamlining the optimisation of this process.

Starting with fluid dynamics, this component provides the necessary kinetic energy for initially detaching fine particles from the soil base and subsequently facilitating their movement throughout the pore space. Various forces are involved when the fluid interacts with these fine particles, including hydrodynamic forces such as drag and lubrication forces, electrochemical forces such as van der Waals and double-layer forces, and Brownian diffusion (Ghidaglia et al., 1996). Nevertheless, for fine particles larger than 10 μm, the drag force F_d is the predominant fluid force governing their transportation (Deen et al., 2007). Consequently, in numerical modelling of fluid dynamics, it is common practice to simplify the system by exclusively considering the drag force (Ma et al., 2022). Calculating F_d is inherently complex due to the numerous influencing factors, including the fluid velocity field and viscosity, as well as the shape and size of the solid particles.

The geometry of the void space plays a crucial role in the circulation and blockage of fine particles. It can be divided into two components: pores and constrictions (Kenney et al., 1985). Pores represent local, larger voids enclosed between filter particles, whereas constrictions are the narrow throats or connections linking neighbouring pores. Figure I.2 illustrate an example of void space components extracted from a numerical sample. Then, constriction sizes primarily govern the blockage of the fine particles by geometric exclusion. If the size of a fine particle exceeds that of a constriction, blockage occurs; otherwise, the particles can pass through it. However, both the flow circulation and movement of fine particles are intricately linked to the pore space topology, particularly the connectivity of pores. As the pore connectivity increases, more paths become available, facilitating the migration of fines (Khilar and Fogler, 1998).

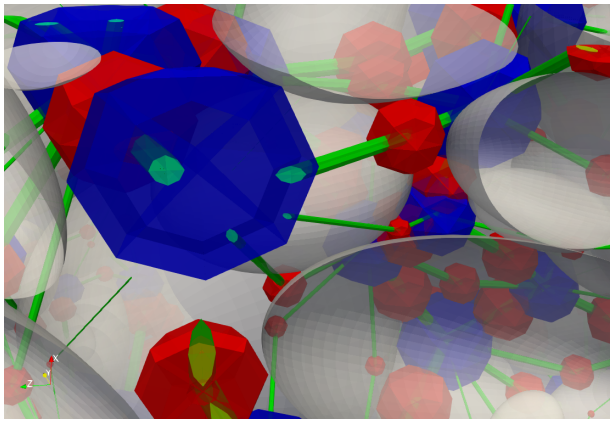

Fig. I.2. Pore space components extracted from a numerical sample: Pores are displayed in blue, constrictions in red, and filter particles in translucent grey.

In the past, different approaches were developed to address questions arising from filtration processes in granular materials and filter design. If laboratory experiments were first carried out to explore both the involved mechanisms and quantification of the void space in terms of pores and constrictions, the development of numerical tools allowed us to obtain more detailed results. These aspects are developed hereafter in more detail.

2. Filtration processes through laboratory tests

Laboratory experiments have been carried out to investigate the filtration processes within granular materials. These investigations have focused on the movement and blockage of fine particles when subjected to hydraulic flow through granular filters. Such filters are composed of either spherical or non-spherical particles. Furthermore, the void space components (pores and constrictions), identified as critical parameters in the filtration process, were extracted via laboratory experiments for analysis. This step aims to establish a connection between the outcomes of filtration and the characteristics of the pore space.

2.1. Observed mechanisms

Adopting a physical approach is inherently complex and requires specialised tools to accurately track the movement of particles within the filter. In light of these challenges, a certain number of laboratory experiments have been conducted involving filters composed of spheres. Only a few of them have been carried out with filters made of non-spherical particles.

Ghidaglia et al. (1996) conducted a comprehensive investigation focused on deep-bed filtration tests involving non-Brownian particles. Their primary objective was to evaluate the depths of particle penetration through a series of wet filtration tests conducted under hydraulic laminar flow conditions and dry filtration tests conducted under the influence of gravity. They also evaluated various particle injection methods, including individual and group injections. For their experimentation, they prepared a filter sample consisting of monosized glass spheres and introduced fine particles that had been coated with a thin layer of gold. In the context of wet filtration (when seepage is involved), these fine particles were observed through visual examination by achieving optical transparency in both the filter sample and the surrounding fluid, which was achieved by carefully matching the fluid refractive indices with those of larger glass spheres.

Their findings indicated that in wet filtration tests, fine particles released in groups penetrate to greater depths than those released individually. However, in dry filtration, this distinction was not observed, suggesting that the group effect could be attributed to hydrodynamic phenomena. Furthermore, in both filtration approaches, when particles were introduced individually, their trajectories remained nearly straight with minimal deviation from this straight direction. In the group injection, the packets of particles exhibited limited spreading, demonstrating strong alignment with the flow direction. Moreover, the penetration depth in dry filtration was slightly lower than that in wet filtration. This suggests that fine particles tend to follow the local maximum flow, associated with larger constrictions, thereby reducing the probability of particle capture. They also found that fine particles were predominantly captured at constriction sites formed between the filter particles. However, additional capture sites, termed "hydrodynamic" sites, originating from the flow stagnation points, were identified. These capture sites were found to be unstable, as sharp flow variations could release fine particles.

Lominé and Oger (2009) conducted another laboratory experiment to investigate the impact of specific parameters on the percolation process, involving a group of fine particles released within a filter in a dry situation. The experimental setup, as illustrated in Figure I.3, consisted of a Plexiglas cell filled with uniform glass beads of diameter D. Simultaneously, a separate container

with small particles of diameter d was suspended above the porous medium, allowing them to pass through it under the influence of gravity. A piezoelectric scale beneath the porous medium recorded the particle passage, which aided in determining the mean transit times. A collecting box divided into square cells was put at the exit of the filter to assess the local particle distribution.

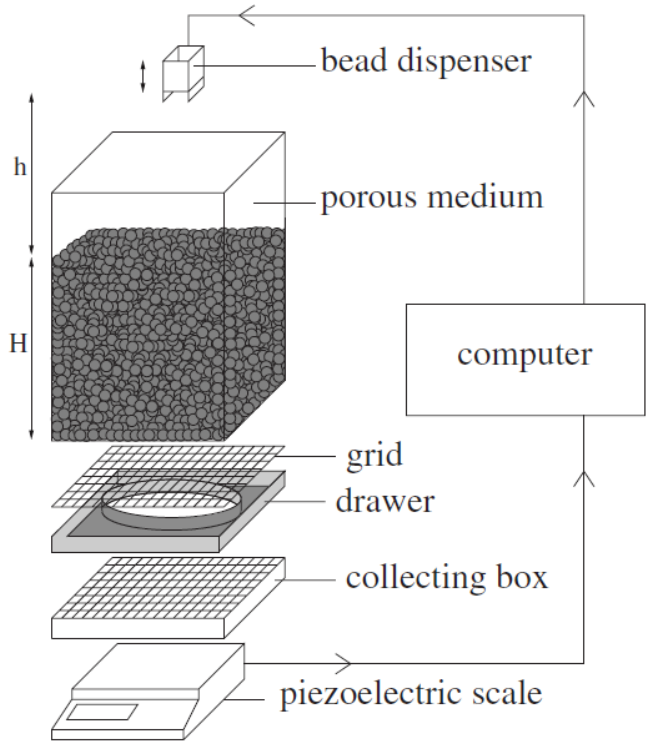

Fig. I.3. Schematic description of the experimental setup of Lominé and Oger (2009).

The results reveal that the fine particle cluster exhibits diffusive behaviour. The number of particles N within the cluster significantly influences the dispersion, with higher N values leading to increased dispersion. The size ratio D/d between the filter particles and released fine particles plays a crucial role in affecting both longitudinal and transverse dispersion. As D/d increases, the pore space becomes more open in all directions; thus, the longitudinal dispersion decreases, whereas the transverse dispersion increases. It arises from larger bouncing on pore walls when D/d increases where fines can find sideways to go head in the filter more easily. Additionally, an increase in particle density results in increased longitudinal dispersion and decreased transverse dispersion. The experimental observations indicated that the combined effects of these parameters can occasionally pose challenges in both theoretical and practical analyses. Although these experiments did not consider the influence of hydraulic flow, they still provide valuable insights that can contribute to a better understanding of the filtration mechanism.

Muresan et al. (2013) conducted similar filtration experiments involving the straining of randomly packed small beads in a filter made of coarse glass beads. The experiments included dry filters, water-saturated filters under hydrostatic conditions, and water-saturated filters under hydrodynamic conditions, to investigate how physico-chemical distinctions between air and water influence straining mechanisms. These findings highlight the significant impact of the presence or absence of water on straining stages and mechanisms. In dry filters, straining is driven by diffusion-

like processes characterised by lateral dispersion resulting from random bounces within the pores. Conversely, under hydrostatic conditions, water-saturated filters exhibit sedimentation-like mechanisms, leading to reduced lateral dispersion and significant deposition in the void space. Under hydrodynamic conditions, even low water velocities were found to be sufficient to guide fines throughout the filter pore network. The results showed that as the water velocity increased, the retention coefficient decreased, while the lateral dispersion increased. Moreover, monitoring the straining process revealed the existence of transient mechanisms that developed sequentially based on the number of fines entering the filters. For instance, as certain pathways become clogged, new preferential pathways emerge.

Aside from the case of spheres which is a typical model for actual granular materials used in the laboratory, other authors tried to establish specific features inherent to actual materials involving non-spherical and/or angular materials. For example, Sherard et al. (1984) conducted an investigation to examine the influence of particle angularity on permeability. To accomplish this, they carefully prepared duplicate samples with identical particle size distributions (PSD) and the same relative density (70%) while varying the particle shapes: subrounded alluvial particles and angular crushed limestone particles. These findings consistently demonstrated that the permeability of the crushed limestone specimens was generally lower than that of the alluvial samples. These results suggest an indirect inference that angular particles possess narrower pore channels compared to their subrounded particles.

To validate this, Barton (2004) conducted an extensive investigation into the filtration performance of granular filters of various shapes. The materials used in this study included glass marbles (DM), rounded river stones (RS), and crushed limestone (DL). The generated samples exhibited nearly identical average porosities of approximately 0.43. In a controlled flow rate experiment, fine particles were released, and the accumulated mass of the retained fine particles in each filter was measured. The results demonstrated that filters composed of crushed limestone exhibited the highest retention capacity, followed by rounded river stones, while glass marbles showed the lowest ability to retain fines.

Therefore, it can be concluded that an increase in the angularity of the filter particles corresponds to enhanced retention capacity. Similar results have been obtained for filters used for drinking water filtration (Trussell et al., 1980; Suthaker et al., 1995; Evans et al., 2002). If the role of particle forms in the retention capacity of granular filters is qualitatively established, quantitative results were not obtained according to the main geometric characteristics of the particles.

Barton (2004) also investigated the impact of relative density on filtration performance by performing filtration tests on a loose sample composed of crushed limestone (LL) with a porosity of 0.5. As anticipated, the denser sample (DL) exhibited a greater propensity to block fine particles than the loose sample (LL). Figure I.4 illustrates the cumulative mass of retained fine particles in four filters as a function of the particle size ratio (S). Here, S is defined as $S = r_f/r_p$, where r_f represents the radius of the filter grain and r_p denotes the sand particle radius. It is worth noting that as S increases, the size of fines decreases.

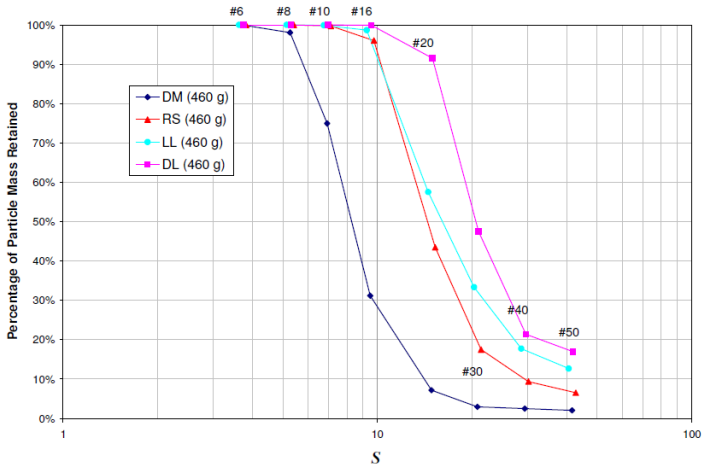

Fig. I.4. Cumulative mass of retained fine particles in four filters (Barton, 2004).

It is worth noting that advanced techniques, such as particle image velocimetry (PIV) and high-speed photography (Wereley and Meinhart, 2010; Chen et al., 2017; Fuller, 2009; Versluis, 2013), can be used for better observation of the filtration mechanism in granular materials. However, PIV may face limitations arising from calibration errors and limited spatial-temporal resolution (Sciacchitano, 2019), whereas high-speed photography often requires the use of advanced cameras to capture complex dynamics, especially in the case of stiff and heterogeneous filters (Xing et al., 2017).

2.2. Pore space extraction and analysis

Numerous experimental techniques have been developed to extract the pore space within granular materials and assess their diverse characteristics, as they hold a key function in the process of filtration in granular materials. Nevertheless, these methods have limitations, owing to their inefficiency and inherent complexity. For example, the replica technique is a useful tool for visualising the void space of granular material, enabling the assessment of the pore network morphology and tortuosity as well as providing insight into void characteristics such as pore connectivity and CSD (Witt, 1986, 1993). This method involves pouring an elastic liquid into the void space of a granular material, which then hardens and gradually removes the particles while preserving the pore space. Although this method is effective in representing the void space, it is time-consuming and can only be used for coarse materials. Figure I.5 shows an example of pores found in a natural gravel material.

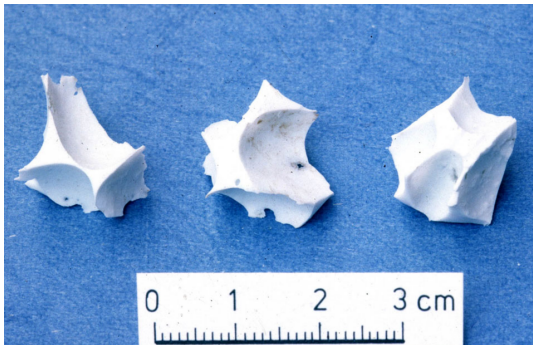

Fig. I.5. Pore imprints of a gravel skeleton (Witt, 1986).

Sherard et al. (1984) employed molten wax to visualise and study the flow channels within gravels, offering valuable insights into their irregular shapes and sizes relative to the characteristics of gravel. In this study, molten wax was poured onto compacted gravel samples, which featured a particle size distribution ranging from 9.5 to 25.4 mm and had a D_{15} value of 11 mm. Once the wax solidified, the sample was carefully sectioned with a chisel, revealing a wax structure mirroring the exact configuration of the underlying pore channels.

The analysis of this wax "skeleton" unveiled several key findings. It showed that the flow channels within the gravel exhibited irregular cross-sectional shapes, with no clear distinction between large and small channels. These channels consistently shared similar maximum and minimum dimensions. The estimated minimum flow channel dimensions capable of capturing suspended soil particles were roughly 0.09 to 0.18 times the gravel's characteristic size (D_{15}). The median "equivalent average" diameter of these flow channels was approximately $0.25D_{15}$ - $0.35D_{15}$, and along the seepage path, the maximum dimension reached around $0.6D_{15}$. Consequently, the cross-sectional dimensions of continuous flow channels spanned from about $0.1D_{15}$ to $0.6D_{15}$. These results are very important for designing filter criteria.

Soria et al. (1993) proposed another method denoted the base suspension method, which was later refined by Sjah and Vincens (2013). This method involves conducting filtration tests on granular filters with different-sized particles to determine the size of the largest particles that can completely cross a filter of a certain thickness. The process of building the underlying CSD requires multiple filters of different thicknesses, which is also time-consuming.

Wu et al. (2012) employed the basic suspension method to explore the impact of particle shapes on the distribution of constriction sizes (CSD). To accomplish this, three distinct materials were used: glass beads, natural alluvial particles (rounded and with a rather high sphericity), and finally elongated and angular particles, all of which had identical particle size distributions. These materials were utilised to create three samples, each in their loosest state, resulting in void ratios of 0.72 for the glass beads sample, 0.69 for the natural alluvial particles, and 0.96 for the elongated and angular particles. Subsequently, the CSDs for these three samples were determined through the basic suspension method (Soria et al., 1993).

The results revealed that both the glass bead and rounded-particle samples exhibited remarkably similar CSDs. In contrast, despite having a higher void ratio, the sample composed of angular particles displayed a greater number of finer-sized constrictions than the other two samples. However, it should be noted that this material also exhibited significantly larger constriction sizes than the previous materials.

3. Filtration processes through numerical approaches

The growth in computational power has significantly supported researchers' ability to use numerical models for conducting quantitative studies on filtration mechanisms rather than relying exclusively on laboratory experiments. Moreover, numerical approaches also allowed access to information about the void space, which laboratory experiments cannot provide easily. They are mainly based on a segmentation of the void space into pores and constrictions.

3.1. Granular filter modelling

One common numerical tool for simulating granular filters is the discrete element method (DEM). DEM is an effective technique for representing the distinctive characteristics of granular materials, including their mechanical properties (Cundall and Strack, 1979). This method is primarily used in the field of granular materials and particle dynamics simulations, offering a robust approach for examining the behaviour of granular assemblies. In DEM, granular assemblies are modelled as discrete individual particles or elements. This method relies on an explicit numerical scheme in which particle interactions are tracked on a contact-by-contact basis, accounting for the individual motion of the particles. In this modelling approach, particles are treated as rigid entities that are capable of interacting through contact forces. This representation accurately captures the inherently discontinuous nature of granular systems, thereby preserving the intricate pore spaces between the particles.

In the context of DEM, the translational and rotational movements of individual particles are governed by Newton's second law of motion. The equations describing these motions are as follows:

$$M\overrightarrow{\ddot{x}}_i = \sum \vec{F}_{j\to i} + \vec{r} \tag{I.1}$$

$$\underline{\underline{I}}\vec{\dot{\theta}}_i = \sum_j \vec{\Gamma}_{j\to i} + \vec{m}_r \tag{I.2}$$

where M and $\underline{\underline{I}}$ are the mass and inertia matrix of particle i, respectively; $\overrightarrow{\ddot{x}}_i$ and $\vec{\dot{\theta}}_i$ are the translational and angular accelerations of particle i, respectively; $\vec{F}_{j\to i}$ represents the force that particle j exerts on particle i and $\vec{\Gamma}_{j\to i}$ represents the moment resulting from $\vec{F}_{j\to i}$ at the centre of gravity of particle i; $\vec{r}$ stands for external forces such as gravitational force and dragging force exerted by fluid, and $\vec{m}_r$ characterizes the moment that $\vec{r}$ exerts at the centre of gravity of particle i. Figure I.6 illustrates an example of a three-dimensional numerical filter modelled using DEM.

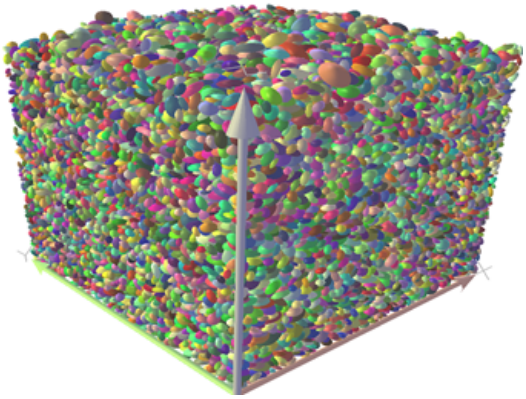

Fig. I.6. Discrete numerical model of a granular filter.

3.2. Filtration modelling

DEM coupled with fluid dynamics models stands as a highly efficient tool for modelling filtration tests and exploring the underlying mechanisms in granular filters. However, given the operational complexities associated with fluid dynamics models, some authors substitute such models with a dry approach (only gravity) with the statement that the main features observed in wet conditions can be retrieved by the former approach.

3.2.1. Case of coupled DEM-fluid approaches

Modelling fluid dynamics in dynamically changing domains presents a significant challenge. Numerous numerical approaches have been introduced in the literature to effectively couple DEM simulations with fluid dynamic models in order to accurately simulate the behaviours of both fine particles and the fluid.

- **Computational fluid dynamics**

The initial approach involves the use of computational fluid dynamics (CFD), which was first introduced by Tsuji et al. (1993). CFD is a well-established domain within fluid mechanics that makes extensive use of numerical techniques and computational resources to comprehensively investigate intricate phenomena involving the interplay between solid bodies and fluids. This method focuses on modelling fluid dynamics by applying the Navier-Stokes equations, which express the fundamental principles governing fluid mass and momentum conservation:

$$\nabla \cdot u = 0 \tag{I.3}$$

$$\rho_f \frac{\partial u}{\partial t} = -\nabla P + \nabla \cdot \tau + \rho_f g \tag{I.4}$$

where u represents the velocity vector, ρ_f corresponds to the density of the fluid; t, g, and τ denote time, gravitational acceleration, and the stress tensor that characterises the rheological properties

of the fluid, respectively.

Various methods have been developed to solve the Navier-Stokes equations on an Eulerian grid, including the finite difference method (Popescu, 2014), the finite element method (Morgan and Peraire, 1998), and the finite volume method (Boudet, 2011). The shared characteristic of these techniques is that they segment the domain into multiple elements using either structured or unstructured grids. Subsequently, they link the elements at the nodes to keep the domain unified.

When it comes to integrate CFD and DEM, three primary approaches can be distinguished based on the ratio of CFD mesh size to particle diameter: Unresolved CFD-DEM has a ratio of 3, representing filtration at the regional scale; semi-resolved CFD-DEM has a ratio near one, depicting filtration at the representative elementary volume scale; and fully resolved CFD-DEM has a ratio of 0.3, providing a detailed representation of pore-scale filtration (Ma et al., 2022). Figure I.7 gives a schematic representation of the modelling of fluid dynamics at different scales. Generally, the pursuit of enhanced simulation accuracy, which involves reducing the mesh size to particle diameter ratio, results in increased computational demands. Consequently, although fully resolved CFD-DEM offers the most accurate portrayal of pore-scale filtration, its significant computational cost makes large-scale numerical experiments nearly impractical.

Feng et al. (2020) investigated how particle size and their concentration in the flow affected particle migration within granular filters composed of spherical particles, using unresolved CFD-DEM modelling. The findings underscore that the size of fine particles and their concentration significantly govern their retention, the formation of an external filtration cake, and the subsequent reduction in permeability. This study establishes a critical size ratio ($Rp = 0.15$), which represents the ratio between the diameter of the fine particles and the diameter of the filter particles, leading to the most significant decrease in permeability. Figure I.8 gives the particle deposition for different injected particle sizes. Furthermore, the study revealed that as the concentration of fine particles increases, permeability experiences a corresponding decrease.

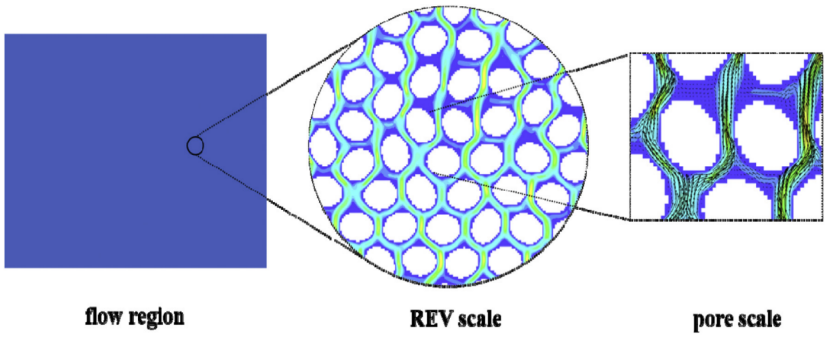

Fig. I.7. Schematic representation of the multi-scale aspects of fluid flow (Song et al., 2021).

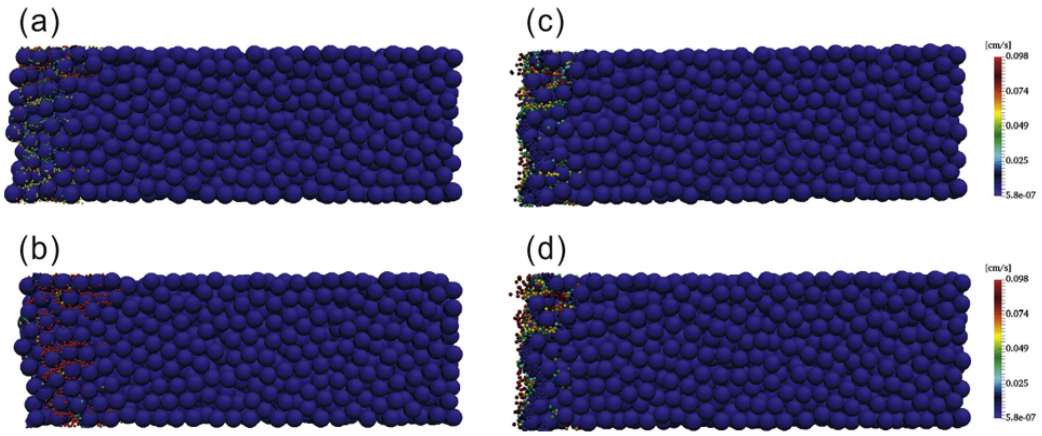

Fig. I.8. Particles deposition and velocity distribution for different injected particle sizes: (a) Rp=0.117; (b) Rp=0.15; (c) Rp = 0.183; (d) Rp = 0.20 (Feng et al., 2020).

Xiong et al. (2023) utilised a coupled CFD-DEM approach to delve deeply into the effects of various configurations of fabric anisotropy on the transport of fine particles under controlled flow conditions. They created granular filters with different initial rotational degrees of freedom and orientations for coarse and irregularly shaped particles. Subsequently, fine particles were introduced at the top of the filter and transported through the filters prepared using hydraulic flow.

The results revealed a clear connection between the migration of fine particles and the anisotropy of each filter, which was defined by the orientation of the particles. Notably, the fine particles exhibited a more pronounced tendency to migrate when the alignment of the filter particles' orientation (longest principal axis) coincided with the flow direction. This phenomenon is associated with the alignment of constriction orientations (normals to the constriction plane) with the flow direction, which enhances the pore connectivity in that particular direction. Figure I.9 gives the trajectory and blockage of fine particles within different filters according to these authors. When the filter particles are randomly oriented (Fig. I.9a), fine particles are more blocked than when the filter particles are all oriented along the direction of the flow, where fines can migrate deeper (Fig. I.9b).

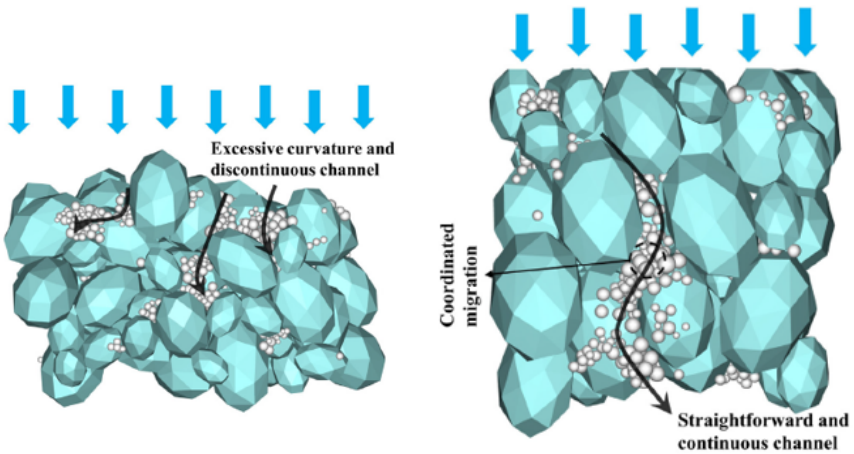

(a) Particles randomly orientated (b) Particles vertically orientated

Fig. I.9. Trajectory and obstruction of fine particles within the two filters (Xiong et al., 2023).

- **Lattice Boltzmann method**

LBM is a discrete mesoscopic methodology that implicitly addresses the Navier-Stokes equations by resolving linear kinetic gas theory equations (Lallemand and Luo, 2000; Ladd and Verberg, 2001). Consequently, this eliminates the necessity for direct solutions to the nonlinear partial differential Navier-Stokes equations, thereby significantly simplifying the modelling process.

LBM models address the fluid as a collection of fictive particles that undergo successive propagation and collision processes within a discrete lattice framework. Similar to resolved CFD approaches, this numerical scheme requires discretizing the pore space. However, unlike CFD, LBM uses a fixed lattice that remains unchanged as the particles move.

When coupling DEM with LBM, the lattice grid can be categorized into three groups: solid lattice, which is entirely located within the discrete particle, outer lattice, which is part of the fluid, and interface lattice, which crosses the boundary of the discrete spherical particle. Figure I.10 illustrates these three lattice categories for a spherical solid particle. The interactions between the fluid and particles can be determined by solving the collisions between fluid and solid nodes near the particle surface.

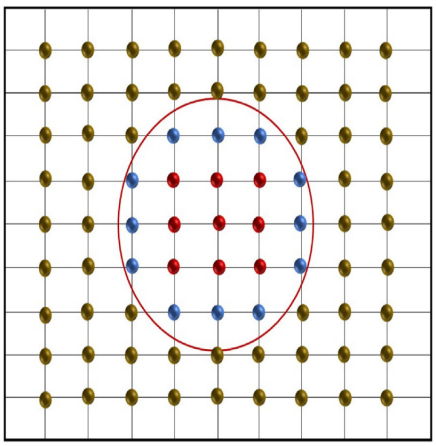

Fig. I.10. Lattice condition of the LBM-DEM coupling: fluid particles (brown), interface particles (blue) and solid particles (red) (Song et al., 2020).

LBM can handle complex boundaries and includes microscopic interactions. Nevertheless, it is worth noting that despite its potential for parallelization, implementing LBM in a three-dimensional (3D) context remains computationally demanding.

Abdelhamid and El Shamy (2016) conducted filtration tests in which the fluid phase was modelled at the pore scale using LBM (Fig. I.11). The primary objective of their study was to explore the response of fine particles under critical flow conditions. The results showed that filters with $D_{15(f)}/D_{85(b)}$ ratios below 4 exhibited a high increase in pressure within the filter zone. Furthermore, the migration of the base particles was directly blocked, leading to clogging after the erosion of less than 20% of the base soil. Moreover, permeability decreased due to the accumulation of fine particles within the filter body. In contrast, filters with a $D_{15(f)}/D_{85(b)}$ ratio greater than 4 experienced erosion of approximately 80% of the base soil. In this scenario, the filter permeability initially decreased owing to the presence of fine particles within the filter body. However, as these particles began to wash out, filter permeability gradually improved. This observation corroborates

the transient phases of filtration previously identified in (Muresan et al., 2013).

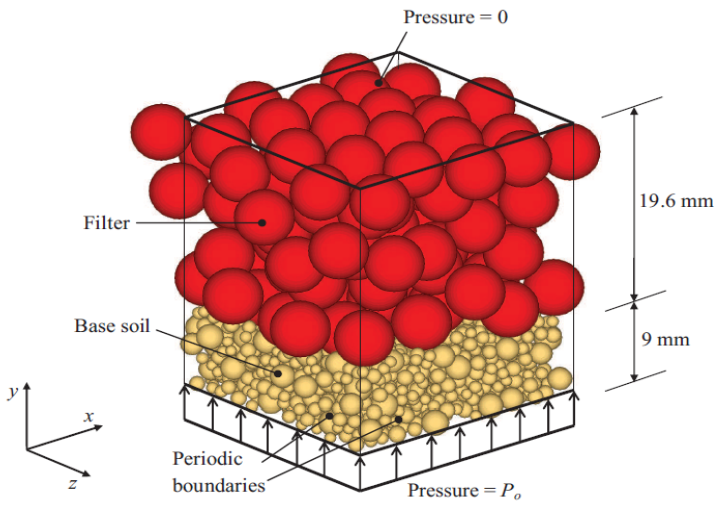

Fig. I.11. Schematic representation of granular deposition for filter simulations (Abdelhamid and El Shamy, 2016).

- **Pore scale finite volume method**

A fluid flow model, known as "pore scale finite volume (PFV)", was introduced by Chareyre et al. (2012) to enhance the representation of flow dynamics within granular materials modelled by DEM.

The PFV model is based on a pore-scale discretization of the Stokes equations for incompressible fluids. This approach involves dividing the pore space within granular materials into interconnected pore bodies using regular weighted Delaunay triangulation. In this method, local pores are defined as voids within tetrahedral cells. Subsequently, the Stokes flow equations were averaged and computed at the pore level using a finite volume scheme. This refinement simplifies the intricate fluid flow dynamics into the Darcy fluid exchange laws between adjacent pores. Following the calculation of the flow between local pores, the fluid forces acting on the particles were determined and integrated into the motion laws of each particle. Additional details regarding the calculation method are presented in Chapter II.

It is important to emphasise that the Delaunay-based spatial segmentation employed in this approach was only developed to address the case of filters composed of perfectly spherical particles. Consequently, this model is not suitable for samples with non-spherical shapes. Moreover, modelling samples containing a large number of particles remains computationally expensive with this method.

Seblany et al. (2021) conducted wet filtration experiments on numerical filters using the PFV model. They correlated the filtration outcomes with the number and size of constrictions, which were extracted from numerical samples using a weighted Delaunay tessellation. The findings revealed a high correlation emerged between the size of the fine particles that were completely blocked within the filter and the mode derived from the probability density function of the constriction sizes, which represents the most frequently occurring constriction size within the filter. Additionally, the study emphasised the importance of ensuring an adequate thickness for the filters

in order to obtain representative filtration results.

3.2.2. Case of dry approach

Given the complexities of modelling fluid dynamics and the significant required computational resources, many filtration tests have been conducted through numerical filters generated by DEM, but under dry conditions where the movement of fines released in the filter is only governed by the gravity force (Sjah and Vincens, 2013; Kerimov et al., 2018; Seblany et al., 2021). In such scenarios, the underlying statement is that the primary characteristic governed by the fluid dynamics model, which is the drag force exerted by the fluid on migrating fine particles, can be roughly modelled by the gravitational force. Nevertheless, it is crucial to emphasise that when subjected to gravitational force, fine particles exhibit unidirectional migration, in contrast to their behaviour under a hydraulic drag force. In the latter case, fines have the potential to undergo lateral movements, aligning with the maximum local flow within the filter, thereby allowing fine particles to migrate further within the filter (Ghidaglia et al., 1996; Muresan et al., 2013). Consequently, this substitution method does not provide a precise modelling of actual wet tests but overall, quantitative results of good quality are obtained in this case.

Lominé and Oger (2009) used the dry filtration method to examine the dispersion of fine particles within numerical filters, aiming to extend and validate the results obtained from their experimental tests. In these numerical experiments, various parameters, including the number, size, density, and restitution coefficient of fine particles, were thoroughly investigated. Furthermore, Sjah and Vincens (2013) used the dry filtration method as a way to acquire the constriction size distribution through a probabilistic approach on the basis of the maximum size of fines able to cross a filter with a given thickness. In addition, Kerimov et al. (2018) conducted dry filtration experiments to explore the mechanical entrapment of fine particles within numerical filters, encompassing monodisperse, bidisperse, and polydisperse packing scenarios. This study introduced criteria based on the sizes of both fine and filter particles to quantify the effectiveness of the filters in retaining fine particles.

3.3. Pore space extraction and analysis

Numerical methods have proven to be an effective alternative to experimental techniques, largely due to their capacity to extract and discretize pore spaces more easily. These methods offer enhanced quantitative outcomes that can be precisely linked to the mechanisms of filtration. However, the definition of a pore is ill-posed as there is no clear mathematical criterion to circumscribe their boundaries. Therefore, different numerical methods that post-process the segmentation to quantify volumes of pores and constriction sizes have been proposed. These approaches can lead to different results, even if the magnitude of derived quantities is mainly conserved. However, within the framework of a given numerical approach, the relation of order when different gradings or sample densities are studied is maintained.

Starting with triangulation-based approaches, these methods rely on extracting the pore space of numerical samples with spherical shapes generated using DEM. An effective tool for this purpose is the weighted Delaunay tessellation algorithm, as described by Reboul et al. (2008). This algorithm involves dividing the pore space into tetrahedrons, with each vertex of the tetrahedron

representing the centre of a particle. Pores are located at the centre of these tetrahedrons, while constrictions are identified on each face of them (Fig. I.12). The subdivision into tetrahedra may lead to an artificial description of the pore space. Merging criteria can be used to erase this aspect, in particular when two adjacent pores are highly connected. It is important to note that this approach is only applicable to spherical shapes, where the pore space can easily be extracted as a dual component of the space from the exact knowledge of the solid space.

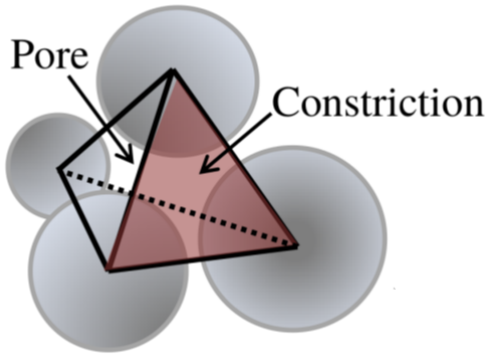

Fig. I.12. Tetrahedron built from the centres of four neighbouring spheres (Reboul et al., 2008)

By employing the Delaunay tessellation method, Reboul et al. (2008) successfully derived void space characteristics from two distinct samples, one densely packed and the other loosely packed, both comprising spherical particles representing uniformly graded materials. The findings revealed that the densification process minimally alters the overall structure of the samples, with changes primarily occurring at the local level. The principal consequence of this transformation lies in the destruction of larger pores, resulting in a more uniform void space. In the loose sample, constrictions and pores exhibited greater heterogeneity, whereas, in the densely packed state, a more uniform distribution prevailed, with enhanced interconnectivity observed among smaller pores.

Using also Delaunay tessellation,Seblany et al. (2021) demonstrated the influence of the PSD on the size of constrictions. As expected, uniformly graded materials exhibit larger constrictions, whereas well-graded materials exhibit smaller constrictions. Moreover, they show that the way samples of spheres are created influences the resulting CSD. Indeed, an isotropic compaction leads to a CSD that is more uniform than when gravity deposition where interactions of particles before equilibrium generate a greater disorder in the sample.

O'Sullivan et al. (2015) also developed a contact-based void partitioning algorithm to determine constriction sizes through a numerical triangulation. This method uses particle-particle contact points to create a triangular tessellation and identifies constrictions as loops enclosing three or four contacts. Importantly, this method avoids the introduction of subjective merging, which results in more reliable results. Nonetheless, it is worth noting that this triangular tessellation approach is also constrained to spherical particles and may not be easily adaptable to materials with non-spherical shapes.

For numerically extracting the pore space from granular materials consisting of non-spherical particle shapes, image-based approaches are more suitable. From a 3D voxelized image obtained either from x-ray tomography of granular materials or from generated numerical samples, the

pore space is extracted directly by some developed algorithm. This image is composed of a set of voxels whose number depends on the size of the sample and the resolution of this image. An attribute is given to each voxel to specify if this latter belongs to the void space or the solid matrix. Based on this segmentation, computations of distances can easily be made. The use of image-based approaches is convenient since this technique can be applied to images that can be derived either from a true numerical sample or an X-ray tomography of actual granular materials.

The medial axis method is an image-based approach that was originally proposed by Lindquist et al. (2000) to study fluid flow within porous rocks. This method is based on the identification of a medial axis or skeleton that traverses through the core of the porous space, maximising its distance from solid particles. From this skeletal distance data, valuable information regarding the centres of the pores and constrictions can be extracted. The centre of the pores corresponds to the nodes along the skeleton that exhibit the most prominent local extrema, whereas the constrictions are defined as the narrowest points within the medial axis.

Another approach, known as the maximal ball method, shares common elements with the medial axis approach. It was initially introduced by Silin and Patzek (2006) and subsequently extended by Dong and Blunt (2009). This technique effectively distinguishes between the pore space and solid matrix in 3D voxelized images. The core idea of the maximal ball method is to locate the largest spheres that can fit entirely within the local void space. A pore is defined at each local void space as the largest sphere with no neighbouring spheres on either side with a greater radius, while constrictions are identified as the smallest spheres situated between two adjacent pores. Figure I.13 presents a schematic illustration of the maximal ball and medial axis methods to extract the pores and a constriction.

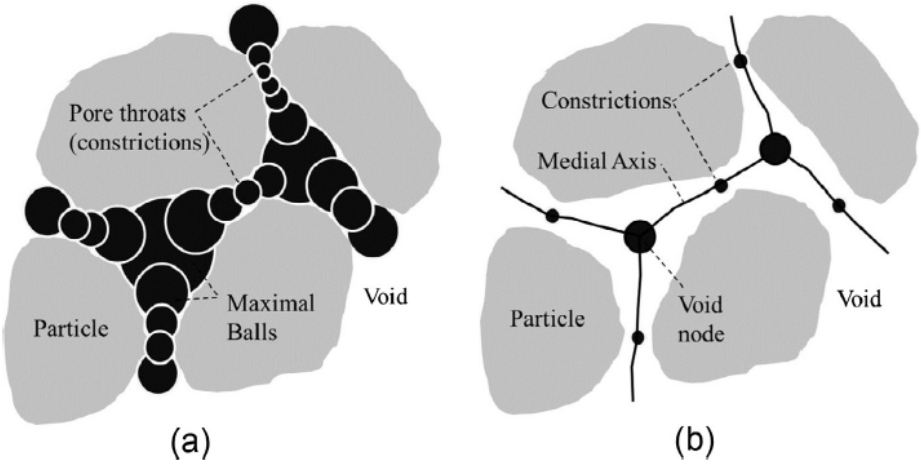

Fig. I.13. Schematic Illustration of two image-based Methods for pore and constriction extraction: (a) Maximal ball method, (b) Medial axis method (Taylor et al., 2015)

Using the maximal ball method, Li et al. (2021a) extracted the pore space of numerical samples consisting of elliptical particles with varying aspect ratios, which are defined as the ratio between the major and minor half-lengths of the geometric elongation axes. They aimed to explore the influence of the particle shape on the porosity of the resulting sample and its inherent pore structure. The findings indicate that increasing the aspect ratio of the particles from 1.00 to 2.50 initially leads to a decrease in porosity. This trend continued until the aspect ratio reached 1.75, at which

point the porosity began to increase. The characteristics of void spaces, such as the mean pore diameter, mean pore spacing, and mean coordination number, exhibit a similar pattern. They first decreased and then increased. Nonetheless, the variability in the porosity of the different numerical samples used in these simulations poses a challenge when attempting to quantitatively assess the direct influence of the particle shape on the void space characteristics.

Shire et al. (2012) conducted a comparative analysis between the Delaunay tessellation (Level 0 no merging) and the maximal ball method. Both techniques were applied to derive the CSD from a numerical representation of the spheres. The findings indicate that the Delaunay method yielded a higher overall CSD value. This is because of the inherent tendency to create excessive void-space segmentation (Al-Raoush et al., 2003). Shire also found that the image-based maximal ball method tends to generate an extended 'tail' of very small constrictions that have a radius ranging from one to three voxels, a phenomenon not observed in the Delaunay method. They suggested that this could be attributed to irregularities in the 3D images produced during the initial voxelization process.

Taylor et al. (2015) introduced a new image-based technique called the "watershed-based method" for extracting the locations and constriction sizes from 3D binary images. This technique is based on the watershed method, which divides void spaces into distinct voids. Subsequently, it scrutinises the boundaries between these voids to pinpoint and measure constrictions. The advantage of this innovative method lies in its ability to generate supplementary visual outputs, such as 3D representations of individual constrictions and voids. This enhanced visual inspection allows users to view a large number of individual pores and constrictions, serving as a valuable tool for discerning variations in the void characteristics. They also found the existence of a tail in the smaller constriction sizes. They suggested eliminating this extended 'tail' by ignoring constrictions smaller than 0.155 times the diameter of the smallest filter particle. This value corresponds to the theoretical size of the smallest constriction that can be formed through mutual contact between the three smallest spheres in the filter, each with a diameter equal to D_0. Nonetheless, this criterion does not apply to non-spherical materials, as it is challenging to determine the size of the smallest constriction using an analytical method. They also conducted a comprehensive comparative analysis of all image-based approaches, and the findings demonstrated that all methods yielded consistent CSD results.

Using this new approach, Taylor et al. (2019) investigated the void space within real materials. First, they took 3D tomography images for the prepared samples and then subsequently employed the watershed-based approach to isolate the pore space. The results revealed that the distribution of constriction sizes is notably more responsive to the grading of the PSD than to variations in shape or density. While there is a degree of sensitivity to shape, the data suggests that angular particles are capable of creating both very small and very large constrictions to a greater extent than their spherical counterparts.

4. Filter criteria for granular filters

Designing an efficient filter is a complex task that requires consideration of numerous factors related to both the filter and the base soil. These factors include geometric and fluid dynamics aspects, among others. Key considerations encompass the PSD of both the filter and base materials, particle shape, pressure gradients, and direction of filtration. However, many proposed criteria

simplify the design process by omitting certain factors.

One of the most widely adopted criteria for filter design primarily focuses on the PSD of both the filter and base soil, which was initially proposed by Terzaghi. These criteria rely on empirical formulas derived from laboratory tests.

Recently, there has been a shift towards the development of new, promising filter criteria based on the constriction sizes of the filter materials (Kenney et al., 1985). This approach holds greater physical significance, as its constrictions directly govern the retention capacity of the filter.

This section provides a comprehensive discussion of these two criteria along with their respective limitations.

4.1. Particle-size based criteria

Particle-size-based criteria were originally proposed by Terzaghi (1922), utilising geometric grading characteristics that rely on the particle size distributions of both the base soil and the filter.

This criterion consists of two requirements for designing a filter that can effectively prevent the base soil from being eroded while permitting the flow to pass through, thus preventing the accumulation of excessive hydraulic pressure.

The two requirements are presented in the form of filter-base soil grain size ratios:

- **Retention requirement**:

$$d_{85} \geq \frac{D_{15}}{4} \tag{I.5}$$

- **Permeability requirement**:

$$d_{15} \leq \frac{D_{15}}{4} \tag{I.6}$$

where D_x and d_x are the filter and base particle diameters, respectively, for which $x\%$ of the material (filter and base soil, respectively) by mass is finer.

Figure I.14 displays a diagram illustrating the initial specifications provided by Terzaghi regarding the grain size of a material appropriate for use in a filter. The shaded area on the left encompasses all possible grain-size curves for the material that requires protection, whereas the shaded area on the right signifies the acceptable range within which the curves for the filter material should fall in.

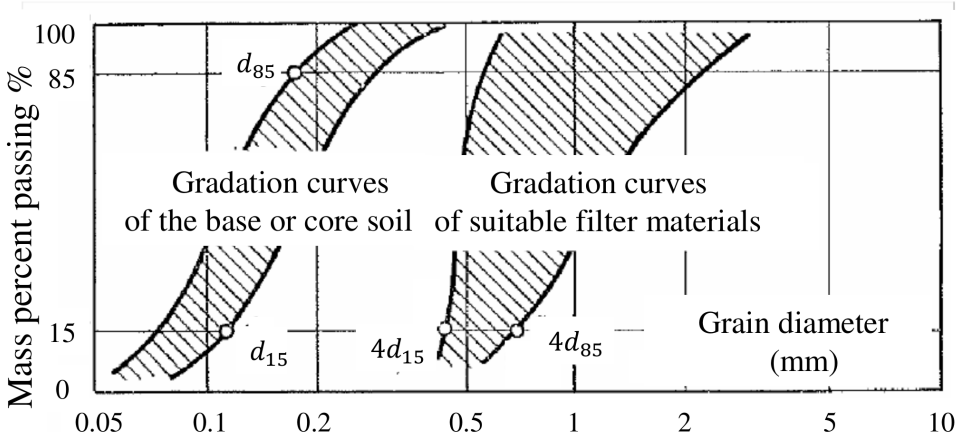

Fig. I.14. Filter and drainage criteria (Terzaghi et al., 1996).

When considering filter materials, the diameter most commonly used to represent the filter material is D_{15}. The selection of this size is justified by considering that the small grains in the filter play a critical role in regulating the size of the voids within the filter itself. These voids, in turn, govern the potential blockage of fine particles (Sherard et al., 1984; Honjo and Veneziano, 1989; Foster, 1999).

For the base soil, Honjo and Veneziano (1989) conducted extensive research that conclusively demonstrated that a filter can be deemed efficient when it is capable of blocking at least 15% of the underlying soil. This is why several studies have embraced the use of d_{85} as the representative size for the base soil in traditional filter design (BERTRAM, 1940; Honjo and Veneziano, 1989; Indraratna et al., 1996). It underlies that the fines greater than d_{85} will penetrate the filter and be blocked in the first layers of the filter reducing the opening size of it and blocking the fines smaller than d_{85}. The process of modification of the filter opening size is denoted as self-filtration.

Other alternative parameters have been examined as representatives of the size of the filter and base soil, such as D_{15}/d_{15} and D_{50}/d_{50} (Karpoff, 1955). However, the results obtained from experiments conducted by Sherard et al. (1984) and Honjo and Veneziano (1989) have jointly demonstrated that using these values in filter design is not suitable because they do not exhibit a significant correlation with filter performance.

Sherard et al. (1984) introduced an improved set of filter criteria to more effectively consider the properties of the underlying soil. As an illustration, when dealing with a base soil containing over 85% fine content, the retention ratio should be modified to consider the fine content such that $D_{15} \leq 9d_{85}$. The reason behind this improvement is that the initial criterion of Terzaghi was designed for non-cohesive uniform soil.

In the case of well-graded base materials, NRCS (1994) suggested the recalculation of D_{85} value for the base soil after the exclusion of coarse particles held back by the 4.75 mm sieve.

Terzaghi criteria, along with the other approaches relying on particle size distribution, are extensively used by engineers for designing granular filters. However, these empirical formulas fail to explicitly consider various critical parameters, such as material grading and density for the filter. Moreover, the direction of filtration is not taken into account as all the laboratory filtration tests are commonly performed in vertical cylinders containing a granular filter material (Terzaghi, 1922;

BERTRAM, 1940; Sherard et al., 1984; Kenney et al., 1985; Locke et al., 2001).

Finally, it is worth mentioning that additional experimental tests are required to determine other criteria related to aspects of the filtering including internal stability. These tests are not detailed herein, as they fall outside the primary scope of this study (Reddi et al., 2000; Deo et al., 2010; Kézdi, 1979; Wan and Fell, 2008).

4.2. Constriction-based criteria

The retention of fine particles within granular filters is primarily governed by the size of constrictions present within the filter structure. Conventional filter design often uses a simplified particle-based approach that implicitly accounts for the filter's opening size ($D_{15}/4$ in the case of Terzaghi geometric criterion) relative to certain characteristic sizes of the base soil. However, these approaches are customised to specific material types, resulting in inaccuracies in representing actual opening sizes when dealing with granular materials and filter densities that do not correspond to those used in laboratory experiments.

Recognising these limitations, Kenney et al. (1985) introduced the concept of controlling constriction size ($D_c{}^*$) as a more explicit representation of the equivalent sieve opening size of the filter. This parameter serves as an important indicator, signifying the largest size of fine particles that the filter can transport effectively. Any particle exceeding this specified size is effectively trapped and retained within the filter. According to Kenney's approach, the controlling constriction size can be estimated based on some characteristic sizes of the filter particles:

$$D_c{}^* \leq \frac{D_{15}}{5} \tag{I.7}$$

$$D_c{}^* \leq \frac{D_5}{4} \tag{I.8}$$

Following this concept, establishing filter criteria that directly correlate with constriction size provides a significantly more accurate representation of retention ability (Locke et al., 2001). From the constriction size distribution (CSD), it is possible to identify two distinct characteristic diameters:

The first representative diameter chosen from the CSD was D_{c35}, which represents the size for which 35% of the constrictions are smaller (Indraratna et al., 2007). The selection of this value as a representative diameter was based on probabilistic studies that indicated the importance of constriction sizes falling within the 30–40% range of the cumulative CSD in controlling the retention capability. For fine particles smaller than this range, there is a higher probability of these particles travelling a considerable distance within the filter before becoming blocked. Hence, D_{c35} was identified as the controlling constriction size beyond which any fine particle exceeding this value would be effectively trapped within the filter.

A second representative diameter was selected to enhance the self-filtration capability of the filter. When the filter becomes blocked with fine particles, these particles play a pivotal role in reducing

the size of constrictions within the filter. Consequently, this leads to the progressive blockage of finer particles (self-filtration concept). It is worth noting that fine particles larger than the largest constriction cannot penetrate the filter, making them inconsequential to the self-filtration process. Hence, when evaluating self-filtration capacity, it is imperative to disregard these coarse particles. Indraratna and Raut (2006) and Raut and Indraratna (2008) chose to specify the dominant constriction size as D_{c95}, representing the size at which 95% of the constrictions are smaller. This dominant constriction size defines the threshold beyond which fine particles larger than this value must be effectively disregarded.

Indraratna et al. (2007) proposed that a filter can be considered as a sieve with an opening size equal to the controlling constriction dimension, denoted as D_{c35}. Accordingly, a criterion based on the constriction size can be established to retain the base soil, outlined as follows:

$$d_{85SA} \geq D_{c35} \tag{I.9}$$

where d_{85SA} is the diameter at which 85% of the base soil by surface area is finer.

Indraratna et al. (2007) proposed a refinement in the methodology for evaluating the representative diameter of the base soil. Instead of relying on the conventional d_{85} value obtained from the mass-based particle size distribution, they recommended using d_{85SA}. This modification has proven to be more representative, particularly when using well-graded soils. The reason for this is that the mass-based approach tends to exaggerate the role of larger particles as they hold a larger mass, even though they are few in number. Indeed, the PSD by mass can be considered adequate for uniform filters, but it fails to deal effectively with well-graded materials.

Later on, Raut and Indraratna (2008) proposed a new filter criterion based on the self-filtering base fraction and the controlling constriction size of the filter. Thus, the PSD of the base soil is modified by excluding all particles coarser than D_{c95}. For an effective base soil-filter combination, the following relationship must be fulfilled:

$${d_{85}}^{*} \geq D_{c35} \tag{I.10}$$

where ${d_{85}}^{*}$ represents the d_{85} value obtained from the modified base soil PSD.

The advantage of these constriction-based criteria lies in their ability to integrate essential filter parameters, including the coefficient of uniformity and porosity of the filter, as the size of the constrictions accounts for these factors. By contrast, particle-size-based criteria focus solely on characteristic sizes and do not adequately represent these important parameters. Moreover, it is worth noting that D_{c35} and D_{c95} models are independent of the base soil properties.

It is crucial to emphasise that these models, which consider dominant and controlling constriction sizes, underwent rigorous validation through experimental filtration tests (Indraratna et al., 2007; Raut and Indraratna, 2008). Consequently, such criteria provide a more physically meaningful perspective than the conventional approach.

Nevertheless, it is important to note that acquiring D_{c35} and D_{c95} involves a more complex procedure than obtaining D_{15} as it necessitates the determination of the CSD for the granular filter. For

simplicity, numerous analytical approaches have been developed to determine the CSD, avoiding the need for experimental or numerical approaches (Silveira et al., 1975; Locke et al., 2001; Reboul et al., 2010; Seblany et al., 2021). Such analytical approaches rely on a probabilistic theory that suggests the presence of reference geometric configurations of particles involved in the creation of a constriction. In this context, particles are generally assumed to be spheres. To determine the constriction sizes, two geometric configurations can be considered depending on the density of the sample being studied as shown in Figure I.15. It should be noted that these configurations are purely geometric and do not reflect the mechanical arrangements found in real materials. Indeed, a numerical sample can be highly heterogeneous in terms of spatial arrangement (Reboul et al., 2008).

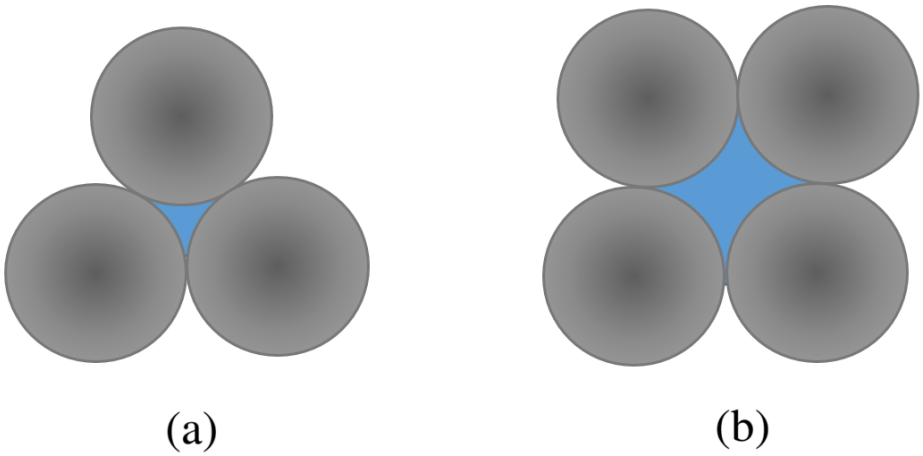

Fig. I.15. Geometric configurations for (a): the densest arrangement (Silveira, 1965); (b): the loosest arrangement (Silveira et al., 1975).

These analytic approaches can deal with filters with different types of PSDs and take into account the filter density. However, they are supposed to be valid only for filters composed of spheres since they were initially developed for this case. Consequently, these methods have limitations when dealing with granular materials with non-spherical particles.

Seblany et al. (2021) suggested a direct estimate of the filter opening size (D_{OS}) which is merely equal to the controlling constriction size and can be associated to a substitute of D_{c35} (Indraratna et al., 2007). The proposal by Seblany et al. (2021) bypasses the computation of the full CSD as required for obtaining D_{c35}. The filter opening size was determined based on an improved analytical approach proposed by Reboul et al. (2010). This approach considers various factors, including the maximum void ratio, actual void ratio, and particle size, characterised by their surface area (D_{50SA}) within the granular material. As a result, the grading, coefficient of uniformity, and porosity of the sample were taken into consideration.

In their study, Seblany et al. (2021) introduced a retention criterion for granular filters based on opening size (D_{OS}):

$$d_{85SA} \geq d_{OS} \tag{I.11}$$

This criterion was subsequently verified using experimental data obtained from previous investigations involving filters with both uniformly and widely graded materials. Furthermore, a comparative analysis was conducted to assess the various retention criteria. The results indicated that retention criteria based on constriction size proved to be relatively more effective in identifying efficient filters than criteria based on particle size.

5. Conclusion

Granular filters are extensively used as protective layers in hydraulic structures to prevent the erosion of the base soil. Under adequate seepage flow, the filtration mechanisms are primarily governed by the geometry of the pore space. Numerous experiments have been conducted to investigate the filtration dynamics within these filters. The findings indicate that, in addition to seepage flow, various factors related to the properties of both fine and filter particles significantly influence the filtration process. However, obtaining quantitative results is challenging because these parameters are closely related, making it difficult to isolate their individual effects. Moreover, visualising, and tracking the movement of fine particles within a granular filter is difficult to achieve. Typically, granular materials are replaced with glass spheres for easier particle tracking. However, even with these adjustments, the process remains complicated.

To address these challenges, researchers have developed numerical models to simulate filtration tests. These models offer insightful and complementary results compared to the experimental outcomes. They simplify the control and tracking of the migration process and make it easier to pinpoint the impact of individual parameters. However, owing to the computational costs involved, the majority of these simulations were carried out using spherical particles, with only a few of them exploring non-spherical shapes.

It is widely recognised that the geometry of the pore space, specifically the constrictions within filters, determines the retention capacity of the filter. Various experimental and numerical methods have been proposed to quantify their size and occurrence in granular materials. Numerical approaches appear to be more effective than experimental approaches in extracting pore space characteristics. Nevertheless, for the sake of simplicity, several analytical methods have been introduced to bypass numerical simulations that may be time-consuming. However, it is important to note that these analytical methods are only valid for packing of spheres since they are based on mathematical equations designed for spherical particles.

Building on prior experimental and numerical studies, several filter criteria have been proposed, each of which adopts a different methodology. The most prevalent approach focuses on the particle size characteristics of both the filter and the base soil. Although numerous criteria based on this approach have been developed, they tend to be applicable mainly to materials with specific characteristics. The characterization of granular materials is influenced by factors such as grading, porosity, and particle shape. However, such criteria often fail to comprehensively account for all of these aspects.

Recently, new filter criteria based on constriction sizes have been introduced. These are more general in their use because they directly address the constriction sizes responsible for particle blockage. As the constriction size is influenced by grading, porosity, and particle shape, these constriction-based criteria offer a more comprehensive view of the filtration mechanism. Nonethe-

less, it is worth noting that constriction sizes are frequently determined using analytical formulas that might not fully account for the effects of particle shape.

A quantitative analysis examining the impact of the particle shape on constriction size and, consequently, the filtration process is still lacking. Additionally, the particle shape can introduce inherent anisotropy in the pore geometry, potentially altering the filter's efficacy in blocking particles depending on the filtration direction. Such an aspect was not taken into account in the present criteria.

In subsequent chapters, we present an in-depth exploration of the influence of particle shapes on the void space and their implications on filtration processes.

Chapter II

DEM Filtration Modeling for Granular Materials: Comparative Analysis of Dry and Wet Approaches

Authored by: Ali Abdallah[1], Eric Vincens[1], Hélène Magoariec[1] and Christophe Picault[2]

[1]. Univ Lyon, Ecole Centrale de Lyon, CNRS, ENTPE, LTDS, UMR5513, 36 Avenue Guy de Collongue, 69134 Ecully, France

[2]. CACOH, Compagnie Nationale du Rhône, 4 Rue de Chalon-sur-Saône, 69007 Lyon, France

This chapter is based on a manuscript currently under review at: *International Journal for Numerical and Analytical Methods in Geomechanics*

Acknowledgments: Part of this work belongs to a project funded by Compagnie Nationale du Rhone. The authors acknowledge the support of CNR for this study.

Abstract

A detailed study comparing two - dry and wet - numerical approaches to model filtration processes at stake in actual granular filters is presented using the discrete element method. In the first approach, the migration of fines is provided by gravitational forces, while in the second, hydrodynamic forces induce their movement. Numerical filtration tests were performed on granular filters involving materials with different gradings and porosities. The study demonstrated that the wet filtration approach generates higher tortuosity due to the possibility for fines to deviate from direct paths towards more open sideways. It leads to a lower coefficient of retention for the filter than if it were characterised using a dry filtration approach. However, the intensity of this feature greatly depends on the grading and the porosity of the granular filter. Finally, an enhanced dry filtration model designated as the "equivalent cyclic wet filtration model" is presented, which better mimics the results obtained through the preferable wet filtration model compared to the original dry filtration model. This new model constitutes a valuable alternative tool for studies of filtration properties in granular materials.

Main results

- Wet filtration showed higher tortuosity and a lower coefficient of retention for fine particles than dry filtration. This difference was attributed to the dragging forces in wet filtration that aligned fine particles with the maximum flux direction, allowing sideways exploration, unlike in dry filtration.
- For narrowly graded materials, there was a more pronounced difference in terms of tortuosity and retention coefficient for wet filtration compared to dry filtration than for more widely graded materials. This arose from the existence of larger heterogeneities in constriction sizes, prompting fine particles to explore more frequently sideways than in other cases.
- In dense materials, the differences between wet and dry filtration in terms of coefficient of retention were less pronounced due to the high pore connectivity. This allowed the fine particles equal chances of exiting pores either from a direct constriction or sideways.
- Relying solely on dry filtration results may not be conservative when determining filter criteria, especially for narrowly graded materials.
- Cyclic wet filtration tests revealed that variations in the hydraulic head could re-launch the initially trapped fine particles. This suggests that in the wet filtration model, fine particles didn't always select larger constrictions when trying to exit a pore. The PFV model highlighted a potential competition between local maximum flux conditions and the movement direction of entering particles. Cyclic tests are necessary to achieve a stabilised and conservative quantification of the retention capacity of a granular filter.
- A new enhanced dry filtration model was proposed to address the limitations of dry filtration as a model for wet (cyclic) filtration. It was validated through comparison with cyclic wet filtration tests. This new model allows for sideways exploration and accurately determines

the equivalent filter opening size. It is computationally efficient and applicable for various particle shapes, provided that the average pore diameter can be estimated.

1. Introduction

The use of granular filters to remove suspended fine particles from fluid streams is a critical process across multiple industries, including geotechnical and environmental engineering, water treatment, mining, and oil industry (Khilar and Fogler, 1998). Designing an efficient and cost-effective filtration system is essential not only for ensuring the quality of the process but also for safety reasons. For instance, filter fouling can have a significant impact on filtration operations, particularly when the applied pressure is driving the flow. When filters become clogged, they can directly reduce the rate of filtrate flux and increase the applied pressure, thereby hindering the overall effectiveness of the filtration process (Iritani, 2013). Similarly, in hydraulic structures and behind retaining walls, clogged filters can unexpectedly create high hydraulic loads on the structure, potentially leading to structural failure (Martin, 2013; Yan et al., 2022). In this case, it may imply critical consequences both in terms of human life loss and economic costs.

In the past, a multitude of experimental tests were conducted to investigate various features. Some focused on studying and characterising the fundamental mechanisms involved in filtration processes, while others were specifically carried out for engineering applications, such as developing filtration criteria for designing granular filters. For example, Ghidaglia et al. (1996) carried out experimental tests to study the penetration depth of fine particles in deep bed filtration for two different particle injection methods under hydrodynamic and gravitational forces (wet and dry conditions, respectively). The results show that in dry conditions (only gravitational forces drive the movement of fines), the fine particles penetrated slightly less deep than in the case where fine particles were dragged by hydrodynamic forces (due to the existence of a water seepage). Furthermore, in the latter case, they remarked that fine particles are trapped not only because of geometrical restrictions existing in the filter, but also because some particles are blocked in "hydrodynamic" sites (associated with stagnation points in the flow). These sites capture the fine particles in a very unstable regime where sharp changes in the flow characteristics due to changes in the inlet property can relaunch these particles.

Within the framework of engineering applications, Terzaghi et al. (1996) conducted several filtration tests on granular filters to develop a filter criterion that can be used for granular filters installed in hydraulic structures such as dams and dikes. Since it was difficult to directly quantify the filter void space and especially the constriction sizes (narrowest paths linking neighbouring pores) within the filter, Terzaghi indirectly related the capacity of a granular filter to retain some class of particles to an equivalent filter particle size. Recently, advanced techniques have been developed to provide more insight on local phenomena involved in the filtration processes, including particle image velocimetry (Wereley and Meinhart, 2010; Chen et al., 2017) and high-speed photography (Fuller, 2009; Versluis, 2013). However, these experimental methods typically offer qualitative information but often fall short in providing quantitative information about fluid-particle interaction (Xing et al., 2017; Sciacchitano, 2019).

Alongside lab experiments involving samples with actual granular materials, researchers have tried to use numerical modelling approaches to complement experimental data and gain a deeper understanding of complex filtration mechanisms. One of the most useful numerical tools is the discrete element method (DEM) coupled with a flow model, as it can provide detailed information on the filtration mechanism at the pore scale. However, the multiphysics coupling scheme remains challenging both in terms of the physical interaction modelling and in terms of computation time. Indeed, while the movement of fine particles is efficiently governed by the DEM computations, the

calculation of fluid motion requires the solvation of the Navier-Stokes equations. This process can be computationally demanding, particularly when high levels of accuracy are required to represent the fluid flow behaviour.

Wautier et al. (2019) listed the different fluid-solid coupling approaches that can be used to model the flow, such as resolved and unresolved computational fluid dynamics (CFD) (Ren et al., 2012; Zhao and Shan, 2013; Xie et al., 2021), lattice Boltzmann methods (LBM) (Lallemand and Luo, 2000; Mansouri et al., 2009; Younes et al., 2022) and pore network models (Bryant et al., 1993; Hilpert et al., 2003). They emphasised that the first three approaches have a prohibitive computational cost when modelling filtration processes in granular materials, while pore network models can offer a cost-effective way to model fluid and grain interactions at a microscale level with fully coupled simulations. Within this framework, Chareyre et al. (2012) proposed an effective up-scaled fluid-flow pore network model called the pore-scale finite volume method (PFV). However, when a large number of filter particles are involved and the moving fine particles are small in size, this technique remains computationally expensive. Moreover, this approach based on the Delaunay-segmentation of the space can only be used for filters composed of perfect spheres.

To overcome this limitation, different authors bypassed the solvation of the fluid dynamics equations and substituted the use of hydrodynamic forces as driving forces on suspended particles with that of only gravitational forces (Reboul et al., 2008; Sjah and Vincens, 2013; Kerimov et al., 2018). The underlying statement was that the main features observed in filtration processes involving water seepage may be found in dry filtration under gravity. There was no proof of the validity of this statement and specially when quantitative results are expected. Indeed, gravitational forces act only in one direction, while hydrodynamic forces influenced by local maximum fluxes in the porous medium can redirect fine particles in multiple directions, allowing them to travel a longer distance in the filter (Seblany et al., 2021). In fact, there is currently no comprehensive numerical analysis that quantitatively assesses the differences between the two approaches and the equivalence between a filtration process mainly driven by hydrodynamic forces and that driven by only gravitational forces.

Building on the insights gained from these previous works, the present study aims to run a thorough analysis of the differences between wet and dry filtration using DEM simulations. This study allows us to outweigh the drawbacks of dry filtration, which is much less time-consuming than wet filtration, particularly when the primary focus only lies on the retention of particles in the filter. Moreover, the notion of cyclic wet filtration tests is introduced. This kind of simulation tries to mimic the natural cyclic variability of hydraulic head in actual hydraulic structures that may disrupt existing unstable retention sites caused by sedimentation or “hydrodynamic” capture (Ghidaglia et al., 1996; Song et al., 2023).

Lastly, this study presents an enhanced dry filtration model, denoted herein as an "equivalent cyclic wet filtration model" able to compensate for the intrinsic limits of dry filtration tests as a model for wet filtration tests. This new approach will be validated based on DEM-PVF simulations of cyclic wet filtration tests. The paper is structured as follows: First, the procedure for generating the numerical sample (granular filter) using DEM is described. Then, dry and wet filtration models, including cyclic wet filtration, are introduced. The difference between these approaches and their impact on filtration results in terms of tortuosity and coefficient of retention are assessed. Next, the equivalent cyclic wet filtration model is presented and validated. Finally, the key findings and conclusions of this study are provided.

2. Generation of numerical samples

To investigate the transportation mechanism of fine particles in porous media, granular filters were numerically modelled as an assembly of spheres using the DEM open-source framework YADE (Šmilauer et al., 2010). In DEM, the numerical sample is defined as packed assemblies of individual interacting particles. Then, local features including pore space properties are well conserved with respect to laboratory experiments if the modelled particles hold the same shape as actual ones. As a result, modelling the movement of the fine particles throughout the filter and recording all necessary information, such as the position, size, and velocity of each fine particle, can be easily processed (Cundall and Strack, 1979).

An elastic-frictional model limited by the Coulomb criterion was chosen for the interaction at contact between particles. The contact is characterised by a normal stiffness k_n, a tangential stiffness k_t, and a Coulomb inter-particle friction φ_c. The normal stiffness k_n and tangential stiffness k_t were set to 5.65 x 10^5 N/m, and the specific weight of particles was assigned as 2,650 kg/m^3. To reduce non-frictional energy and particle bouncing during the preparation phase, a local damping coefficient of 0.7 was introduced (Cundall and Strack, 1979).

The numerical filter samples were created by gravity deposition of a group of spheres inside a well-defined box, where this deposition was designed to mimic the filter installation procedure in actual engineering projects. To minimise wall boundary effects and reduce the number of particles involved in the computations, lateral periodic boundary conditions were implemented. The preparation process was considered complete when the assembly achieved a stable equilibrium state, characterised by an average unbalanced force ratio of less than 0.05 (Seblany et al., 2021). This ratio is defined as the ratio between the mean resultant forces at contact divided by the mean contact force over the sample. After equilibrium was obtained, the coarse matrix was fixed since filters are supposed to be internally stable. It allows for the optimisation of computation times since in this case, contact forces and kinematic torques for coarse particles are not updated throughout a filtration test.

To broaden the scope of the investigation, three types of granular materials with different gradings were used including narrowly-graded (NG), intermediate-graded (IG) and well-graded (WG) materials (Figure II.1). In order to model the loosest and densest states of the filter for each material type, two samples were prepared with inter-particle friction φ_c set to 0.3 and 0, respectively (Seblany et al., 2021). The values of the model parameters used for generating the numerical samples are given in Table II.1.

Table II.1: Mechanical and numerical parameters for DEM simulations in the generation phase.

Parameter	Magnitude
Normal stiffness (K_n)	5.5 x 10^5 N/m
Tangential stiffness (K_t)	5.5 x 10^5 N/m
Specific weight of spheres (ρ)	2650 kg/m^3
Global damping (α)	0.7
Inter-particle friction (μ)	0.3 (loosest state) 0 (densest state)

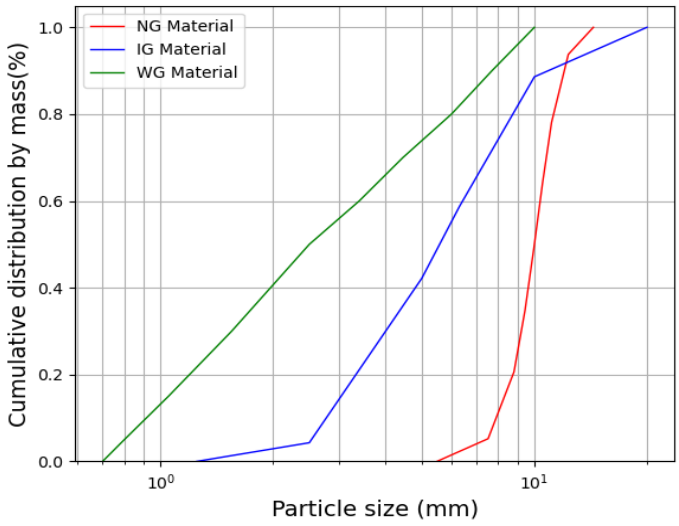

Fig. II.1. Particle size distributions of the numerical filters.

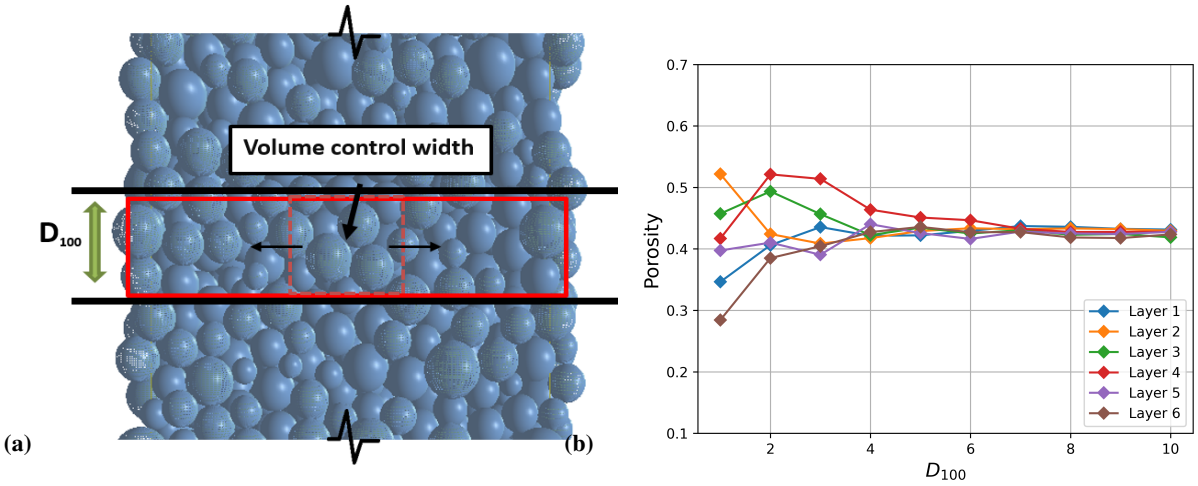

Fig. II.2. Determination of the representative elementary volume of the granular sample: (a)- Layers division within the sample, (b)- Porosity with increasing volume control width in each layer in the loosest state of NG filter.

The dimensions of the boxes were chosen to be greater than the representative elementary volume (REV). A preliminary study was conducted to confirm the appropriate sample size, using a methodology similar to that employed by Reboul et al. (2008) and Sjah and Vincens (2013). First, the sample was divided into layers with a thickness equal to the largest particle diameter D_{100} (Figure (II.2-a)). The porosity of each layer was then computed along the lateral direction with an increasing volume control width. The REV was determined by identifying the minimum size at which the porosity in each layer stabilised around a similar value. In Figure II.2-b, for example, the porosity of horizontal layers of a loose NG sample is given, which demonstrates the fulfilment of the REV condition. This condition is met when the porosity becomes steady at the volume control width of $8D_{100}$, corresponding to $14.5D_{50}$. Using a similar method, samples with widths of $6D_{100}$ ($17.5D_{50}$) and $4D_{100}$ ($16D_{50}$) were chosen for IG and WG materials, respectively.

Selecting the appropriate filter thickness and the required number of coarse particles to create the samples can be challenging. Indeed, as the filter thickness increases, the number of constric-

Table II.2: Characteristics of numerical samples.

Material	Coefficient of uniformity (C_u)	Number of particles loose / dense	Void ratio e_{max}/e_{min}
NG	1.2	4,000 / 4,400	0.75/0.57
IG	2.2	10,000 / 11,000	0.62/0.43
WG	3.7	18,400 / 20,000	0.48/0.33

tions along a pathway also increases. As a result, it increases the probability of fine particles being trapped in the filter. It means that different retention properties can be assigned to a filter depending on its thickness. However, above a certain thickness, a further increase does not significantly affect the results (Witt, 1993). Sherard (Sherard et al., 1984) stated that fine particles can pass through all possible combinations and permutations of pore network sizes and shapes after travelling a relatively short distance of approximately $5D_{15}$. According to Seblany et al. (2021), for the results to be reliable, a fine particle needs to pass through at least 40 constrictions. The transcription of the number of required constrictions on a pathway into a sample thickness can be performed assuming that the pore space is a multilayered cubic network model of pores interconnected by constrictions, as proposed by Schuler (1996). Then, the computation of a sample thickness H is defined by the relationship $H = N_c * s$ where N_c denotes the number of constrictions in a given straight direction and s the average pore diameter, which is herein also the average distance between two successive constrictions. It can be calculated by the equation II.1 designed by Wu et al. (2012) and improved by Seblany et al. (2018b). This formula takes into account both the grading of the material and its density :

$$s = \frac{1}{0.7}\sqrt[3]{\frac{e}{e_{max}}}s_{max} \tag{II.1}$$

where e and e_{max} are the actual and maximum void ratios for the material. s_{max} is the mean pore diameter in the material for the loosest case. An estimate for s_{max} can be obtained by taking a value equal to $0.5D_{50SA}$, where D_{50SA} represents the particle diameter at which 50% of the material is smaller than from a particle size distribution (PSD) of the material defined in terms of surface area. The validity of this estimate for s_{max} can be found in (Seblany et al., 2018b).

In this work, a thickness of 12 cm and 30 cm for NG and IG filters, respectively, was assigned to ensure that at least 40 constrictions are encountered for both loose and dense cases. However, in the case of WG filter, the number of constrictions was deliberately reduced to 30, equivalent to a thickness of approximately 3 cm. This adjustment was made to restrict the particle count to 20,000, considering the substantial number of particles necessary for sample creation and the subsequent increase in computational time required for conducting filtration tests. The values of the physical properties of the obtained samples are given in Table II.2.

3. Numerical filtration models

A set of 200 mono-sized fine particles belonging to a given class of diameter were released randomly on top of the filters, and five repetitions of the same test for each fine particle class were processed where the initial position of the fine particles was different between repetitions. It allowed us to be sure that enough individual particle paths were explored through the filter and that the characterization of the filtration properties of the filters was representative. The release conditions and the chosen number of fine particles ensured that individual particle paths were explored with few interactions between fines, avoiding group effects and bridging (Kerimov et al., 2018; Seblany et al., 2021).

The smallest size for the investigated fine particles for the filtration tests was selected to be slightly smaller than the smallest constriction (D_0/6.5). This value is obtained by the mutual contact of three of the smallest particles of the filter. Indeed, only particles smaller than the smallest constrictions have a non-null probability of being blocked by a filter irrespective of its thickness. A test was considered complete when all fine particles of a chosen size either crossed the full thickness of the filter or were found trapped inside and at equilibrium.

During filtration tests, the inter-particle friction φ_c at the contact between filter particles and fine particles was set to zero. This "lubrication" allows the friction forces to be reduced and allows the fine particles to migrate more ahead in the filter (Sari et al., 2011). Moreover, the coefficient of restitution e was set to a low value of 0.3 in order to prevent the excessive bouncing of the fine particles on the surface of the filter particles (Reboul et al., 2008; Kerimov et al., 2018).

Density scaling is a widely used technique to reduce the computational cost of DEM simulations, as demonstrated in previous studies (Thornton, 2000; Cui and O'sullivan, 2006; Zhao et al., 2018; Zhao and Zhao, 2019). The influence of particle density on computational time varies depending on the specific type of numerical experiment conducted. In this study, the density of particles was increased by a factor of 10^3 to scale up the mass of particles. For the wet filtration model, the hydraulic pressure was also increased by a factor of 10^3 in order to conserve the same dragging forces on the fine particles and hence the same accelerations for them. In the dry filtration model, the acceleration of fines is introduced by gravity, and changing particle density does not modify the gravitational force. A parametric study was conducted to evaluate the effect of density scaling on filtration results. The results indicated that the technique had no significant impact on the final results, as tortuosity and coefficient of retention remained unaltered for dry and wet filtration with density amplification with respect to the case with no density scaling. Herein, the computational time was reduced by 10 to 25 times.

3.1. Dry filtration

In the dry filtration model, the movement of the suspended particles in the granular filter is only governed by the gravitational force. The use of this simplified model for filtration processes is generally motivated by a reduction of computational time but also allows the question of the fluid modeling together with the modeling of fluid-solid interactions to be bypassed. Herein, the procedure for modelling a dry filtration test is straightforward. Once the numerical sample had been prepared by gravity deposition and filter particles had been fixed, the set of 200 fines was

released under gravity on the top sample.

3.2. Wet filtration

There are several approaches available to simulate coupled fluid-solid systems. In this work, the pore scale finite volume method (PFV) was selected as it has been demonstrated to be an efficient tool for simulating the solid-fluid interaction in laminar fluid flows through spherical granular materials (Catalano et al., 2014).

The PFV method performs a segmentation of the space in granular materials into locally connected pore bodies by means of a regular weighted Delaunay triangulation, where local pores are represented by the void inside the tetrahedral cells. Stokes flow equations are upscaled at the pore level and calculated using a finite volume scheme. By assuming constant fluid pressure in each pore and using the Darcy form to compute fluid fluxes, the flux q_{ij} between two connected pores i and j is computed as:

$$q_{ij} = g_{ij}\frac{p_i - p_j}{l_{ij}} \tag{II.2}$$

where p_i and p_j are the pressure in pore i and j respectively, g_{ij} is the hydraulic conductance of the throat linking pores i and j, and l_{ij} is the length between the centres of the two connected pores.

To obtain the pressure field within the void space of granular material, the equation of continuity for the fluid is solved within each pore. It means that the rate of volume change for each pore can be calculated by summing up the fluxes through the four facets of the tetrahedral pore element. Considering pore i, the continuity equation is computed as follows:

$$\dot{V}_i^f = \sum_{j=1}^{j=4} q_{ij} \tag{II.3}$$

where $\dot{V}_i^f$ is the volumetric strain rate of the pore i obtained from the particle velocities at the four vertices of the tetrahedron i. Finally, the dragging force applied by the hydraulic flow on each particle with a boundary surface $\partial\Gamma_k$, is calculated in function of pressure p and viscous shear stress τ (note that the gravitational forces are neglected):

$$\vec{F}^k = \int_{\partial\Gamma_k} p\vec{n}ds + \int_{\partial\Gamma_k} \tau\vec{n}ds \tag{II.4}$$

where $\vec{n}$ is the unit normal to the surface $\partial\Gamma_k$.

Then, the complexity of the fluid-solid problem is simplified and can be solved efficiently by the

inversion of sparse matrix algorithms. More details can be found in (Chareyre et al., 2012).

In this study, the granular filters were exposed to a hydraulic charge of 2,000 *kPa* imposed in the same direction as gravity in dry filtration. This high value actually takes into account the effects of the amplification of the particle density but actually corresponds to a hydraulic head of 20 cm. The fluid viscosity was set to 0.001 kg/ms. To isolate the effect of hydrodynamic forces on fine particle movement in fluid filtration processes, gravity was set to zero. In fact, when hydraulic gradients are high and relatively lightweight particles are involved, hydrodynamic forces dominate over gravitational forces, making the latter negligible.

3.3. Cyclic wet filtration

Granular filters can experience variations in flow rates over time in many different applications. For instance, in hydraulic structures like dams and dikes, the water level can periodically rise and fall due to factors such as rainfall or tides. Similarly, in industrial engineering, such as water treatment, the flow of water through a granular filter is not always steady and may stop and start again periodically. Experimental results show that fine particles trapped in unstable sites, like "hydrodynamic" sites can be dislodged and mobilised again when subjected to transient conditions in the porous domain. Such transience can be induced by sharp changes in flow conditions, including complete flow cessation and subsequent relaunch or flow direction reversal. Note that a gradual increase or decrease in flow does not introduce this mobilisation (Ghidaglia et al., 1996).

Herein, the possibility of cyclic conditions that may quantitatively modify the results in terms of retention coefficient was taken into account. Its objective was to consider trapped particles that could be released and subsequently migrate further into the filter and thus characterise the retention capacity of the filtration from a conservative perspective. A cycle was composed of two phases: in the first phase, fluid flow was activated with the appropriate boundary conditions. The filtration test was stopped when all fine particles had reached a state of equilibrium or had totally crossed the sample. The particles that passed the filter entirely were removed, while the particles that were found blocked were kept at their exact blockage site for the next cycle (Figure II.3-a). In the second phase, fluid flow was deactivated and the blocked particles were subjected to a movement in the opposite direction of the flow of the previous cycle. This movement is equal to half of the mean pore diameter (Figure II.3-b) which can be computed based on the equation (II.1). This technique was implemented to regulate the mobilisation phase and ensure an uniform exposure of all fine particles to similar conditions. Indeed, attempting to mobilise the blocked particles through a sharp increase in flow is not effective in numerical simulations, as the PFV method gives the solution to the problem in the established regime. Then, for the next cycle, the flow was reactivated which allowed the launched blocked particles to be re-engaged with streamlines characterised by the highest flux. This model offers blocked particles the opportunity to migrate once again within the filter if enough large sideway constrictions exist in the pore (Figure II.3-c). Cycles were repeated continuously until stabilised filtration results were obtained, indicating that no more fine particles could pass through the filter.

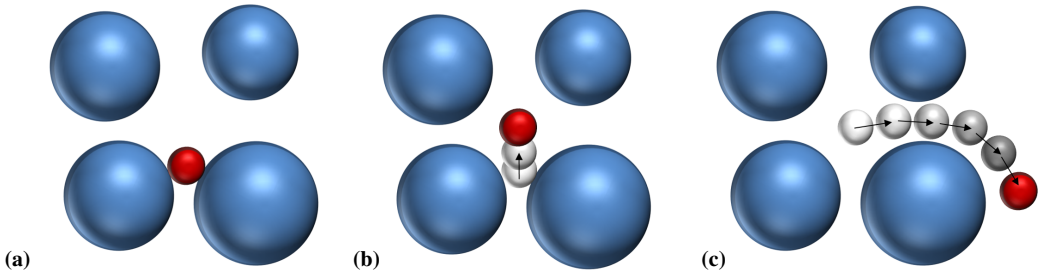

Fig. II.3. Schematic drawing of a trapped fine particle in cycle i being released from the pore in cycle $i+1$: (a) - cycle i, phase 1: trapped particle at the end of the phase, (b) - cycle i, phase 2: relaunching phase, (c) - cycle $i+1$, phase 1: reactivated flow and filtration test.

4. Results and discussion

Since the trajectories of fine particles were tracked throughout the simulations, different filtration characteristics for the filter can be computed, including tortuosity and retention coefficient, among others.

4.1. Tortuosity

Tortuosity is often considered a key property of granular materials describing the geometry of the void space and transport properties. Herein, tortuosity refers to the degree of curviness of the path taken by fine particles as they travel through a filter. Specifically, it is defined as the ratio between the actual path length of the particles within the filter and their vertical straight-depth penetration. The size of fine particles used to explore tortuosity for the three different filter materials was sufficiently small to warrant a 100% success of filter crossing (Table II.3). Results are only given for the case of dry and wet filtration results since the behaviour of fine particles in cyclic wet filtration was found to be similar to that obtained through wet filtration.

Table II.3 gives the average tortuosity computed for filters NG, IG, and WG in both the loosest and densest cases using fine particle sizes of 1 mm, 0.2 mm, and 0.1 mm respectively. Through dry filtration computation, the average tortuosity is about 1.34 irrespective of grading and porosity. In fact, when fine particles encounter a filter particle on their pathway, they are bound to follow the

Table II.3: Average tortuosity for NG, IG WG filters in the loosest and densest state with the dry and wet filtration models.

Material	Size (mm)	Dry	Wet
NG L	1	1.34 ±(0.03)	1.60 ±(0.07)
NG D	1	1.34 ±(0.02)	1.60 ±(0.06)
IG L	0.2	1.34 ±(0.04)	1.61 ±(0.09)
IG D	0.2	1.34 ±(0.03)	1.59 ±(0.07)
WG L	0.1	1.35 ±(0.05)	1.51 ±(0.09)
WG D	0.1	1.34 ±(0.05)	1.48 ±(0.08)

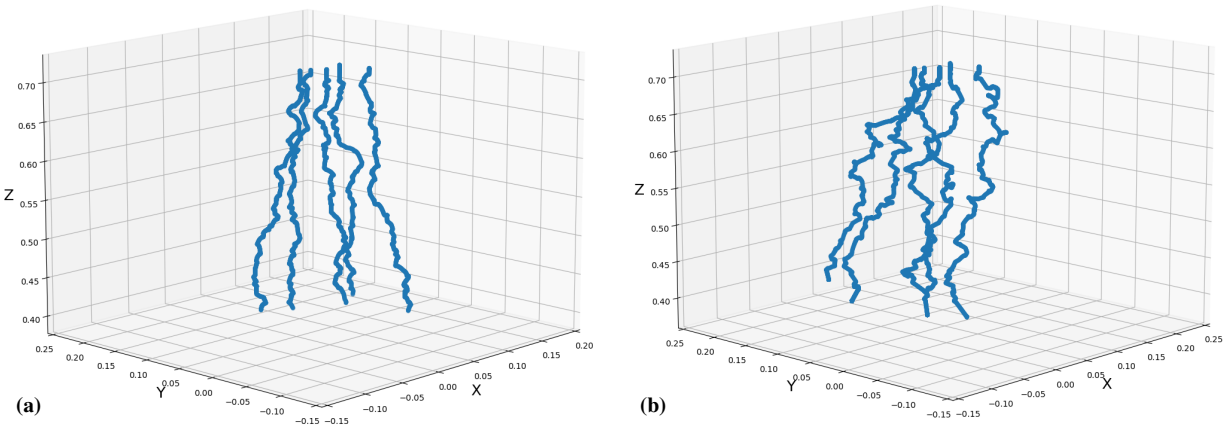

Fig. II.4. Path trajectory of fine particles in the densest state of NG filter: (a)- dry filtration, (b)-wet filtration.

curvature of the filter particle until there is no more contact. Then, they resume falling straight until they encounter another filter particle. Since filters only involve spherical particles, the filter particles hold the same curvature, regardless of the filter grading or porosity, which explains why there is the same average tortuosity for all studied filters.

The results obtained for the wet filtration showed a different feature, revealing a consistently higher average tortuosity compared to the dry filtration model. The values are indeed 10% to 16% larger in this case than in the case of dry filtration. A higher tortuosity indicates that not all particles took direct pathways but explored sideways, increasing their average path length in the filter. It may be attributed to the influence of dragging forces that align fine particles with the direction of maximum fluxes between local pores, inciting them to explore sideways. As a consequence, path lengths are bound to be larger than those found in dry filtration tests. Figure II.4 shows the path trajectory of the fine particles under dry and wet filtration models in the densest state of NG filter. It is clear that in wet filtration, the trajectory of the particles is more tortuous than what can be observed in dry filtration.

The results from wet filtration also indicated that the average tortuosity is greater in IG and NG materials than in WG materials. It may indicate that fine particles explore more sideways in NG and IG materials than in WG materials. Reboul et al. (2010) and Seblany Seblany (2018) showed that the probability density function (PDF) of construction sizes in NG materials is more spread than in well-graded materials. In Figure II.5, this PDF is given for narrowly-graded material and well-graded materials with a coefficient of uniformly equal to 1.7 and 3.9, both in a loose state (Seblany, 2018). The larger difference in constriction sizes within the same pore in NG materials may result in a greater variety of values for the fluxes exiting a pore and thus for the values of dragging forces (Figure II.6 (a-b)). This may induce more opportunities for fines to explore sideways in NG materials when the maximal local flux is in the direction of the sideway (Figure II.6-b). In WG material, the contrast between constriction sizes of a given pore may be smaller, providing fine particles with less chance to deviate from the average direction of the fluid flow (Figure II.6-c).

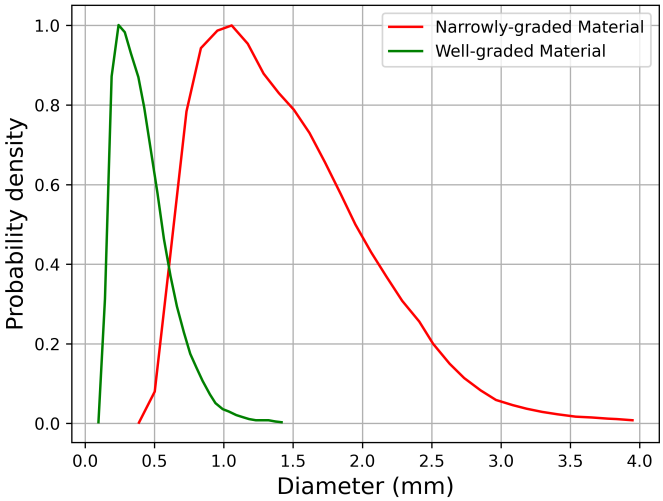

Fig. II.5. Probability density function of constriction sizes for a narrowly-graded and a well-graded material in a loose state (Seblany, 2018).

4.2. Coefficient of retention

The study investigated the retention capacity of different classes of fine particles by six numerical filters using dry, wet, and cyclic wet filtration models. Comparing the wet and dry models, Figure II.7 reveals a difference between the two models irrespective of grading and porosity. It seems that the filter is less efficient at stopping fines in wet filtration than in dry filtration. This difference can be attributed to the reorientation of some fines through constrictions corresponding to a condition of local maximum flux in the wet filtration model. These particles deviate from a direct path using sideways with larger constrictions, which increases the opportunity for them to go ahead in the filter.

However, comparing NG and WG grading, one can note that in the latter case, there is little difference between dry and wet filtration in terms of retention whatever the particle size released in the filter. As mentioned before, in dry filtration, direct paths (parallel to gravity direction) throughout the filter are always favoured by fines. In the case of wet filtration, since WG materials

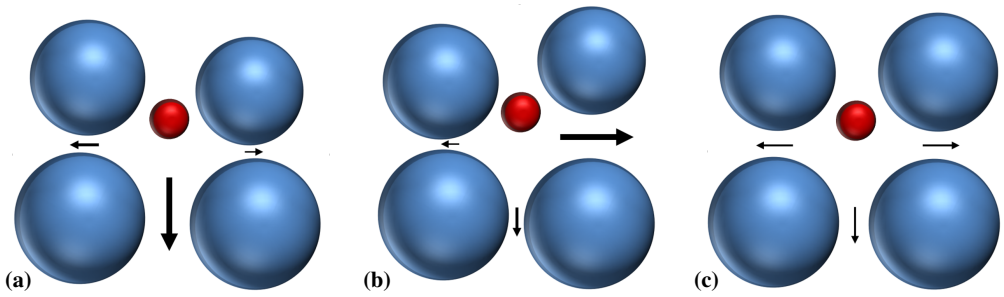

Fig. II.6. Effect of heterogeneity in constriction sizes on the values of local dragging fluxes at pore exits: (a) - constrictions with very different sizes resulting in a high flux parallel to the direction of the flow, (b) - constrictions with very different sizes resulting in a high flux perpendicular to the direction of the flow (c) - constrictions with similar sizes.

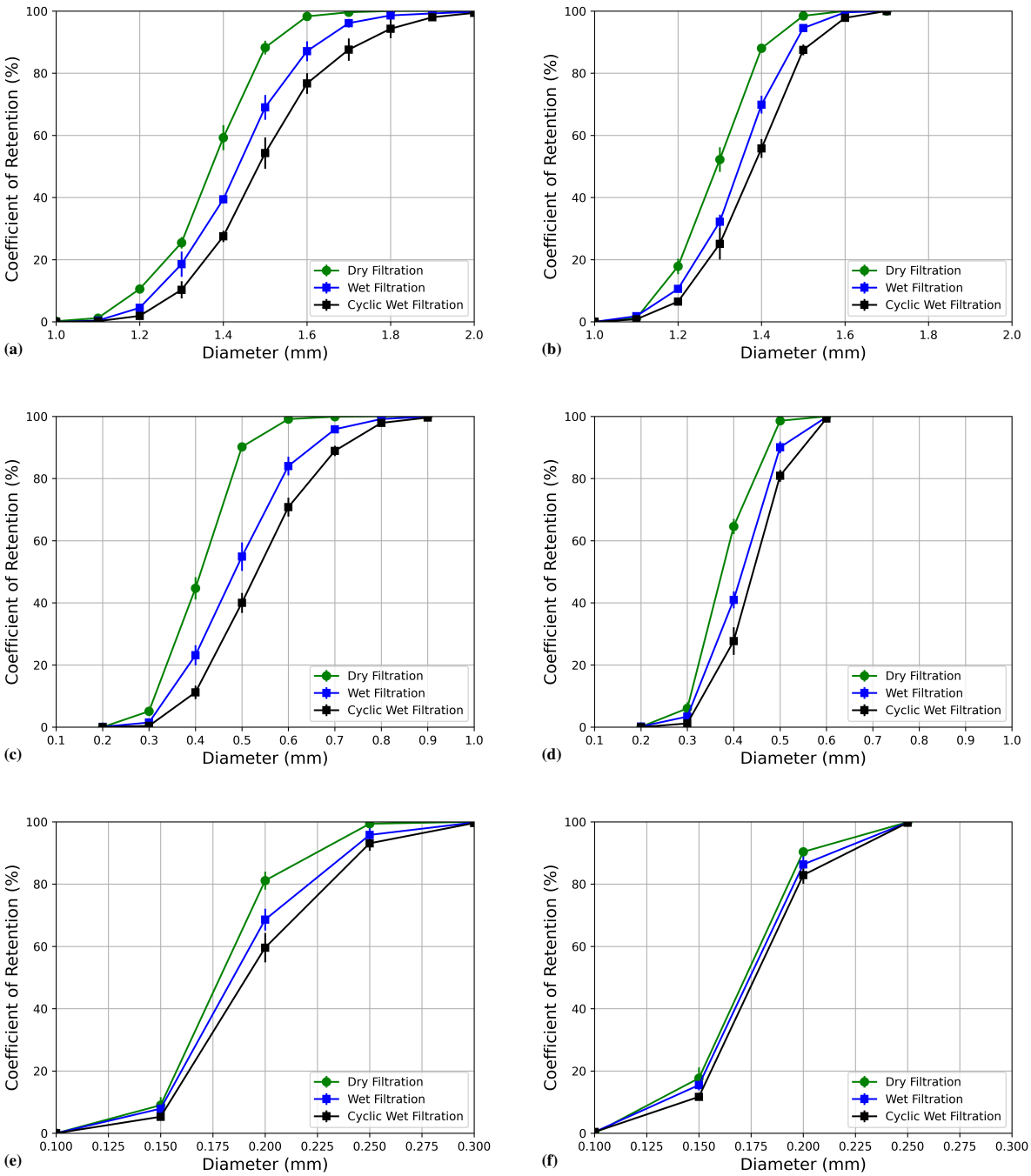

Fig. II.7. Coefficient of retention of fine particles in the filters according to their size and the kind of filtration model: (a-b): NG, (c-d): IG, (e-f): WG at loosest (a-c-e) and densest (b-d-f) states.

hold a pore network that is more uniform than NG materials, there is not a great contrast between the constriction sizes of a given pore and thus the direct path (parallel to the average direction of flow) is also privileged in this case. In the case of NG grading, the contrast is greater and more fines are deviated towards sideways according to the condition of local maximum flux that involves larger constrictions. It results in a greater gap between the results provided by dry and wet filtration.

Porosity also influences the gap between the retention factors found in dry and wet filtrations.

As density increases, the number of constrictions per pore increases, and as a consequence, the void space of the material becomes more connected (Reboul et al., 2008). Then, it is easier for a fine particle of a given size to find a way across the filter with a movement close to the average direction of the fluid flow as in dry filtration. It explains why the difference in the retention factor between dry and wet filtration decreases when density increases.

The study also revealed that, regardless of the porosity, a similar value for the percolation size (i.e., the largest particle size associated with a 100% probability of completely passing through the filter) is observed for the same material type. This characteristic is supposed to also be equal to the minimum constriction size of the filter since fines smaller than its size have a 100% probability of crossing a filter irrespective of its thickness. For the three materials investigated in the study, the theoretical minimum constriction sizes were estimated to be 0.85 mm, 0.19 mm, and 0.1 mm for NG, IG, and WG materials, respectively. These values were found to be in close agreement with the obtained percolation sizes (Table II.3).

However, when attempting to determine the equivalent opening size of the filter that corresponds to the size of fines with a 100% chance of being blocked during filtration tests (other choices can be taken for the percentage associated with the criterion of blockage (Seblany et al., 2021)), the dry filtration model always leads to a smaller value than the wet filtration model, especially for NG and IG materials (Figure II.7(a-d)). One must remind that, in general, the wet filtration model always incites fine particles to select more open pathways than in dry filtration and the filter is envisioned as a less efficient filter. Then, it indicates that relying solely on dry filtration outcomes to design filter criteria may not be conservative, especially when dealing with IG and NG materials. In such cases, the chosen equivalent opening size may underestimate the size of larger fine particles that can entirely cross the filter. However, for WG materials, dry filtration tests may be sufficient to determine the filter opening size (Figure II.7 (e-f)).

The cyclic wet filtration model enabled additional possibilities for fine particles to go ahead in the filter, in the range of explored fine sizes (Figure II.7 (a-f)). In fact, some particles that were initially blocked at a constriction site in the wet filtration model seemed to have been relaunched into the filter and were bound to explore sideways in the case of the cyclic wet filtration model.

It seems that the existence of sideways paths associated with a local maximum flux (compared to other exits) does not always guarantee the migration of fine particles through the associated constriction. In reality, fine particles have an initial velocity and a dragging force acquired from their past trajectory when they enter a pore. If the value of the local dragging force at stake in a pore towards sideways is insufficiently high, the fine particle may be incited to choose the direct path with a constriction size smaller than its size instead, leading to its blockage. In cyclic wet filtration, fine particles are propelled towards the centre of the pore and subsequently follow the path of the highest dragging force from an initial zero velocity state. It enables fine particles to explore sideways more efficiently and to potentially follow a different path than in a previous cycle.

Regarding the difference in filtration mechanisms depending on porosity, our simulations demonstrate that cyclic filtration is more effective in releasing fine particles for loose filters compared to dense ones. This aspect is consistent with what was previously mentioned: a less-connected void space in loose material results in fewer pore exits, which limits the opportunities for particles to exit. Cyclic filtration provides these particles with more opportunities to exit pores by exploring sideways. In contrast, dense filters have more exits per pore, providing fine particles

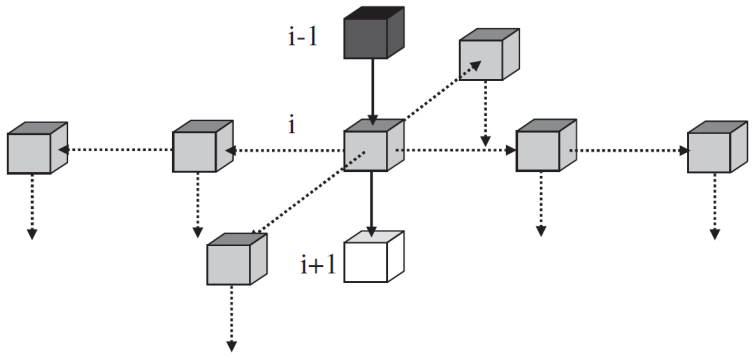

Fig. II.8. Cubic pore-network model (Schuler, 1996).

with greater opportunities to leave a pore through wet filtration. Therefore, cyclic wet filtration provides limited additional benefits for dense filters compared to loose filters.

5. Equivalent cyclic wet filtration

5.1. Framework

Dry filtration tests have emerged as a cost-effective alternative to computationally expensive wet filtration models for studying the migration of fines in granular filters. However, our analysis revealed that the underlying physical phenomena involved in the simulations are very different in nature. For example, in dry filtration tests, the movement of fine particles in a filter is mainly driven by gravity forces. As a consequence, their trajectory is mainly parallel to the gravity direction. Fine particles are always bound to choose a direct path to exit a pore which tends to reduce their chance of finding an exit larger than their size. In a wet filtration test (PFV method), the condition of local maximal fluxes related to the existence of larger constrictions connecting adjacent pores seems to incite fine particles to also explore sideways to exit a pore. Then, in this case, more chances are given to fine particles to go ahead in the filter.

This study introduces a novel filtration model, called the equivalent cyclic wet filtration model (which is, in fact, an enhanced dry filtration), which overcomes the limitations of existing numerical dry filtration models. This model combines the advantages of both wet and dry filtration models by allowing fine particles in a dry filtration test to explore sideways.

More precisely, the proposed model is based on some features associated with the pore network model originally proposed by Schuler (1996). In this model, the pore space is envisioned as a regular network of void cubes, where each pore body is connected to others by constrictions on each face (Figure II.8). When a fine particle enters a pore, it can exit the pore along a unidirectional path (direct path) or sideways (towards lateral pores on the same layer) through one of four possible exits. Building upon this framework, the proposed dry filtration model incorporates a combination of both gravity force and imposed sideway movements to enable fine particles to explore sideways as a possible successful exit.

To simplify the model, the constrictions are assumed to be centred on the cube face. Then, on

average, a fine particle located at the centre of a pore can reach a sideway if it crosses a distance equal to half the average pore diameter. This assumption will be used hereafter to define the average sideway movements that are imposed on trapped fine particles. The computation of the average pore diameter for a filter composed of spherical material is based on the equation II.1.

The proposed methodology for the filtration test is decomposed into cycles. Each cycle has two different phases. Throughout the first phase, fine particles are gradually released under gravity until a steady state is obtained for their position (either passing through the filter or becoming trapped inside it). The penetration depth of each fine particle in the filter at the end of this first phase is computed. In the second phase, gravity is set to zero, and a movement towards sideways equal to half of the mean pore diameter is imposed on trapped fine particles with a random orientation. This movement is enforced by setting gravity in a random direction perpendicular to the natural one for a defined period of time to potentially allow blocked fine particles to move a distance equal to half of the mean pore diameter. At the end of the imposed movement, gravity's direction is set again to its natural direction, and the velocity of the fine particles is set to zero. Figure II.9 shows a sketch of a trapped fine particle being released after the imposed sideway movement.

In the next cycle, initially trapped particles that successfully exited a pore through a sideway migrate again ahead in the filter until further blockage occurs and a new steady state for the positions of all fine particles is obtained. These cycles are repeated until a stop criterion is achieved, which is defined based on the difference between the penetration depth of each blocked particle throughout two consecutive cycles. When this difference is less than half of the mean pore diameter for each blocked particle, the simulation is stopped. It means that no fine particle is able to leave the pore they have been trapped in.

5.2. Validation

The proposed model was designed to address the high computation time associated with wet filtration computation in the context of the filtration of fine particles by granular filters. The new model involved a combination of cycles of dry filtration where sideway imposed movements were applied to fines to give them the opportunity to explore sideways. The number of cycles required to reach the stop criterion in cyclic filtration was not significantly influenced by the grading or porosity of the filter material. Instead, the primary factor affecting the number of cycles was the number of fine particles initially blocked in the filter. The maximum number of cycles observed

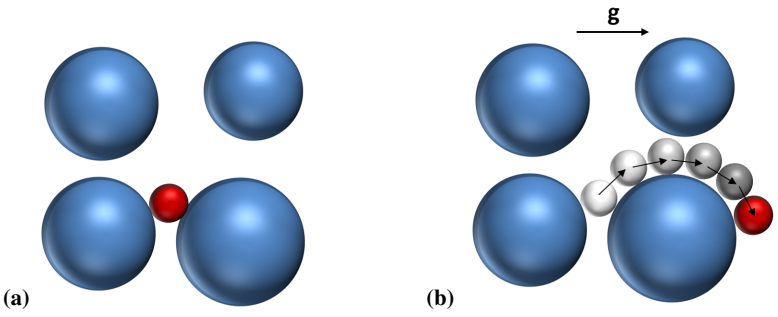

Fig. II.9. Schematic drawing of a trapped fine particle being released by the imposed sideway movement in the equivalent cyclic wet filtration model: (a) - blocked particle, (b) - imposed sideway movement.

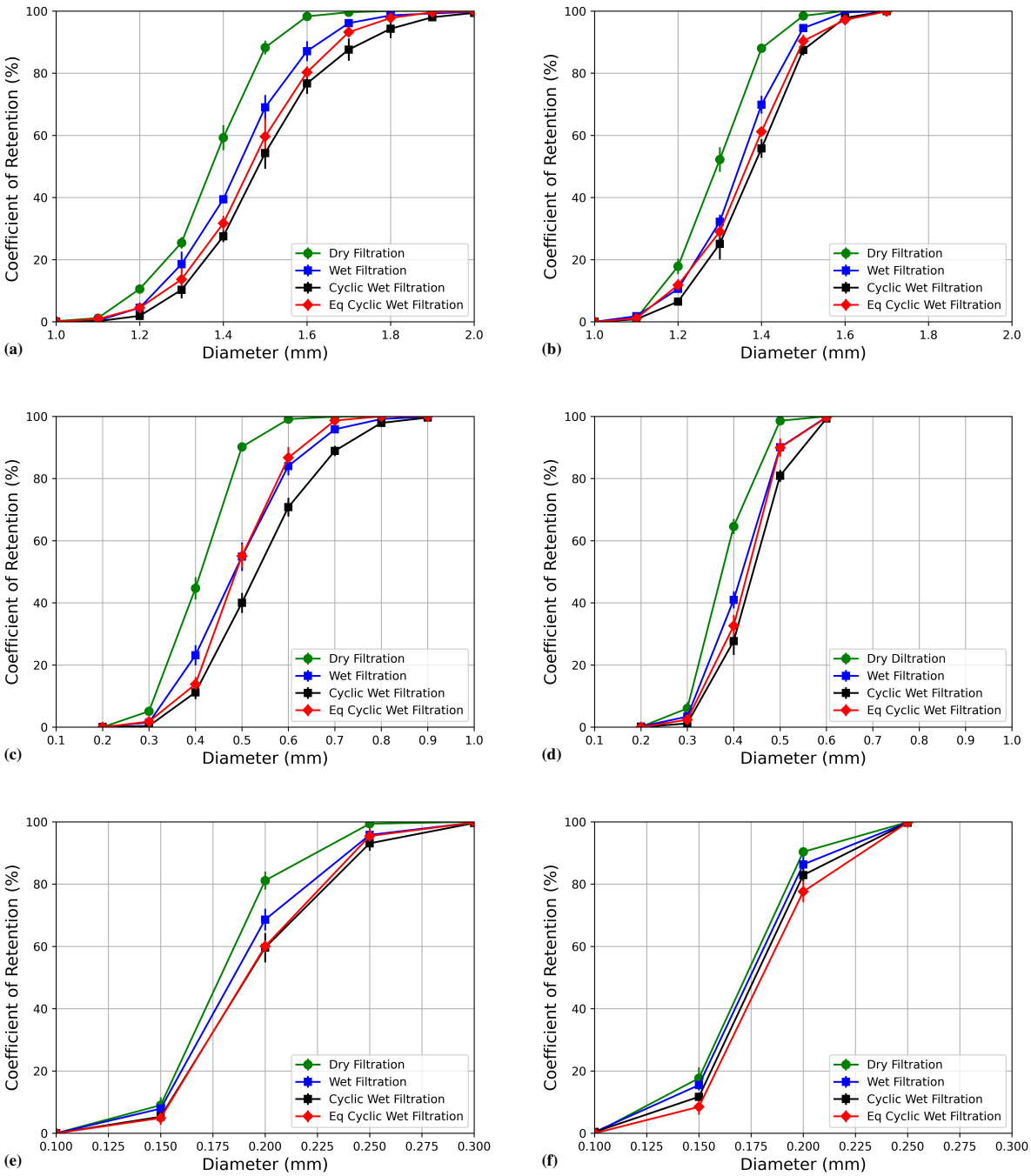

Fig. II.10. Coefficient of retention of fine particles against their size in the filtration tests under different models: (a-b): NG, (c-d): IG, (e-f): WG at loosest (a-c-e) and densest (b-d-f) states.

in our study was found equal to about 30 cycles, which was observed for the class of fine particle diameters that were slightly smaller than the equivalent opening size of the filter.

Figure II.10 (a-f) illustrates a comparison of the results obtained using the new model with those obtained using previous models. It is noteworthy that the retention curve achieved by the new model closely approximates that of wet or cyclic wet filtration. However, there are occasional fluctuations in the new results, which at times align more closely with either wet filtration or cyclic wet filtration. Considering the cyclic nature of the computation and the model's attempts

to explore sideways, one would expect the results to exhibit greater consistency with cyclic wet filtration.

In fact, the equivalent cyclic wet filtration model has limitations as it only considers a few aspects of fluid flow through granular materials and the interaction between fluid and flowing particles. The filtration mechanism depends mainly on the value of the imposed lateral movement on the fine particles. Indeed, some fine particles are trapped in pores with a diameter larger than the imposed lateral movement, thus they will not be able to exit through the sideway. However, imposing high lateral movement may cause fine particles to exit the pore through a lateral exit and continue migrating laterally, which is unrealistic. To address this issue, we correlated the value of the imposed lateral movement with a physical parameter that has a tangible meaning such as the average pore diameter. It's important to note that the empirical equation (II.1) used to estimate the average pore diameter is based on a probabilistic approach, which can result in either an overestimation or an underestimation of the actual value. As a result, this may account for the fluctuation in results observed between wet and cyclic wet filtration curves.

The equivalent cyclic wet filtration model holds definitive advantages for quantifying the retention characteristics of a granular filter. First, it successfully retrieved the equivalent filter sieve opening size, which is a crucial property of the material for the design of a filter. Secondly, it allows faster computations than wet filtration in spite of the involved cycles, taking five to fifteen times less time. It is even more efficient when compared to the cyclic wet filtration model. For instance, in the case of WG sample, an equivalent cyclic wet filtration test can complete a filtration test in 12 hours, while a wet (non-cyclic) filtration test takes 103 hours. Compared to the PFV model, which is a simplified tool and faster than traditional CFD models for simulating wet filtration, the proposed model offers greater flexibility as it can be applied to any particle shape as long as the average pore diameter of the granular filter is known.

6. Conclusion

Researchers have extensively used the discrete element method to explore and quantify the filtration mechanisms in granular filters. Two common approaches are generally chosen to model filtration tests including wet filtration models that couple DEM with fluid dynamic models and dry filtration models that apply gravity as the driving force for the movement of suspended particles. The latter approach is preferred because it circumvents the complexity associated with dynamic fluid models and has a favourable computation time. This paper aims to present a comprehensive numerical analysis that quantitatively compares these two approaches by conducting filtration tests on six distinct numerical filters involving various materials and porosities.

The filtration tests conducted using both wet and dry filtration models demonstrated that the former was associated with a higher tortuosity and a lower coefficient of retention of fine particles, compared to the latter. It was mainly due to the existence of dragging forces that aligned the fine particles with the direction of maximum fluxes between local pores, causing them to explore sideways alongside direct paths. This possibility is not given by the dry filtration model, where only pathways close to the gravity direction can be explored. Herein, different features were obtained according to the grading and porosity of the filters. For narrowly-graded materials, the larger heterogeneities in terms of constriction sizes created more opportunities for fines to explore sideways in the wet filtration model, leading to a higher difference in tortuosity and coefficient of retention

compared to dry filtration. On the other hand, for dense materials, the high connectivity of the pore space allowed the fine particles to have equal chances of exiting the pores from all directions, resulting in reduced differences between the wet and dry filtration models in terms of coefficient of retention.

Regarding the efficiency of the filter in completely trapping a specific size of fine particles, the dry filtration model led to a smaller value for the equivalent opening size of the filter compared to the wet filtration model. The findings suggest that using only dry filtration results to establish filter criteria where this geometrical characteristic holds a key role may not be conservative, especially when dealing with narrowly-graded materials. However, for well-graded materials, conducting dry filtration tests alone could be adequate for determining the filter opening size.

Additionally, this investigation included cyclic wet filtration tests to examine how perturbations in the hydraulic head affect the stability of trapped particles in the filter. The simulations revealed that cycles allowed the initially trapped fine particles to migrate more through the filter. It means that in the wet filtration model, fines did not necessarily choose the larger constrictions in an attempt to exit a pore. It demonstrated that in the PFV model, there may exist a competition between the effects of the conditions of local maximum fluxes and the velocity vector of fine particles entering a pore on their dynamic movements. It may either lead fine particles to favour a direct path but with a constriction smaller than their size or to choose a sideway path.

Overall, this study provided valuable insights into the filtration mechanism in granular filters by comparing the wet and dry filtration models and investigating the effects of grading, porosity, and the perturbation of the hydraulic head effects on particle retention. The results highlighted the importance of dragging forces in wet filtration tests, especially when dealing with narrowly-graded materials but also granular filters in a loose state.

Finally, this study presented an enhanced dry filtration model called the "equivalent cyclic wet filtration model" that addresses the limitations of dry filtration tests as a model for wet (cyclic) filtration tests. This model, which allowed sideways exploration, successfully retrieved the value for the equivalent filter opening size. Furthermore, the equivalent cyclic wet filtration model allowed significant gains in computation time. Highly flexible, it can be used irrespective of the involved particle shapes as long as the average pore diameter of the granular filter can be estimated.

Chapter III

Effect of Particle Shape on the Void Space in Granular Materials: Implications for the Properties of Granular Filters

Authored by: Ali Abdallah[1], Eric Vincens[1], Hélène Magoariec[1], Mohsen Ardabilian[2] and Christophe Picault[3]

[1]. Univ Lyon, Ecole Centrale de Lyon, CNRS, ENTPE, LTDS, UMR5513, 36 Avenue Guy de Collongue, 69134 Ecully, France

[2]. Univ Lyon, Ecole Centrale de Lyon, CNRS, LIRIS UMR 5205,36 Avenue Guy de Collongue, Ecully,69134,France

3. CACOH, Compagnie Nationale du Rhône, 4 Rue de Chalon-sur-Saône, 69007 Lyon, France

This chapter is based on a manuscript that will be submitted to: *Granular Matter*

Acknowledgments: Part of this work belongs to a project funded by Compagnie Nationale du Rhone. The authors acknowledge the support of CNR for this study. Additionally, special thanks go to Edgar for invaluable contributions to the Pn-extract algorithmic code.

Abstract

This study investigates the influence of particle shape on the pore space morphology and topology in granular materials. Numerical samples with spherical and rounded non-spherical particle shapes were generated using the Discrete Element Method. A segmentation algorithm was used to extract the pore space characteristics. The results revealed that particle shape significantly affect both constriction and pore sizes, with distinctive features according to flatness index or elongation ratio, the former being more significant than the latter. Simulations of filtration tests were performed and confirmed the findings obtained from the pore space extraction. The study revealed the importance of considering particle shape in the design of granular filters, emphasising its significant impact on pore space characteristics and filtration performance.

Main results

- Particle shape significantly influenced constriction size characteristics. Flat particles generally had smaller constrictions and narrower distributions, while spherical particles had larger constrictions and a broader range. Elongated particles displayed even larger constriction sizes and the widest distributions.
- Partially rounded and spherical particles shared a very similar constriction size distribution, which indicated that the filter criteria designed for spherical particles were applicable for partially rounded particles.
- The characteristics identified for constriction sizes mirrored those of pore sizes. The samples with flat particles demonstrated the highest average number of constrictions per pore, whereas the sample with elongated particles presented the lowest value.
- Simulations of filtration tests confirmed the findings of the pore space extraction method. Filters with flat particles had the highest blockage rate for certain fines, while those with elongated particles had the lowest blockage.

1. Introduction

Granular materials have emerged as a highly effective solution for filtering and separating fine particles during seepage transport (Terzaghi et al., 1996). The movement and blockage of fine particles circulating within hydraulic fluids are profoundly influenced by the morphology and topology of the filter pore space (Khilar and Fogler, 1998). Pore space within granular materials comprises voids with intricate geometries located between grains and can typically be classified into two primary categories: pores, denoting the larger voids existing between particles, and constrictions, representing the narrowest throats or channels that interconnect neighbouring pores. The trajectory and circulation of fine hard particles, as well as the flow streamlines within the porous medium, are predominantly governed by the connectivity of pores and the dimensions of the constrictions encountered along their paths (Reboul et al., 2008). A well-connected pore network facilitates the existence of multiple pathways for suspended fine hard particles carried by the flow, while the blockage of these particles is primarily contingent upon the geometric restriction associated with constriction sizes. If the dimensions of the suspended fine hard particles exceed those of the constrictions, the particles become trapped in the filter.

Hence, the constriction size distribution (CSD), which holds a tangible physical significance, is recognised as a crucial parameter for quantifying the retention capacity of granular filters (Kenney et al., 1985). Kenney introduced the notion of controlling constriction size as a geometric characteristic of the void network within granular filters, which establishes the maximum particle size capable of passing through the filter. This finding served as a basis for a novel filter criterion framework designed on the distribution of constriction sizes in a granular filter (Indraratna et al., 2007; Seblany et al., 2021). However, due to the complexity of accurately determining the actual sizes of constrictions within a filter, their determination is generally constructed upon a probabilistic approach based on the knowledge of the particle size distribution (PSD) and on the density of the filter material (Silveira et al., 1975; Locke et al., 2001; Reboul et al., 2010). Such CSD-based approaches hold certain limitations, including the statement of spherical shape for the filter particles, which simplifies the analytical and numerical calculations of constrictions and pore sizes.

The assumption of spheres as a model for actual material has long been considered relevant for deriving the key features observed in actual granular packings. While this approach has provided valuable insights, it has overlooked an important factor, including the influence of particle shape, on the characteristics of the void space. This gap is all the more critical as the shape of particles used for processing granular filters is contingent upon the kind of material available on site. Rounded particles are commonly found along rivers and sea sites, while particles derived from large crushed rocks in quarries tend to exhibit a more angular shape. Numerous studies have demonstrated that the particle shape exerts a direct influence on the complexity of pore morphology, thereby impacting various phenomena, including hydraulic conductivity (Ren and Santamarina, 2018; Zheng et al., 2021; Nguyen and Indraratna, 2020), fluid-particle interactions (Torskaya et al., 2014; Rong et al., 2015; Zhao and O'Sullivan, 2022), and tortuosity (Espinoza-Andaluz et al., 2020). However, when considering the influence of particle shape on the size of constrictions, which governs the retention capability of a filter, several studies have been carried out but did not comprehensively cover all shape-related characteristics (Trussell et al., 1980; Suthaker et al., 1995; Evans et al., 2002; Barton and Buchberger, 2007; Wu et al., 2012; Li et al., 2021b).

The shape of a particle can be quantified by different features depending on the chosen scale.

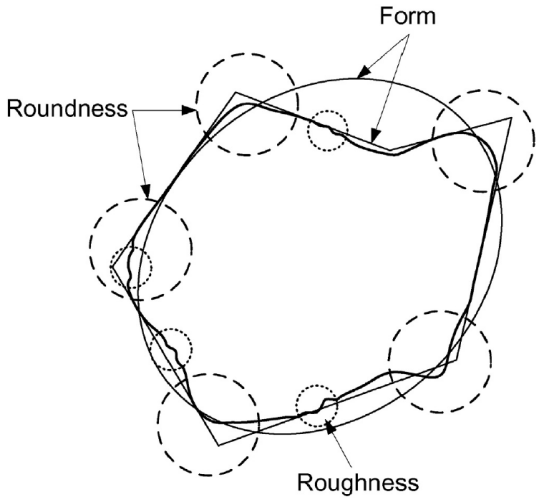

Fig. III.1. Particle shape across three different scales Zhao and Wang (2016).

In the literature, there are several classification systems for particle morphology, which can be summarised primarily by three parameters: form, angularity (or roundness), and roughness at macro, meso, and micro scales, respectively as shown in Figure III.1.

For a given porosity, particle form and angularity can directly influence the shape and size of constrictions and pores. Numerous studies have demonstrated that angular materials exhibit greater effectiveness in blocking fine particles compared to rounded particles (Trussell et al., 1980; Suthaker et al., 1995; Evans et al., 2002; Barton and Buchberger, 2007). However, the influence of particle form, represented by elongation and flatness ratios, remains poorly understood. Li et al. (2021b) conducted numerical simulations using elliptical particles with varying aspect ratios, defined as the ratio between the major and minor half-lengths of the geometric elongation axes, to investigate the effect of particle form on the pore space. However, the numerical samples used in these simulations did not possess the same porosity, making it challenging to quantitatively analyse the direct impact of particle form on the void space and, in particular, on constriction sizes.

This study aims to build upon previous investigations and by introducing non-spherical rounded particle shapes with well-defined forms, to conduct a comprehensive analysis of the influence of particle form on the pore space, particularly the size of constrictions, and its impact on the filtration mechanisms at stake in granular filters. The discrete element method (DEM) is used to generate several numerical samples with consistent grading and porosity but with particles having different aspect ratios (elongation and flatness ratios). Subsequently, a pore space extraction is processed, including constrictions and pores, from these numerical samples to quantify these quantities. Additionally, filtration tests are conducted on these numerical samples to evaluate the correlation between the observed constriction sizes and the obtained retention coefficient for the granular filter. This study aims to provide direct evidence of the effect of particle form on the pore space and, consequently, on the filtration properties of granular filters.

2. Numerical samples

2.1. Materials

Particles that are found in nature and used in various industries, such as sand or pebbles, exhibit significant variations in their sizes and shapes. To fully comprehend the effects of such complex shapes, it is crucial to accurately characterise the properties associated with particle shape. However, quantifying these parameters is not a straightforward task and often requires advanced techniques for measurement. From an engineering standpoint, engineers often employ simpler methods to determine the particle's shape. A commonly used approach involves measuring the three principal axes of the particle to identify its overall form, which can range from elongated to flat or rounded. Additionally, for assessing angularity or roundness, engineers can use visual charts, such as Krumbein's chart (Krumbein, 1941), which offers a convenient means for an average estimate (Figure III.2). These charts enable a qualitative assessment of particle angularity by comparing them to reference images.

The fundamental approach in physics involves simplifying complex systems to their core elements, often employing toy models that retain essential features to demonstrate the desired effects (Schaller, 2017). Accordingly, in this work, ellipsoids have been selected as a preferred shape due to their systematic nature, offering a comprehensive pathway to explore the influence of particle form on pore space morphology. By adjusting the aspect ratio, particle shape can continuously vary from highly flat to highly elongated.

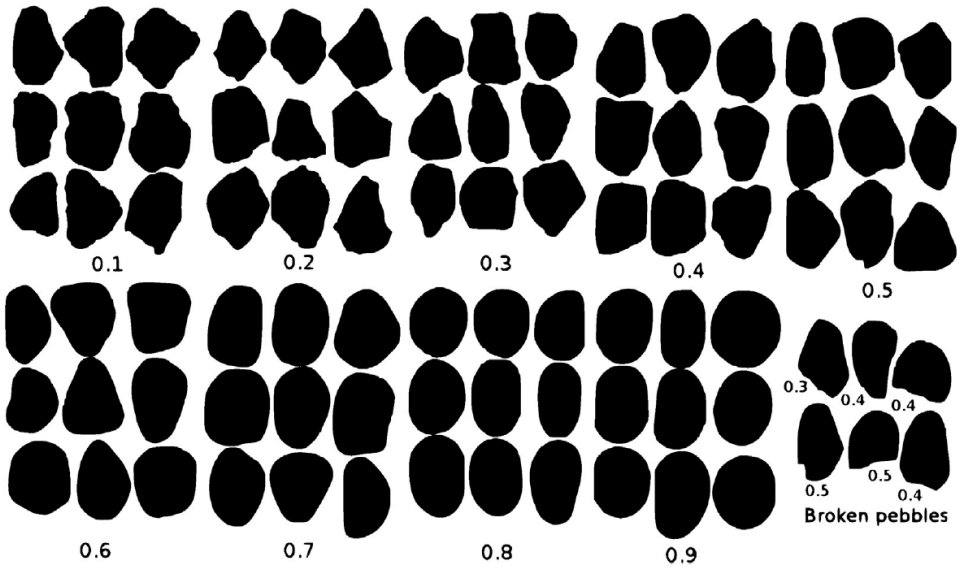

Fig. III.2. Visual angularity assessment using Krumbein's chart (Krumbein, 1941).

The Elongation Index (*EI*) and Flatness Index (*FI*) are defined as follows:

$$EI = \frac{L_1}{L_2} \qquad FI = \frac{L_3}{L_2} \tag{III.1}$$

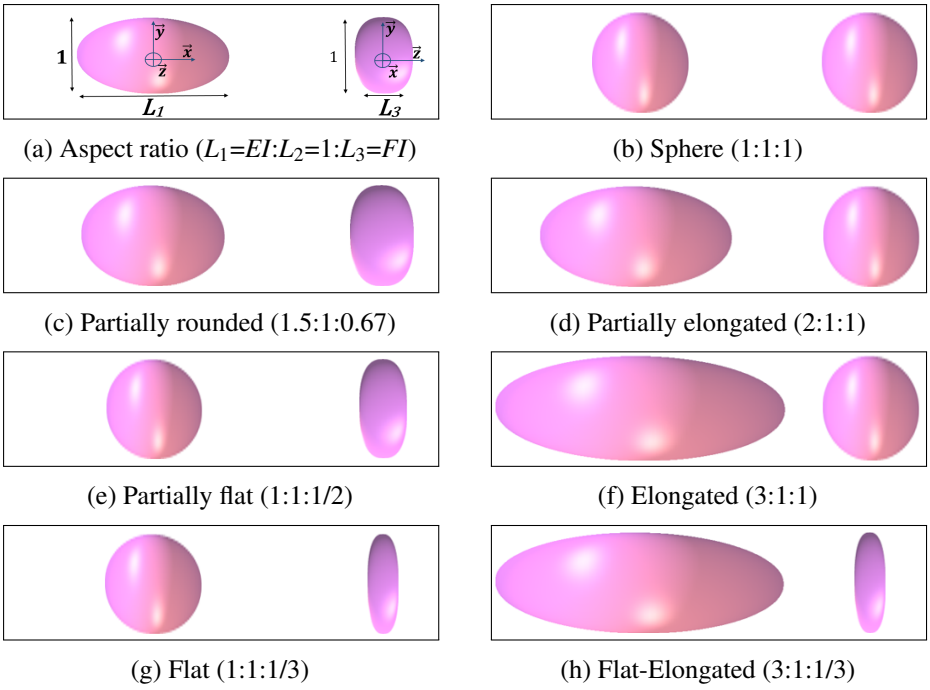

(a) Aspect ratio (L_1=*EI*:L_2=1:L_3=*FI*)

(b) Sphere (1:1:1)

(c) Partially rounded (1.5:1:0.67)

(d) Partially elongated (2:1:1)

(e) Partially flat (1:1:1/2)

(f) Elongated (3:1:1)

(g) Flat (1:1:1/3)

(h) Flat-Elongated (3:1:1/3)

Fig. III.3. Different aspect ratios for filter particles.

where L_1, L_2, and L_3 are the lengths of the maximum, intermediate and minimum principal axes of the ellipsoid.

Elongated particles are defined as those with an elongation index (*EI*) greater than 1.8, while flat particles are characterised by a flatness index (*FI*) less than 0.6 (Kwan et al., 1999). To investigate the influence of particle shape, seven ellipsoids with varying aspect ratios (L_1=*EI*:L_2=1:L_3=*FI*) were modelled (Fig. III.3). The shapes considered in this study included flat, partially flat, partially rounded, spherical, partially elongated, elongated, and flat-elongated particles (Tab. III.1). The selection of these aspect ratios was deliberate in order to specifically examine the isolated effects of each shape category as well as the combined influence of all three categories to determine which category holds greater dominance.

An intermediate-graded material with a coefficient of uniformity of 2.2 was implemented for all the samples. The intermediate diameter *L*2 was considered equal to the particle size (Fig. III.4), since theoretically, *L*2 controls if the particle can pass a sieve with an opening of *L*2 or more. *L*1 and *L*3 were calculated according to the aspect ratios defined for each particle shape.

2.2. Generation of samples

In this study, a series of numerical samples were prepared using SudoDEM, an open-source discrete element software developed by Zhao and Zhao (2021), which is based on the open-source code Yade (Šmilauer et al., 2010). The generated samples involved ellipsoid particles with seven different aspect ratios, as outlined in Tab. III.1.

Interaction between particles is governed by a linear elastic law involving two parameters: normal stiffness (k_n), and tangential stiffness (k_t), while the incremental tangential force is limited by a

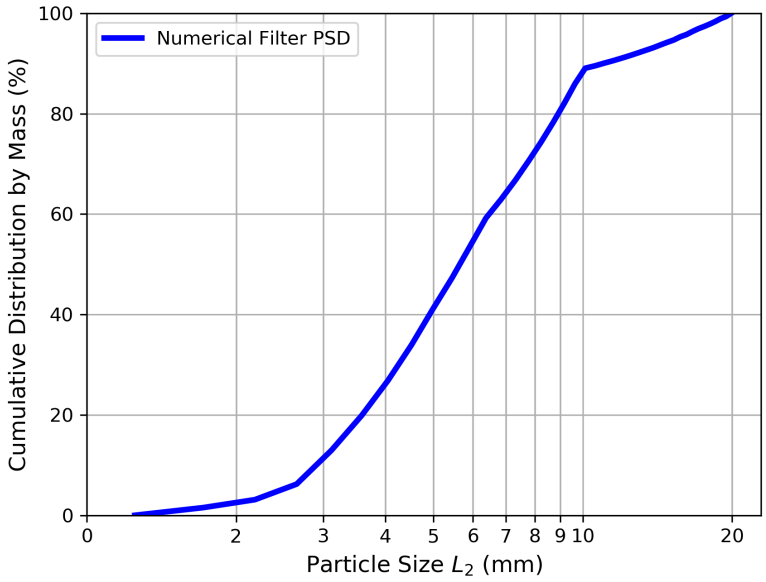

Fig. III.4. Particle size distribution of the material.

Coulomb law, which requires the definition of the Coulomb inter-friction coefficient φ_c. To maintain the integrity of the void space and prevent significant particles overlap, k_n and k_t were set to a high value of 5.65 x 10^5 N/m without excessively penalising computation time. Furthermore, the particles were characterised by a specific weight of 2,650 kg/m^3, and a local damping coefficient of 0.7 was introduced to dissipate non-frictional energy and minimise particle bouncing during the preparation phase, as outlined by Cundall and Strack (1979).

The particles were deposited into a box with rigid walls using the gravity deposition method, mimicking the installation procedure used in lab scenarios. A cubic box with a width size of $6D_{100}$ (D_{100} represents the maximum intermediate diameter L_2 of particles in the sample) was chosen to ensure generating numerical samples greater than the Representative Elementary Volume (REV).

The range of void ratios that can be achieved for each sample is influenced by the shape of the particles they are composed of (Maroof et al., 2022). Consequently, a relatively high value of porosity equal to 0.41 was selected to ensure that all samples could reach it in any case. During the preparation phase, this porosity was achieved by adjusting the inter-friction coefficient between

Table III.1: Particle shape's aspect ratios.

Shape of particles	Aspect ratio (L_1=EI:L_2=1:L_3=FI)
Flat	1:1:1/3
Partially flat	1:1:1/2
Partially rounded	1.5:1:0.67
Spherical	1:1:1
Partially elongated	2:1:1
Elongated	3:1:1
Flat-Elongated	3:1:1/3

the particles.

This adjustment was carried out under the condition of reaching a sufficiently low average unbalanced force ratio. This ratio is defined as the ratio between the sum of overall forces acting on particles and the average force magnitude on interactions. A threshold for the average unbalanced force ratio of 0.05 was chosen to ensure that a state close to equilibrium is reached for the samples (Reboul et al., 2008; Seblany et al., 2021).

3. Extraction of the pore space

Several methods have been developed to extract the pore space in granular materials. Vincens et al. (2015) and Taylor et al. (2015) have listed the different approaches for determining the distribution of constriction sizes, including laboratory testing, analytical, numerical triangulation-based methods, and image-based methods.

Experimental approaches often encounter limitations when attempting to extract and quantify the pore space in granular materials. For example, the replica technique involves filling the void space of granular material with a highly elastic liquid (Witt, 1986, 1993). Once the liquid is hardened, the particles from the granular materials are gradually removed, and the pore space is conserved. While this technique effectively represents the void space, its use is mainly restricted to coarse materials. Another laboratory test, known as the base suspension method, was proposed by Soria et al. (1993) and later refined by Sjah and Vincens (2013). This method involves conducting filtration tests on granular filters where fine particles of different sizes are infiltrated into the filter. The size of the largest particle able to completely cross a filter of a given thickness is determined. Different filters with different thicknesses are required to build the underlying CSD. Then, the CSD is obtained at the expense of a heavy and somehow time-consuming process.

Analytical methods such as those proposed by Silveira et al. (1975), Locke et al. (2001) and Reboul et al. (2010) are typically efficient tools to extract the constriction size for uniformly graded soils consisting primarily of spherical particles. However, these methods do not apply to non-spherical shapes since there are no simple mathematical equations available to describe the dual volume of the solid part.

Numerical triangulation-based approaches are based on extracting the pore space of numerical samples with spherical shapes generated using DEM. An effective algorithm for extracting the void space is derived from the weighted Delaunay tessellation (Reboul et al., 2008). This method involves partitioning the pore space into tetrahedrons, where each vertex of the tetrahedron corresponds to the centre of a particle. Pores are mainly located at the centre of these tetrahedrons, while constrictions are found on each face of them (Bryant and Blunt, 1992). However, this tessellation method is limited to spherical shapes, as a defined centre and radius are necessary to construct the tessellation. O'Sullivan et al. (2015) also introduced an algorithm for constriction size determination through numerical triangulation. The method is based on particle-particle contact points to establish a triangular tessellation, where constrictions are identified as enclosed loops containing 3 or 4 contacts. This approach avoids subjective merging, yielding consistent outcomes. Nonetheless, its applicability is also constrained to spherical particle shapes and is not directly adaptable to materials with irregular shapes.

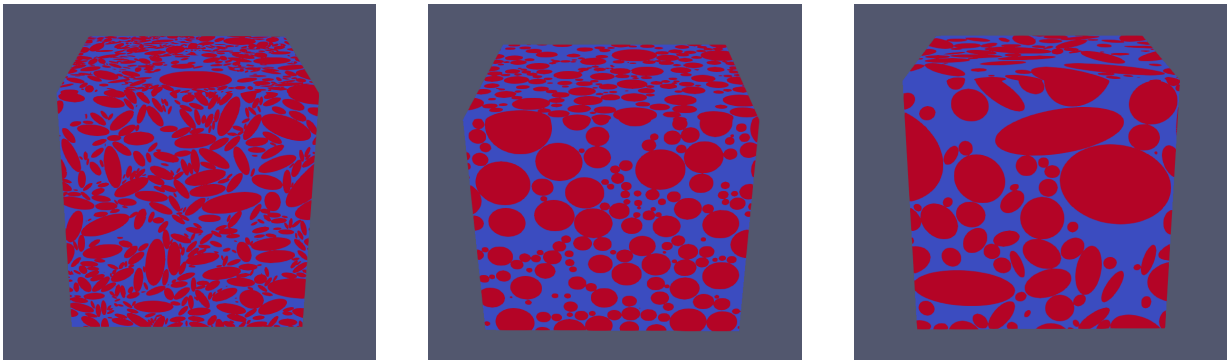

(a) Flat particles. (b) Spherical particles. (c) Elongated particles.

Fig. III.5. 3D binary images for samples constructed from flat, spherical, and elongated particles; Red color is associated to the solid part and blue color to the void space.

The image-based methods seem to be more suitable for analysing complex, irregular shapes. From a 3D voxelized image obtained either from x-ray tomography of granular materials or from generated numerical samples, the pore space is extracted directly by some developed algorithm. A Voronoi computation that is based on the Euclidean distance to the solid can be used where pore centres and constrictions are determined as extrema along the medial path (Yang et al., 2002; Lindow et al., 2011; Homberg et al., 2012). However, merging criteria must be used to damp out excessive segmentation of the pore space (Seblany et al., 2018a). The maximal ball method is another approach initially introduced by Silin and Patzek (2006) and later developed by Dong and Blunt (2009). It shares common features with the previously mentioned segmentation procedure. This method effectively distinguishes the void space from the solid matrix in 3D voxelized images. The fundamental principle of the maximal ball method involves identifying the largest inscribed void spheres within the void space. A pore is defined as the maximum sphere that does not have any neighbouring maximum spheres (from both sides) with a greater radius, while constrictions are identified as the smallest maximum spheres that lie between two neighbouring pores.

An image-based method using the maximal ball approach is used in this work to extract the void space. The numerical samples that have been previously prepared are discretized into 3D binary images. These binary images are composed of voxels, where each of them is assigned a value of either 1 or 0 to represent the solid space (particles) or the void space, respectively. This discretization process is carried out using MATLAB code. Figure III.5 shows an example of 3D binary images with a resolution of 2400x2400x2400 for samples constructed from flat, sphere, and elongated particles.

3.1. Pn-extract tool

In this study, an image-based method called Pn-extract algorithm developed by Raeini et al. (2017) is adopted, which is based on the maximal ball method proposed by Dong and Blunt (2009). By leveraging the hierarchical arrangement of maximal balls identified along the resulting medial axis, the algorithm effectively captures the intricate void space between non-spherical particles, encompassing both pores and constrictions. The proposed methodology is outlined as follows: First, a distance map is computed for each voxel within the void region, where the distance be-

tween the centre of each voxel and the nearest solid voxel is calculated. Subsequently, the distance map calculations are used to extract the medial axis, which serves as the main skeleton of the void space. The medial-axis mesh is comprised of points that exhibit maximum equidistance from two or more points on the solid boundary. Then, these points are associated with a maximum radius capable of fitting inside the pore, resulting in the creation of maximal spheres.

To establish the connectivity of the medial surface, a hierarchical structure of maximal spheres is used. This hierarchy organises the resulting maximal spheres based on a parent-child relationship, similar to the maximal-ball algorithm (Raeini et al., 2017). The merging is determined by considering larger spheres as parents of smaller spheres when they exhibit partial overlap. The maximal spheres that lack neighbouring spheres larger than themselves indicate a local maximum of the distance map. Thus, they are assigned as top-level spheres for the definition of pores. The centre of each top-level maximal sphere represents the centre of a corresponding pore, while its radius determines the pore radius. Additionally, each maximal sphere is assigned a pore label, which is also inherited by all of its children. This process results in the segmentation of the medial surface, allowing for the assignment of every voxel of the 3D binary image to a specific pore. This segmentation facilitates the subsequent identification of constrictions, which are defined as the common voxel faces shared between neighbouring pores. The radius of each constriction is determined by the maximal sphere that can fit within the constriction surface, possessing the largest value in the distance map. Consequently, the pore space is discretized into interconnected pores and constrictions, with each pore represented by a parent maximal sphere and each constriction represented by a child maximal sphere. More comprehensive details can be found in (Raeini et al., 2017).

3.2. Representative Elementary Volume

To ensure the representativeness of the 3D image volume obtained from the numerical sample in terms of constrictions and pores, a parametric investigation was conducted on the 3D image volume. A control volume of a cubic shape whose centre is confounded with the centre of the numerical sample is defined for the statistics (Fig.III.6).

Different sizes for this volume, ranging from $0.5D_{100}$ to $3D_{100}$ were studied, and the CSD was computed for each case. As an example, Figure III.7 displays the CSD for the sample composed of partially spherical particles with a high resolution (voxel size of $D_0/60$, see more details in subsection 3.3, where D_0 stands for the smallest particle size of the granular material). For a control volume greater than $2D_{100}$, the CSD stabilises, indicating that a further increase in the control volume does not significantly impact the distribution of constrictions.

The same procedure was carried out for all the numerical samples to examine the associated REV. Ultimately, a cubic control volume with a side length equal to $2.5D_{100}$ ((5x5x5 cm³) was adopted, whatever the particle shapes involved in the numerical samples. This volume size systematically excluded the zones of the samples affected by wall effects. It was observed herein that this distance can reach a maximum range of a value equal to D_{100} from the wall for all the samples.

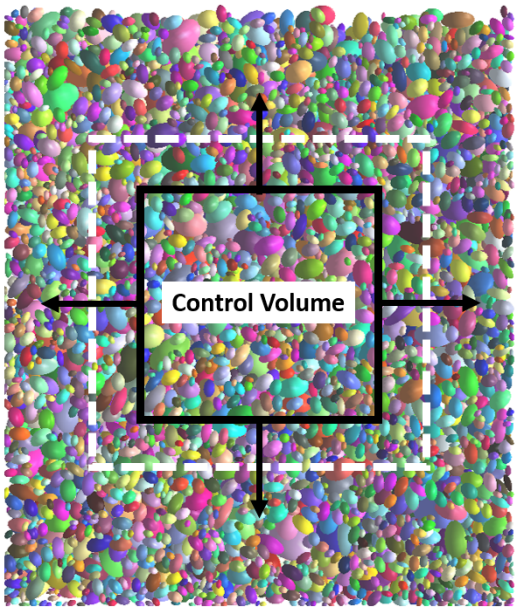

Fig. III.6. Control volume for determining the REV.

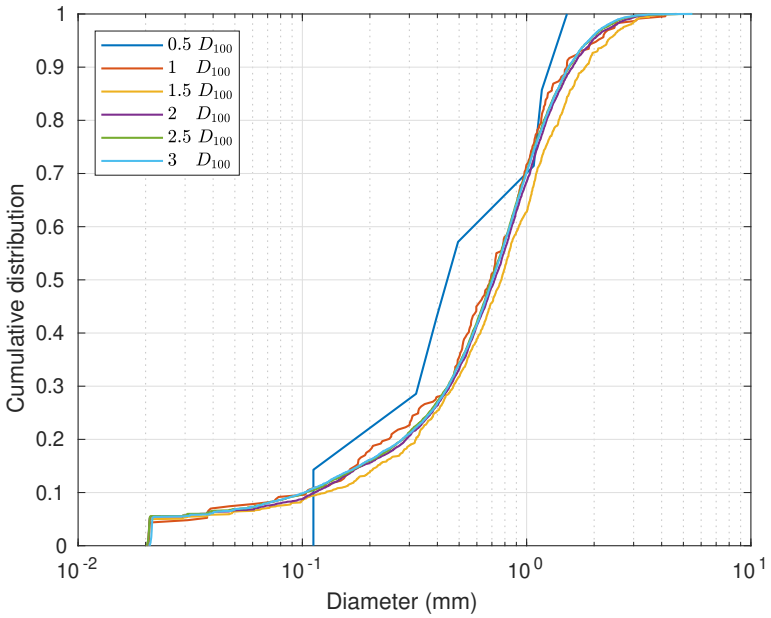

Fig. III.7. Constriction size distributions computed within a control volume of different sizes.

3.3. Resolution of the 3D images

For a precise representation of the pore space, the 3D binary images must have a sufficiently high resolution. The term resolution refers to the level of detail and clarity that can be displayed in the images. It is typically defined by the number of voxels along each dimension. Shire et al. (2012) carried out a study aiming to investigate the effect of the number of voxels on the constriction

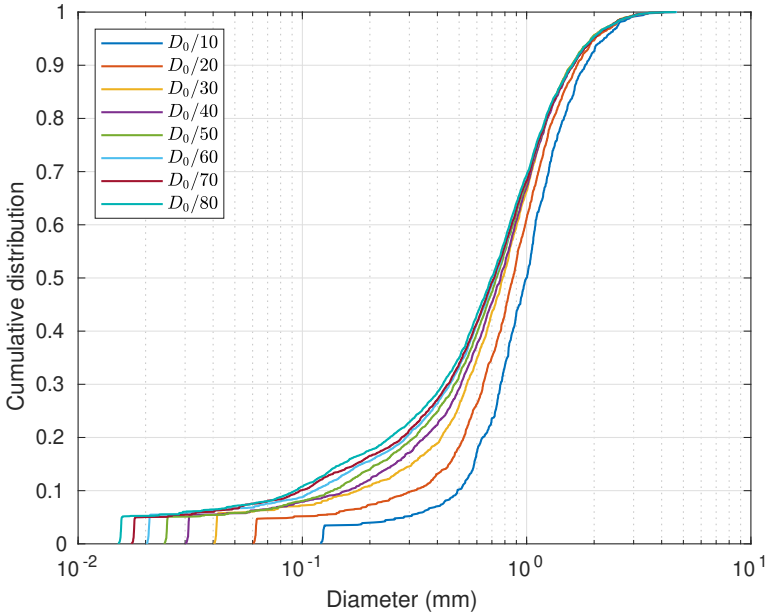

Fig. III.8. Genuine constriction size distributions with different resolutions.

sizes for a sample composed of uniformly graded spheres. The results show that the accuracy significantly increases as the number of voxels per radius of the sphere increases until there are 50 voxels per radius. Above this value, the results are only slightly modified. However, due to the huge amount of data to store and available memory, for samples of larger size, a radius represented by 25 voxels was used by these authors. Independently of the resolution, the results show that there exists a "tail" of very small constrictions that are considered artificial. The authors justified the presence of this artificial "tail," attributing it to the irregularities in the 3D image generated during the initial voxelization process, such as small gaps at particle contacts. Taylor et al. (2015) proposed to remove all the constrictions that have a size smaller than $0.155D_0$. This value represents the analytical solution of the size of the smallest constriction that can be built on the basis of the mutual contact of the three smallest spheres of the filter with a diameter equal to D_0. However, this threshold does not apply to samples made of non-spherical materials, as the size of the smallest constriction cannot be easily represented by an analytical approach.

In this work, to deal with this issue, a parametric study was carried out on one of the generated samples to evaluate the effect of the resolution on the derived CSDs. A 3D image with a volume of 4x4x4 cm ($2D_{100}$) was taken from the sample with partially rounded particles and was voxelized with different resolutions. The size of the voxels was chosen to be equal to D_0/n_v, where n_v represents the number of voxels per diameter ($L2$) of the smallest particle. Note that all constrictions located within a 0.5 cm range of the boundary zone were disregarded, as they can be influenced by the boundaries of the 3D image. Figure III.8 gives the CSD as a function of the resolution with values between $D_0/10$ up to $D_0/80$, which corresponds to 3D images with a resolution of 320x320x320 to 2560x2560x2560 voxels, respectively. The study reveals that resolution does not only affect the size of the computed constrictions in the range of larger sizes but also the size of the "tail" related to so-called artificial constrictions in the sense that they do not hold physical meaning. Unexpectedly, as the resolution increased, the size of the tail also increased, where additional constrictions of smaller size were found. Moreover, one can note that the size of the smallest constriction was found almost equal to the defined size of the voxel, which was not

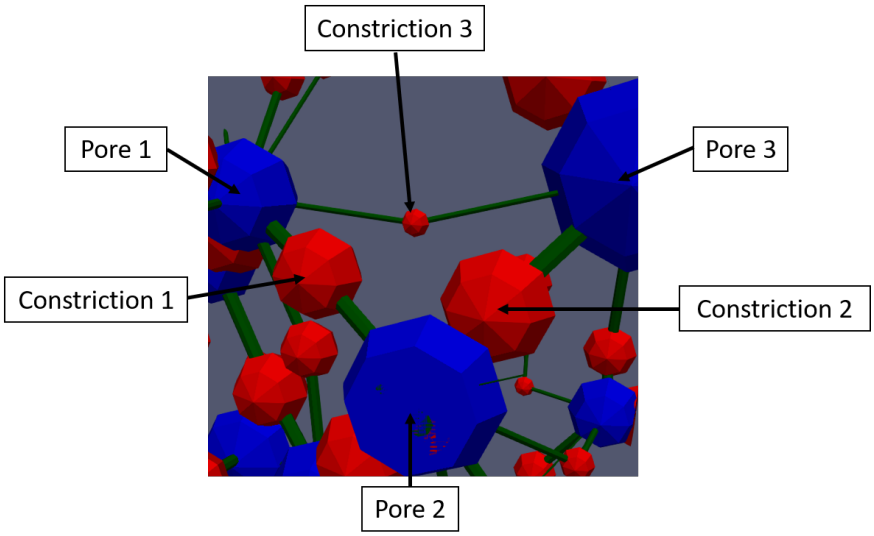

Fig. III.9. Pore space interconnection.

expected.

Before delving into the origin of these artificial constrictions, it is essential to reiterate the definition of a constriction that holds a physical significance. As previously mentioned, a constriction denotes the narrowest passage or channel (throat) interconnecting adjacent pores. When viewed from the perspective of a filtration mechanism, it is supposed to constitute a local geometric restriction to transport and as such have the capability to obstruct fine particles if the size of the latter exceeds that of the constriction. To enable this passage to effectively block fine particles, it must be conceptualized as a tube with well-defined boundaries. These boundaries are merely filter particles that limit the constriction size. To ensure the constriction possesses well-defined boundaries in the constriction plane, a minimum of three filter particles must constitute its borders.

Then, after a comprehensive visual inspection of the pore space, two categories of constrictions lacking physical significance were identified. The first category encompasses constrictions that are tangible, connecting two pores but lacking well-defined boundaries (with at least three points of contact). The second category consists of constrictions that arise from existing gaps introduced between two particles that are in contact resulting from artefacts introduced by the voxelisation process of the 3D image.

As an illustration of these cases, Figure III.9 gives the interconnection existing between pores (tainted blue) and constrictions (tainted red), while the filter particles are hidden to enhance the visibility of the void space. Three pores (1, 2, and 3) were identified, connected by corresponding constrictions (1, 2, and 3). The constriction planes for each constriction were subsequently plotted (Fig. III.10). Both constriction 1 and constriction 2 possess a plane that establishes three contact points with the filter particles (Fig. III.10a- III.10b), they hold the expected physical meaning for a construction. However, constriction 3 exhibits two contacts only (Fig.III.10c) and the geometric restriction in the constriction plane is not correctly satisfied in all directions. They should not be considered as valid constrictions and should be removed from the statistics for constriction sizes.

The second category leading to the classification of a constriction as "invalid" was investigated through visual analysis using Paraview software (Ayachit, 2015). Figure III.11 displays a voxelized 3D image depicting two filter particles in contact, along with the surrounding constrictions

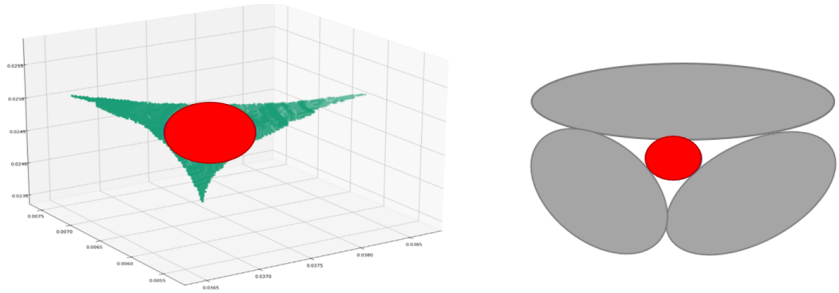

(a) Constriction 1

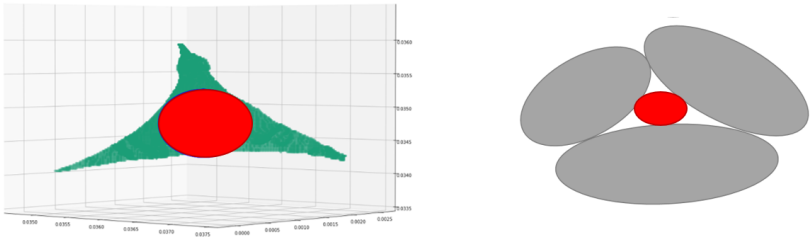

(b) Constriction 2

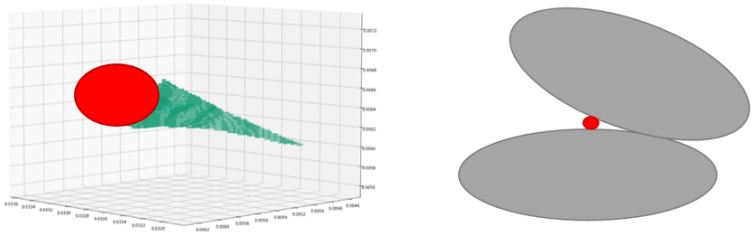

(c) Constriction 3

Fig. III.10. Constriction planes.

and pores derived from the Pn-extract process. In this instance, the voxelization process applied to the numerical sample failed to accurately represent the contact point between these two filter particles, leaving a gap between them. PN-extract algorithm interpreted this void as a connection between two pores located in front and behind the two filter particles. Consequently, this resulting constriction (circled in purple in Fig. III.11) is considered as artificial and must be excluded from the statistical analysis of constriction sizes.

As a synthesis of this peculiar study, since a very high resolution cannot remove the artificial constrictions but only makes them larger in number, new systematic solutions need to be adopted to identify and remove them from the statistics. Based on the criterion that constrictions must have at least three contacts with the filter particles to hold a physical meaning, one can take advantage of the DEM model as it can easily provide the number of contacts for each particle. To obtain this value, first, the coordinates of the centres of all the constrictions and their sizes were extracted from Pn-extract. Then, in SudoDEM, equivalent spheres representing the constrictions were created at the exact location of constrictions with the same diameter. Finally, the number of

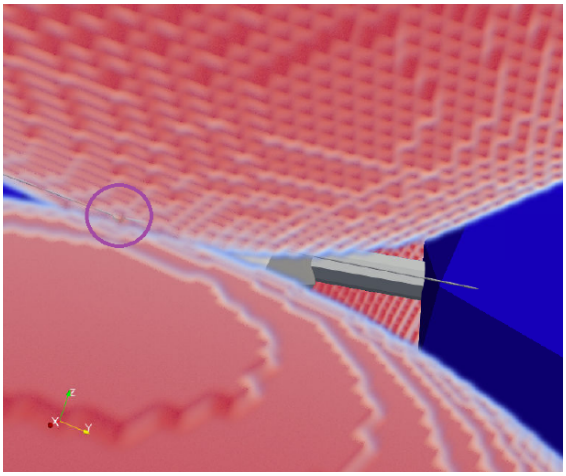

Fig. III.11. Visualization of a small constriction (circled in purple). Red color stands for solid particles, and blue color for pores.

contacts existing between them and the filter particles was computed. All the constrictions that had fewer than three contacts were deleted.

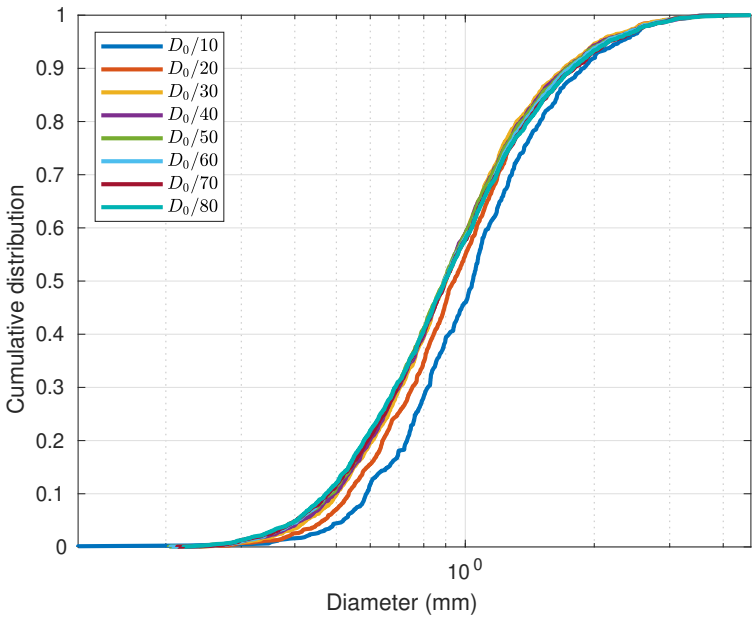

Fig. III.12. Post-processed constriction size distributions with different resolutions.

Figure III.12 shows the post-processed CSD as a function of the resolution after the treatment. The artificial tail with odd constrictions totally vanished, which allows us to conclude the appropriate resolution to use in order to obtain precise results. In Figure III.12, one can note that a resolution greater than $D_0/40$ does not provide a significant change to the CSD. No more change is noticeable for a resolution greater than $D_0/60$. This latter value was chosen in this study.

4. Results and discussion

4.1. Effect of particle shape on the constriction sizes

After establishing a well-defined methodology for extracting a well-representative CSD from the numerical samples, while ensuring the exclusion of non-physical constrictions, the CSDs for all the numerical samples were re-computed. Even though the sample porosity is the same for all samples, significant departures in the CSDs depending on the involved particle shapes have been obtained as shown in Figure III.13. Remarkably, the CSD for highly flat particles exhibits the smallest constriction sizes, while the curves progressively shift towards larger diameters for more spherical particles. The sample with the most elongated particles manifests the largest constriction sizes. Moreover, one can note that the CSD of the sample with flat-elongated particles aligns more closely with that of flat particles than that of elongated particles. It means that the degree of flatness exerts a more pronounced impact on the CSD than the elongation ratio. This feature can be attributed to the different types of contact that can be established between particles according to particle shape. Flat particles can exhibit quasi-plane contacts, leading to the possibility of generating smaller constrictions, while elongated particles can only create contact points, resulting in the creation of larger constrictions.

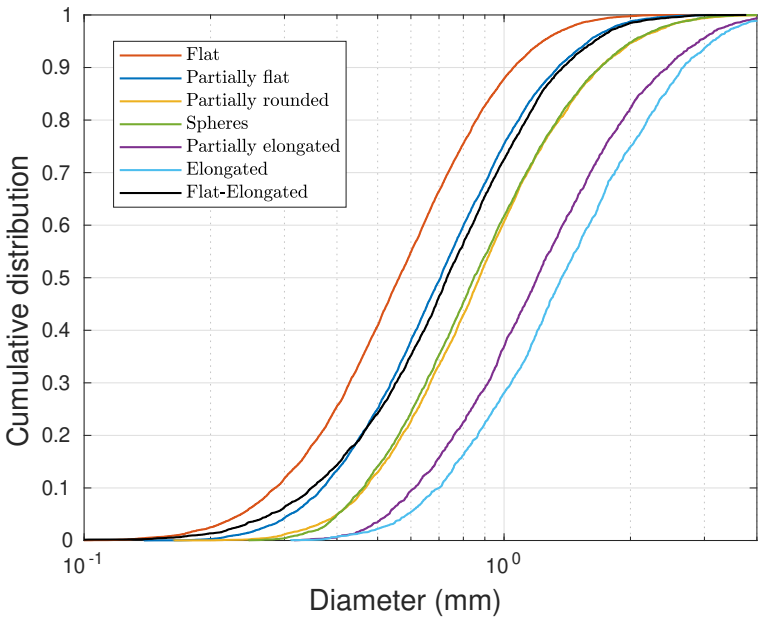

Fig. III.13. Effect of particle shapes on the constriction size distributions.

Interestingly, the CSD of partially rounded particles demonstrates a notable concurrence with that observed for spherical particles. Additionally, it is noteworthy that the minimum constriction size is influenced by the shape of the filter particles, which was expected. Consequently, the prescribed cut-off value of $D_0/6.5$ ($0.155xD_0$), which serves to exclude artificial constrictions below a certain size, cannot be universally applied to non-spherical particles. However, it is worth noting that for samples involving spherical particles, the minimum constriction size was found to be equal to 0.2 mm, which is close to $D_0/6.5$ (0.195 mm), the expected value.

Figure III.14 gives the probability density function associated with the CSDs. It allows us to

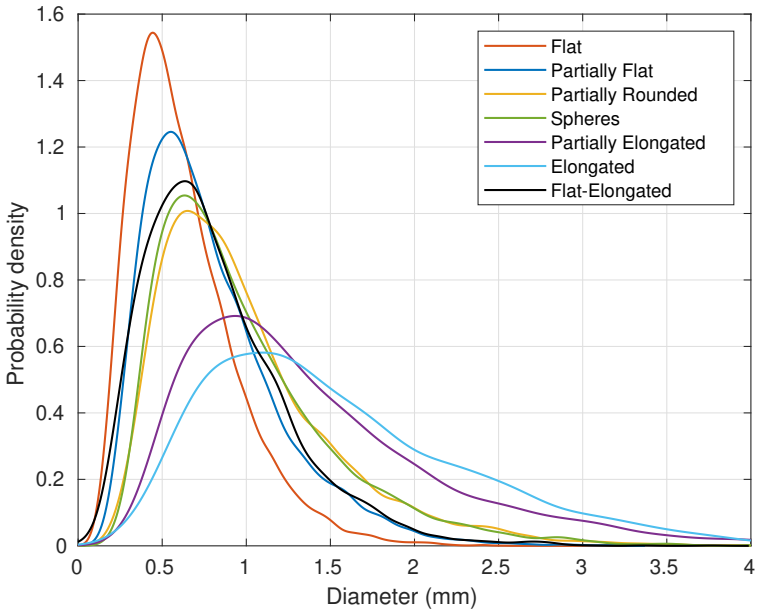

Fig. III.14. Probability density function of constriction sizes for samples with different shapes.

exhibit the size associated with the mode of the distribution, the most represented constriction size in the sample. Specifically, the diameter related to the mode is the smallest for samples with highly flat particles, then gradually increases as the sphericity of the particles increases, and becomes the largest for samples with extremely elongated particles. The relative difference of 66% between the smallest and largest mode positions is notable. Moreover, for flat particles, the CSD curve assumes a narrow and tall shape, indicating a certain degree of uniformity in constriction sizes. As the particle shape of the granular materials becomes more spherical, the CSD curve tends to spread and flatten, resulting in increased variability in constriction sizes. This spread attains its maximum width in samples containing elongated particles. Table III.2 gives the values of the smallest constriction and the mode diameter for all the samples.

Table III.2: Size of the smallest constriction and the mode value of the CSD for the different samples.

Shape of particles	Smallest constriction size (mm)	Mode size (mm)
Flat	0.09	0.44
Partially Flat	0.17	0.55
Partially rounded	0.21	0.63
Spheres	0.24	0.65
Partially elongated	0.30	0.95
Elongated	0.31	1.19
Flat-Elongated	0.12	0.64

Moreover, Table III.3 presents the number of particles and constrictions obtained for the seven numerical samples. It is important to note that the volume of particles varied depending on their shape, resulting in different numbers of particles in each sample. Specifically, when considering the same volume (5x5x5 cm^3), the samples comprising flat particles contained approximately

7,000 particles. However, as the particle shape transitioned from flat to spherical and elongated, the involved solid volume increased, leading to a decrease in the number of particles (Tab.III.3). Consequently, since the number of constrictions is contingent upon the number of particles, an increase in the number of particles leads to an augmented number of constrictions.

Table III.3: Number of particles and constrictions in 5x5x5 cm^3 samples according to involved particle shape.

Shape of particles	nb of particles	nb of constrictions
Flat	7,200	17,500
Partially Flat	4,690	10,125
Partially rounded	2,350	5,340
Spheres	2,597	5,495
Partially elongated	974	2,373
Elongated	549	1,610
Flat-Elongated	1,819	5,785

4.2. Effect of particle shape on pore sizes

Figure (III.15) illustrates the probability density function (PDF) of pore sizes according to particle shapes. Consistent with the findings for constrictions, the mode of the pore size distribution corresponds to a smaller size for the sample made of flat particles, followed by that made of rounded particles and elongated particles. Moreover, the pore curve for flat particles exhibits a narrower shape compared to rounded particles, while elongated particles display the widest curve. These results, coupled with the findings regarding constrictions, provide evidence that the pore space in filters containing flat particles is relatively homogeneous, whereas it is more heterogeneous in the case of elongated particles. Table III.4 shows the obtained mode of the PDF of the pores for all the samples.

In the sample with flat-elongated particles, the sizes of the pores closely resemble those obtained for samples with flat particles, thereby indicating that the flatness index leads to smaller pore sizes. Furthermore, similar to the findings regarding constrictions concerning the number of particles, the number of pores also increases as the number of particles increases (Tab. III.5).

The average coordination number N_c is computed, which quantifies the number of constrictions per pore within the sample. This parameter serves as an indicator of the connectivity of the pore space, revealing the capacity of the pores to facilitate the flow transportation Khilar and Fogler (1998). The results indicate that samples containing flat particles exhibit the highest coordination number, with a value of 5.8. As the particle shape transitions from flat to rounded and eventually elongated, the coordination number decreases. Filters with elongated particles possess the lowest coordination number, with a value of 5, indicating the lowest level of connectivity among the investigated particle shapes.

In the sample with flat-elongated particles, the observed coordination number closely aligns with that typically found in elongated samples. This suggests that the elongation index plays a more significant role in determining the connectivity of the filter compared to the flatness index.

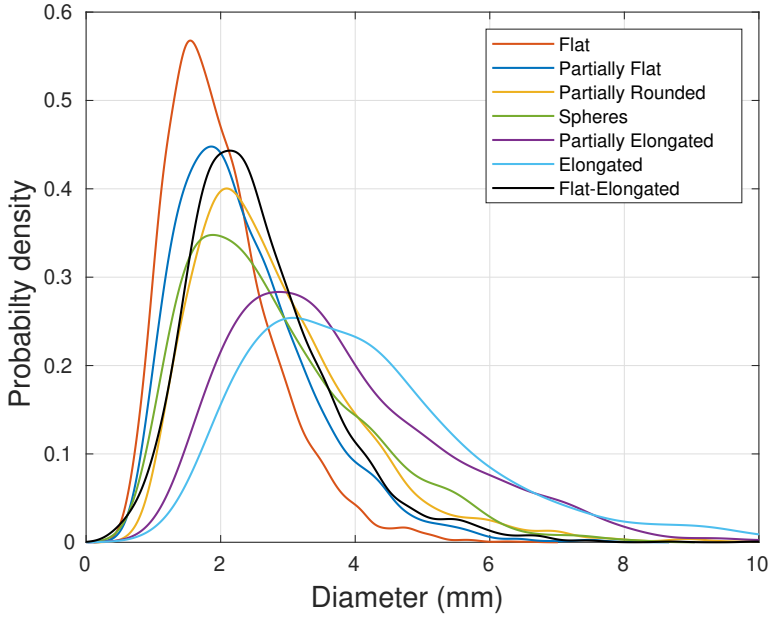

Fig. III.15. Probability density function of pore sizes for samples with different particle shapes.

Table III.4: Mode of the PDF of pores for the different samples according to involved particle shape.

Shape of particles	Mode size (mm)
Flat	1.57
Partially Flat	1.85
Partially rounded	2.09
Spheres	1.91
Partially elongated	2.71
Elongated	3.01
Flat-Elongated	2.15

Furthermore, similar to the findings regarding constrictions concerning the number of particles, the number of pores also increases as the number of particles increases (Tab. III.5).

The average coordination number N_c is computed, which quantifies the number of constrictions per pore within the sample. This parameter serves as an indicator of the connectivity of the pore space, revealing the capacity of the pores to facilitate the flow transportation (Khilar and Fogler, 1998). The results indicate that samples containing flat particles exhibit the highest coordination number, with a value of 5.8. As the particle shape transitions from flat to rounded and eventually elongated, the coordination number decreases. Filters with elongated particles possess the lowest coordination number, with a value of 5, indicating the lowest level of connectivity among the investigated particle shapes.

In the sample with flat-elongated particles, the observed coordination number closely aligns with that typically found in elongated samples. This suggests that the elongation index plays a more significant role in determining the connectivity of the filter compared to the flatness index.

Table III.5: Number of pores and coordination number in 5x5x5 cm^3 samples according to involved particle shape.

Shape of particle	nb of particle	nb of pores	Coordination number N_c
Flat	7200	6036	5.8
Partially Flat	4690	3575	5.7
Partially rounded	2350	2022	5.3
Spheres	2597	2024	5.4
Partially elongated	974	887	5.3
Elongated	549	643	5
Flat-Elongated	1819	2537	4.6

4.3. Implications for filtration properties of granular materials

The filtration efficiency of granular filters is primarily determined by the constriction sizes. When these constrictions are smaller than fine particles, they block the passage of such particles. Additionally, an increased count of constrictions enhances the likelihood of capturing fine particles within the filter. Since filters with equivalent thicknesses but varying particle shapes do not hold the same number of constrictions, they may exhibit distinct retention properties for the same given porosity.

Analyzing the outcomes of pore extraction from the previous sections, particularly focusing on the size and number of constrictions, filters constructed from flat samples are theoretically expected to display the highest retention coefficient for two reasons. First, it can be attributed to their smaller constriction sizes in comparison with the other samples. The second reason lies in the higher number of constrictions than in the other samples. In comparison, filters made from spherical particles would come next in retention capability, while those constructed from elongated particles, characterised by larger constrictions and a lower number of constrictions, would have the lowest retention coefficient for the same porosity. The results also suggest that the original filter criteria devised for spherical particles remain valid when applied to partially rounded shapes, as they both share almost the same CSD and a similar number of constrictions. This result is compatible with what was found by Wu Wu et al. (2012) from lab filtration tests with a filter composed of rounded natural material.

5. Numerical filtration tests

To support the conclusions made through a direct analysis of the pore space characteristics by means of the pore extraction technique, simulations of filtration tests have been performed.

Samples containing non-spherical particles can pose computational challenges due to the requirement for fluid-solid coupling. Indeed, it requires the use of resolved and unresolved computational fluid dynamics (CFD) methods (Ren et al., 2012; Zhao and Shan, 2013; Xie et al., 2021) or lattice Boltzmann methods (LBM) (Lallemand and Luo, 2000; Mansouri et al., 2009; Younes et al., 2022), which can be prohibitively expensive when simulating filtration processes in granular mate-

rials (Wautier et al., 2019). To address this issue, dry filtration tests have generally been developed to examine the migration of fines in granular filters (Reboul et al., 2008; Sjah and Vincens, 2013; Kerimov et al., 2018). However, it is essential to note that the underlying physical phenomena in this type of model for filtration tests are fundamentally distinct from those at stake in actual samples.

In dry filtration tests, the movement of fine particles within a filter is primarily driven by gravity forces, resulting in trajectories that are predominantly aligned with gravity direction. Conversely, in wet filtration tests, due to the existence of a seepage, fine particles follow the local maximum flow, leading them to explore sideways during their migration in the filter. Thus, it provides increased opportunities for them to pass through the filter (Seblany et al., 2021; Abdallah et al., 2023b).

In this work, an improved dry filtration model called the "equivalent cyclic wet filtration model," as proposed by Abdallah et al. (2023b), was used. This model addresses the limitations of traditional dry filtration tests by incorporating sideways exploration, allowing for a more comprehensive examination of potential pore exits. A brief overview of the model is provided in the appendix, while a more comprehensive explanation can be found in (Abdallah et al., 2023b).

To ensure consistency in the filtration process, all the numerical filters having the same porosity and grading used in the study had a standardised thickness of 10 cm, derived from the initial set of the generated samples featuring diverse particle shapes. Fine spherical particles were randomly dispersed onto the surface of each filter and released. Each simulation is associated with a given class of sizes for the fines, with a number of fine particles equal to 200. The deliberate selection of this relatively small particle count was aimed at mitigating any potential strong interactions between fines (group effects among others) that could arise while guaranteeing that the variety of possible paths in the filter were able to be explored by them.

Figure III.16 displays the coefficient of retention associated with each class of diameters for the released fines in the filters. Notable disparities can be observed in relation to the particle shapes of the granular filters. The filter incorporating flat particles demonstrated the highest extent of blockage for a given class of fines. Interestingly, the sample with partially spherical particles exhibited a behaviour similar to that of spherical particles, while the sample composed of elongated particles displayed the lowest level of blockage. Moreover, it was observed that the smallest fine particle that starts to be blocked in the filter varied depending on the particle shape of the filter, with a value close to $D_0/6.5$ in the case of spheres and partially spherical materials. All the trends obtained throughout these filtration tests validate the outcomes obtained from the void space extraction and are especially related to the CSDs. Specifically, flat particles were associated with the sample with the smallest constriction sizes, partially spherical and spherical particles exhibited intermediate-sized constrictions, while elongated particles manifested the largest constriction sizes. Furthermore, there is a strong correspondence between the smallest constriction C_0 (Tab. III.2) and the smallest fine particles that have a zero percentage of blockage. For example, flat and flat-elongated particles have a C_0 equal to 0.09 and 0.12 mm, respectively, and the size of the fine particle that corresponds to zero blockage is found to be 0.1 mm. The same feature can be found in the other samples.

Furthermore, when comparing the results obtained from the samples containing flat-elongated particles with those comprising elongated particles and flat particles, it is notable that the retention curve closely aligns with that of the flat particle samples. This observation further supports the

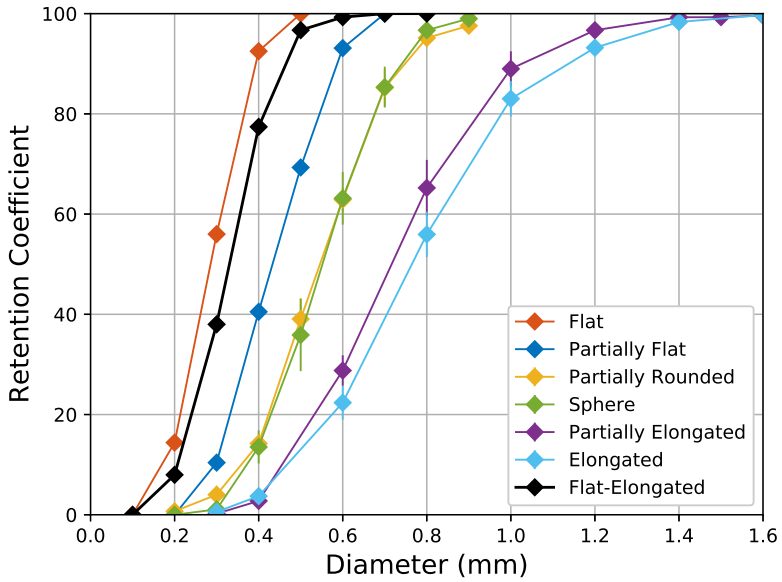

Fig. III.16. Coefficient of retention for the filters according to involved particle shape.

earlier findings obtained by void space extraction, where the CSD derived from the flat-elongated particles closely matches that of flat particles rather than elongated ones.

However, it is crucial to note that discrepancies in the retention curves may arise from two different aspects, including the average number of constrictions along a given path and the size of the most represented constriction in the granular filter. For the same filter thickness, a sample having a given number of constrictions and a given mode value of the most represented constriction sizes can have the same retention coefficient as another sample with a larger number of constrictions associated with a larger mode value of the most represented constrictions. In the study involved herein, when there is a greater number of constrictions there is also a smaller size for the most represented constriction. It means that this bias cannot be obtained herein at the time when deriving conclusions. In fact, particle shape has a double influence that tends to amplify the influence of particle shapes on the filtration properties of granular filters.

6. Conclusion

The study proposed herein investigated the influence of rounded particle shape on the morphology and topological properties of the pore space within granular filters. Some implications in terms of filtration properties for these kinds of filters have been derived. Numerical samples with the same grading and porosity but different particle shapes have been created using DEM, and a pore extraction technique was used to characterise the void space. Numerical filtration tests were also conducted to validate the results and establish a correlation between constriction sizes and retention properties of granular filters.

The influence of particle shape on the size of constrictions exhibited distinct variations across different particle shapes. Highly flat particles demonstrated in general smaller constriction sizes,

the smallest mode, and the narrowest constriction size distribution, while more spherical particles exhibited progressively larger sizes of constrictions, a larger mode, and a larger distribution range. The sample containing elongated particles exhibited the opposite trend in terms of particle shape effects, displaying larger constriction sizes, the largest mode, and the broadest distribution for constriction sizes. In general, the degree of flatness had a more pronounced effect compared to the elongation ratio. Additionally, the CSD of partially rounded particles is closely aligned to that of spherical particles. Both samples exhibit intermediate characteristics between samples with flat particles on one hand and elongated particles on the other.

The number of constrictions in a given volume was found to be directly related to the number of particles, leading to the highest number of constrictions for the sample with flat particles and the lowest for the samples with elongated particles. An increase in the flatness ratio directly corresponded to a greater occurrence of constrictions.

All features found for the constriction sizes were also found for the pore sizes. Furthermore, in the sample with flat particles, the pores exhibit a higher average number of constrictions. In contrast, the samples with elongated particles presented the lowest value.

The simulations of filtration tests validated what could be deduced from the pore space extraction technique. For filters of the same grading, same porosity, and same thickness, the filter containing flat particles showed the highest blockage rate for a given class of released fines. In contrast, the sample with elongated particles demonstrated the lowest level of fine particle blockage. The effect of particle shape on retention properties was found to be amplified due to a cumulative effect. When there are smaller constrictions, there are also a larger number of constrictions, which constitute a larger number of obstacles to overcome for a fine of a given size to cross the filter.

Overall, considering the significant impact of particle shape on pore space characteristics and filtration performance, it seems crucial to take particle shape into account within filter criteria.

Appendices

Equivalent cyclic wet filtration model

The model is build upon a pore network model proposed by Schuler (1996), representing the pore space as a regular network of interconnected void cubes with a constriction on each face. Fine particles within the pores can exit through a direct path or sideways towards neighbouring pores on the same layer. The proposed model assumes that when a fine particle is blocked inside a pore, it can still find a sideway exit by traversing a sideway distance equal to half of the average pore diameter. If the sideway constriction is larger than the fine particle, the particle has the opportunity to exit the pore and migrate further within the filter.

The filtration test methodology consists of cycles with two phases. In the first phase, fine particles are allowed to freely descend inside the filter under the influence of gravity until a stable condition is reached. In the second phase, gravity is deactivated, and the trapped particles undergo a sideway displacement equal to half the average pore diameter. This displacement occurs in a randomly determined direction perpendicular to the gravity direction. Following the sideway movement,

gravity is restored to its natural direction, and particles that successfully exit the pore continue to migrate within the filter. These cycles are repeated until stable filtration results are obtained, indicating that no more fine particles can pass through the filter.

The calculation of the average pore size relies on equation III.2 originally developed by Wu et al. (2012) and subsequently modified by Seblany et al. (2018b). This formula considers both the grading of the granular material and its density for computing the average pore size in the packing of spheres.

$$s = \frac{1}{0.7}\sqrt[3]{\frac{e}{e_{max}}}s_{max} \tag{III.2}$$

where e and e_{max} denote the actual and maximum void ratios for the material, respectively. s_{max} represents the average pore diameter in the material in the loosest state. An estimate for s_{max} can be obtained by assigning a value equal to $0.5D_{50SA}$, where D_{50SA} signifies the particle diameter at which 50% of the material is smaller than, based on a particle size distribution (PSD) of the material defined in terms of surface area. More details about the derivation of this estimate can be found in (Wu et al., 2012). Equation III.2 is valid for spherical particles. However, as illustrated in Figure III.15, the size of the pores varies depending on the shape of the particles. The case of spheres results in an intermediate case between that of flat particles and that of elongated ones. Equation IV.6 will be used as a first estimate for the average pore diameter irrespective of the involved particle shape.

This simplified approach was validated on a reference case where coupled fluid-solid simulations were performed. The samples consisted of spherical particles, and various fines from distinct diameter categories were introduced into these samples. The main criterion for assessment was the percentage of blockage of fines within the samples, categorized by their diameter. More details can be found in (Abdallah et al., 2023b).

Chapter IV

Effect of Fabric Anisotropy on Filtration Mechanisms in Granular Filters

Authored by: Ali Abdallah[1], Eric Vincens[1], Hélène Magoariec[1] and Christophe Picault[2]

[1]. Univ Lyon, Ecole Centrale de Lyon, CNRS, ENTPE, LTDS, UMR5513, 36 Avenue Guy de Collongue, 69134 Ecully, France

2. CACOH, Compagnie Nationale du Rhône, 4 Rue de Chalon-sur-Saône, 69007 Lyon, France

This chapter is based on a manuscript that will be submitted to : *Granular Matter*

Acknowledgments: Part of this work belongs to a project funded by Compagnie Nationale du Rhone. The authors acknowledge the support of CNR for this study.

Abstract

This study explores the impact of fabric anisotropy on directional filtration mechanisms in granular materials, arising from anisotropic particle shapes and preparation methods. Using the discrete element method, diverse samples underwent extensive numerical filtration tests. Subsequently, an extraction algorithm facilitated comprehensive pore space analysis. Results highlighted the notable influence of the gravity deposition method, intensifying anisotropy and affecting directional filtration. The pore space analysis revealed connectivity variations between directions, justifying differing retention coefficients. This study underscored the need for a comprehensive approach that accounts for constriction size, number of constrictions larger than, and connectivity to yield precise results. It contributes valuable insights into anisotropy's role in granular materials, sheds light on complex directional filtration mechanisms, and advances related applications.

Main results

- The filtration tests showed that the gravity deposition method caused anisotropy in samples because of anisotropy in particle contact. This resulted in a higher retention coefficient in the vertical direction (parallel to gravity) compared to the horizontal direction, irrespective of the particle shape.
- The more anisotropic the particle shape became, the more pronounced the anisotropy in the filtration process was. However, the difference between retention coefficients obtained in the horizontal and vertical directions was relatively insignificant from an engineering perspective.
- An analysis of the pore space revealed that there wasn't a significant discrepancy between the CSDs obtained based on the orientation of the average constriction plane. Hence, they didn't explain the disparate retention coefficients observed based on the direction of filtration. But they did clearly explain the varying retention coefficients observed for the different samples linked to different particle shapes.
- The anisotropic particle shapes exhibited systematically smaller connectivity in the vertical direction than in the horizontal direction. This might explain the higher retention coefficients observed in such scenarios. For larger size ranges, flatter particles tended to result in a less connected material, while more elongated particles led to a more connected material.

1. Introduction

Granular materials have found extensive utility as filtration mediums across various engineering domains. For example, granular filters can serve as a protective layer on hydraulic structures such as dams and dikes (Locke et al., 2001; Bonelli, 2013). Their role in this context is to prevent the migration of fine particles from the structure or its foundation, mitigating the risk of internal erosion and subsequent structural failure. Furthermore, granular filters play a pivotal role in environmental engineering, particularly in water management, including the treatment of water from storms and sewage sources (Jackson and Letterman, 1980; Siriwardene et al., 2007; Ho et al., 2011). Within this domain, they are employed to efficiently eliminate particulate waste from fluid flows, enhancing the overall quality of the treated water.

The flow orientation and the subsequent movement of fine particles through granular filters can exhibit significant variation depending on several factors, including the geometric layout, underlying soil conditions, and hydraulic gradients. As an illustration, in the context of earth embankment dams, the path of seepage flow tends to fluctuate downward (in alignment with gravity) when it migrates from the impervious core of a zoned dam into the filter (Fig.IV.1a). Conversely, in a situation of mitigation of internal erosion (repair) when filters are installed on the downstream side of a dike, seepage flow tends to follow a horizontal trajectory (Fig.IV.1b).

In granular filters, when flow aligns with the direction of gravity, filtration is generally denoted as vertical filtration, whereas when flow is perpendicular to the gravitational force, it is denoted as horizontal filtration (Skouras et al., 2011). These denominations are taken in this paper for better legibility. Existing design criteria for granular filters, such as particle-size based criteria (Terzaghi et al., 1996) and constriction-based criteria (Indraratna et al., 2007; Seblany et al., 2021), neglect the direction of flow with respect to gravity assuming that the retention capacity of a granular material is a non-oriented property.

However, it is widely acknowledged that granular materials on-site exhibit a state of anisotropy stemming from factors such as particle shape, deposition methods (inherent anisotropy), and applied loads generating deviatoric stresses (induced anisotropy). Anisotropic features in granular materials can be evaluated by assessing their initial fabric. The term "fabric" represents the spatial arrangement of the particles and their associated voids as defined by Oda (1972). Fabric

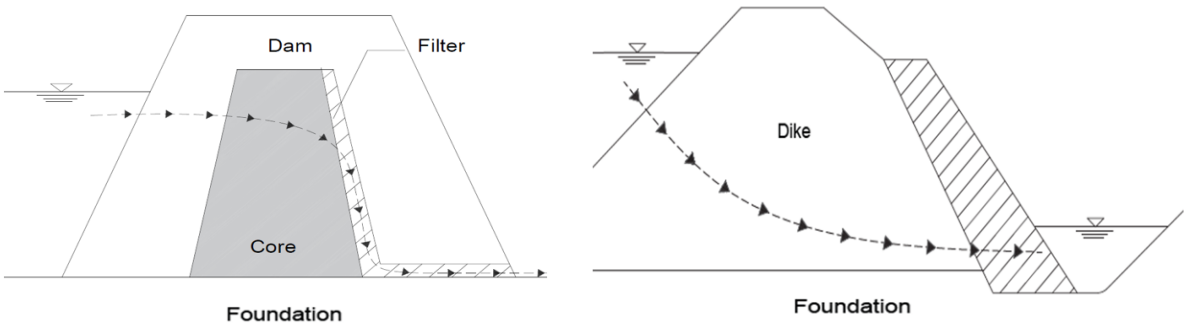

(a) Direction of the seepage flow in dam

(b) Direction of the seepage flow in dam

Fig. IV.1. Schematic of different seepage directions in hydraulic structures

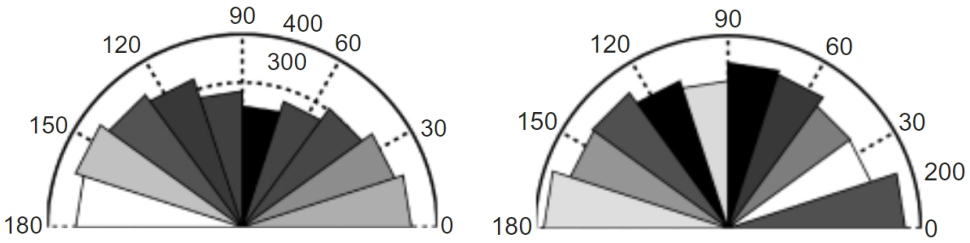

(a) Before loading (b) After loading

Fig. IV.2. Projection of the void long-axis of pore orientations onto the vertical plane before and after loading (Fonseca et al., 2013)

anisotropy can be measured in function of particle orientation, contact normal orientation, branch vector orientation, and void orientation (Oda et al., 1985). This anisotropy exerts an influence over both mechanical and hydraulic characteristics of granular soils, including attributes like stiffness, shear strength, and permeability (Kuhn et al., 2015). Consequently, these properties can induce variations in the material response or failure modes contingent on the direction of applied loads.

In a directional seepage flow analysis, the directional permeability parameter is considered a valuable tool for effectively capturing the inherent characteristics of the granular material's pore space. Numerous studies have been conducted on the anisotropic nature of permeability in granular materials (Mansur and Dietrich, 1965; Chapuis et al., 1989; Masad et al., 2002). In the majority of granular homogenous samples created by gravity deposition, the findings consistently revealed a greater permeability coefficient when the flow is horizontal. The ratio r_k between the horizontal permeability coefficient and the vertical permeability coefficient ranges from 1.1 to 4.1. However, for dynamically compacted samples, this ratio was found ranging from 0.87 to 1.00, indicating a slightly higher coefficient of permeability in the vertical direction than in the horizontal one (Chapuis et al., 1989). Since permeability depends among others on properties such as pore sizes, constriction sizes (throats connecting neighbouring pores) and pore connectivity (Bryant et al., 1993; Vogel and Roth, 2001), such properties may be oriented properties in actual materials

In a filtration test, the circulation of non-cohesive fine particles under seepage flow is also controlled by the pore space properties, including pore connectivity, while the blockage of the suspended particles is mainly controlled by geometric constraints imposed by the constriction sizes (Kenney et al., 1985; Khilar and Fogler, 1998; Reboul et al., 2008).

Shire et al. (2013) conducted a numerically comprehensive study for quantifying the role of stress-induced anisotropy in the orientation of inter-void constrictions within numerical samples. These samples were generated from spheres that underwent true triaxial loading conditions. Their findings revealed that larger constriction diameters exhibit more alignment with the major principal stress direction, whereas smaller constrictions display a tendency to deviate from the major principal stress orientation. Masad et al. (2002) revealed that the disparity in void sizes between the horizontal and vertical directions in glass bead specimens. In the case of sands, Fonseca et al. (2013) analysed samples made of Reigate sand and observed that pore orientations exhibited a subtle horizontal inclination, mirroring the particle arrangement (Fig.IV.2a). Indeed, the orientation of non-spherical particles is primarily horizontal as a consequence of the gravity deposition (Nouguier-Lehon et al., 2003). This preferential orientation for the long-axis of the pores may vanish if shearing is applied (Fig. IV.2b).

The anisotropy in the transportation of detached non-cohesive fine particles resulting from seepage flow within granular materials consisting of spherical particles has been well observed (Wautier et al., 2019; Ma et al., 2021; Liu et al., 2022). These studies indicate that the erosion rate is notably increased when the seepage flow aligns with the principal stress direction. Xiong et al. (2023) conducted an in-depth investigation into the transportation behaviour of fine particles across various granular internally stable filters generated from particles having the same shape but with controlled orientations. The findings demonstrated a clear correlation between the transportation of fine particles and the anisotropy of each filter, which was characterised by particle orientation. Notably, fine particles had a tendency to display a more pronounced migration when the alignment of the filter particles' orientation (longest principal axis) coincided with the direction of the flow. This phenomenon was found to be linked to the alignment of constriction orientations (normal of the constriction plane) with the flow direction. As a result, pore connectivity was found to be greater in that direction.

Despite the extensive body of research in this field, a comprehensive understanding of how the filtration mechanism can vary based on the direction of flow/filtration within a granular sample remains elusive. Particularly, the impact of the direction-dependency of the filtration on the retention capacity of the filter is not yet fully elucidated. It is important to emphasise that the degree of fabric anisotropy exhibits fluctuations contingent upon the form of particles (Zhao et al., 2017). Consequently, it is expected that the intensity of the direction-dependency of filtration mechanism varies accordingly upon particle forms. Notably, Abdallah et al. (2023a) explored the influence of particle shape on constriction sizes and their correlation with the filter retention coefficient when flow is parallel to gravity. Their analysis did not encompass a specific study involving different directions of filtration with respect to the fabric anisotropy of studied samples.

Then, the primary objective of this work consists of a comprehensive evaluation of the influence of the direction of flow with respect to the fabric anisotropy within granular filters on their retention capability. Using the Discrete Element Method (DEM), this investigation involves the generation of multiple numerical samples sharing the same grading for the material and the same porosity, but each is characterised by distinct particle shapes. Samples made of spheres and prepared by isotropic compaction on the first hand and gravity deposition, on the other hand, will constitute references for the study. Subsequently, numerical filtration experiments are performed under two perpendicular directions, enabling the assessment of the retention capacities of filters in these directions.

To establish a comprehensive relationship between the anisotropic filtration outcomes and the underlying anisotropic pore structure, an extraction algorithm will be used to retrieve the pore space data from the numerical samples. Specifically, the orientation of the constrictions (orientation of normals of constriction planes) and the possible directional connectivity of the pore space will be analysed in detail. This approach will facilitate a deeper understanding of how directional filtration results are intricately connected with the geometrical characteristics of the pore space and with the particle forms in granular materials. Herein, only the case of rounded filter particles is addressed.

2. Methodology

The impact of the fabric anisotropy on the filtration mechanism was examined through filtration tests conducted on numerical samples with particles exhibiting diverse shapes. These samples were generated using a DEM code. Then, the filtration experiments were executed by employing an equivalent cyclic wet filtration model, as detailed in (Abdallah et al., 2023b). This model provides an effective tool for conducting filtration analyses involving particle shapes for the filter that deviates from perfect sphericity. Ultimately, the extraction of the pore space properties was carried out to complement the filtration results, involving the analysis of constriction sizes and examining the pore space connectivity.

2.1. Generation of the numerical samples

The Discrete Element Method (DEM) has been widely used in modelling numerical experiments on granular materials. This tool facilitates the investigation of the constitutive behaviour of these materials at a representative elementary scale while simultaneously yielding insights into the intrinsic mechanisms operating at the individual grain scale (Sibille et al., 2019). Within the framework of DEM, granular materials are represented as assemblies of individual particles that mutually interact (Cundall and Strack, 1979). This approach preserves the pore space existing between particles, affording valuable insights into its intricate nature.

In this study, the modelling of numerical samples incorporating diverse particle shapes was executed using the open-source DEM code SudoDEM (Zhao and Zhao, 2021). Built based upon the open-source code YADE (Šmilauer et al., 2010), SudoDEM demonstrates remarkable efficiency in modelling non-spherical shapes.

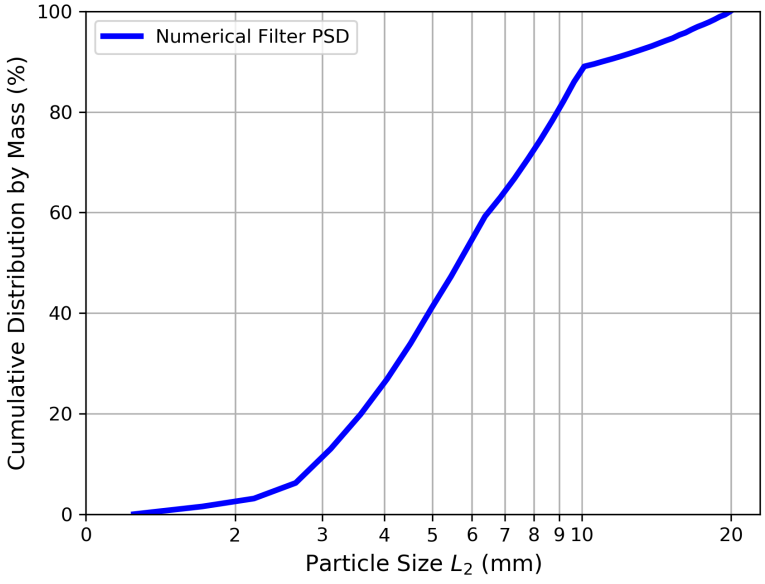

Fig. IV.3. Particle size distribution of the considered material.

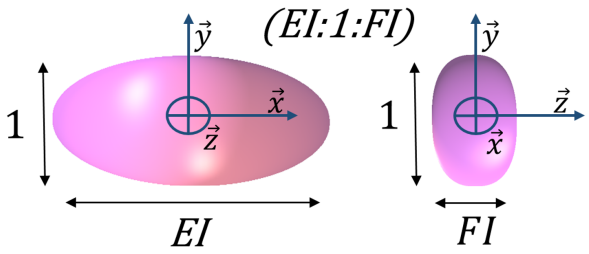

Fig. IV.4. Graphic representation of the aspect ratios of a particle

2.1.1. Materials

The numerical samples were all generated using an intermediate-graded material, characterised by a coefficient of uniformity of 2.2. Figure IV.3 gives the particle size distribution of this material where the minimum particle size D_0 is equal to 1.25 mm and the maximum particle size D_{100} is equal to 20 mm.

Ellipsoidal shapes were selected to model rounded grains due to their inherent capability to imitate a variety of non-spherical rounded particle geometry. Ellipsoidal particles are characterised by their three principal axes: $L1$, $L2$, and $L3$, which respectively represent their maximum, intermediate, and minimum dimensions, respectively. The intermediate diameter $L2$ was deemed to be equivalent to the particle size (Fig. IV.3). This is because $L2$ is the dimension between the three that determines whether a particle can traverse through a sieve or not. The values attributed to $L1$ and $L3$ define the particle's form, covering a spectrum that ranges from highly flattened to significantly elongated configurations. A good representation of particle morphology can be achieved through the utilisation of the elongation index EI and flatness index FI, also denoted as aspect ratios (Fig.**??**) and defined such as:

$$EI = \frac{L_1}{L_2} \qquad FI = \frac{L_3}{L_2} \tag{IV.1}$$

Particles can be categorised as elongated when their elongation index EI surpasses 1.8, whereas those classified as flat exhibit a flatness index FI below 0.6, as defined by Kwan et al. (1999).

In order to expand the range of anisotropy levels of particle geometry, various numerical samples were generated, encompassing particles with distinct aspect ratios. All particles were chosen such as $L2$ dimension is equal to 1 mm. Then, the triplet ($L1$, $L2$,$L3$) characterising the particle dimension is equivalent to the triplet (EI, 1, FI). Table IV.1 gives the six different aspect ratios (herein equivalent to particle dimensions) that were employed to encompass a broad spectrum of shapes, ranging from flat particles to elongated ones.

2.1.2. Inter-particle contact law

The interaction between ellipsoidal particles is determined by the Parametric Common Normal (PCN) algorithm, which calculates the depth of penetration (overlap) for two particles that are in contact (Wellmann et al., 2008).

Table IV.1: Particle shape's aspect ratios.

Shape of particles	Aspect ratio *EI*:1:*FI*
Flat	1:1:1/3
Partially flat	1:1:1/2
Partially spherical	1.5:1:0.67
Spherical	1:1:1
Partially elongated	2:1:1
Elongated	3:1:1

The contact interaction between these particles follows the Coulomb friction model, which relies on three essential parameters: the normal stiffness k_n, the tangential stiffness k_t, and the inter-contact friction angle φ_c. The normal contact force $\vec{F}_n$, and the tangential contact force $\vec{F}_t$, are determined by the following equations:

$$\vec{F}_n = k_n \delta_n \vec{n} \tag{IV.2}$$

$$\Delta\vec{F}_t = -k_t \Delta\vec{u}_t \qquad \text{with} \qquad || \vec{F}_t || \leq || \vec{F}_n || \tan\varphi_c \tag{IV.3}$$

$\vec{n}$ represents the unit vector normal to the contact plane. The normal contact force is directly proportional to the overlap distance δ_n through the normal stiffness k_n. The calculation of $\vec{F}_t$ is carried out incrementally due to the non-linearities introduced by Coulomb friction. Within the elastic regime, this tangential force is directly proportional to the relative tangential displacement $\Delta\vec{u}_t$ at the contact point, governed by the tangential stiffness k_t.

In order to preserve the pore structure and avoid substantial particle overlap, the values of k_n and k_t were elevated to a sufficiently high value equal to 5.65 x 10^5 N/m. This adjustment was made while ensuring computational efficiency was not excessively compromised. Additionally, the particles were defined by a specific density of 2,650 kg/m^3. φ is adjusted according to particle shape to achieve the targeted porosity for the sample. To manage non-frictional energy and minimise particle rebound throughout the preparation stage, a global damping coefficient of 0.7 was incorporated, following the approach detailed by Cundall and Strack (1979). All the mechanical and numerical properties can be found in Table IV.2. More details are given for φ in section 2.1.3.

Table IV.2: Mechanical and numerical parameters for DEM simulations.

Parameter	Magnitude
Normal stiffness (k_n)	5.65 x 10^5 N/m
Tangential stiffness (k_t)	5.65 x 10^5 N/m
Specific weight of spheres (ρ)	2,650 kg/m^3
Global damping (α)	0.7
Inter-contact friction (φ)	Tuned [0.7; 0]

2.1.3. Preparation of the samples

The fabric anisotropy exhibited by granular samples can be significantly influenced by the used preparation methodology. In typical scenarios on site, granular filters are subjected to deposition under gravitational force, followed by a compaction aimed at achieving the desired porosity level. In numerical approaches, various techniques exist for the preparation of granular samples, each yielding to distinct particle arrangements. To align with site conditions, this study generally adopted a gravity deposition for generating numerical samples. In this method, particles were first randomly positioned and oriented within a defined cloud of specific dimensions. Subsequently, under the influence of gravity, these particles were deposited within a rigid box. The compaction process to attain the target porosity was regulated by tuning the contact friction angle φ. This adjustment functions as a lubrication parameter, facilitating the compaction of the sample. The target porosity was set to 0.41 for all the samples.

It is widely recognized that particle shape is a critical factor influencing both the maximum and minimum void ratio (e_{max} and e_{min}) achievable within a granular sample (Maroof et al., 2022). A preliminary study enabled us to ascertain that this porosity value (0.41) was achievable across all samples (between e_{max} and e_{min}). It is important to note that the range of values for φ was different for each sample. Initially, the φ parameter was set at a high value of 1. Until equilibrium was found, porosity was assessed iteratively and φ was adjusted until the target porosity was achieved.

Equilibrium was considered achieved when the average unbalanced force ratio reached a value lower than 0.05 (Reboul et al., 2008; Seblany et al., 2021). The average unbalanced force ratio is defined as the sum of overall forces acting on particles divided by the average magnitude of forces in interactions.

The particles were introduced into a well-defined rigid box with a width equal to six times the largest particle diameter D_{100}. This choice of dimensions was deliberate, ensuring the generation of numerical samples surpassed the scale of the Representative Elementary Volume (REV). More details can be in sections 2.2 and 2.3 for the definition of the REV.

Six numerical samples were generated using the intermediate granular material with the specified particle shapes (Tab. IV.1).

Furthermore, in order to assess the impact of the generation method on the anisotropy level, a reference sample consisting of spheres was generated with an isotropic compaction within a parallelepipedic cell featuring periodic boundary conditions. The spheres were compacted uniformly from all sides of the cell until the targeted porosity was achieved, under a confining pressure of 350 kPa. Additional details regarding this preparation technique can be found in (Aboul Hosn et al., 2017).

2.1.4. Fabric anisotropy of the generated samples

To assess the impact of particle shape and generation method on the anisotropy of the particle orientation in the numerical samples, the fabric anisotropy was quantified. Zhao et al. (2017) conducted an extensive analysis of the effect of the particle shape on the anisotropy using various fabric vectors, including particle orientation, contact normal, and branch vectors. Their findings suggested that branch vectors exhibit lower sensitivity to particle shape compared to particle orien-

tation and contact normal vectors. Since particle orientation vectors are inapplicable for spherical shapes, the tensor of the contact normal vectors, which represents the orientation of contact normal vectors between particles in contact was adopted (Satake, 1982):

$$\Phi = \frac{1}{N}\sum_{k=1}^{N} \mathbf{n}_k \cdot \mathbf{n}_k^T \tag{IV.4}$$

where $\mathbf{n}_k$ is the contact normal unit fabric vector and N is the number of all contact vectors.

The three eigenvalues λ_1, λ_2 λ_3 of tensor Φ were computed together with the three associated eigenvectors. The fabric anisotropy magnitude was calculated using the formula (Barreto et al., 2009):

$$\lambda_d = \frac{1}{\sqrt{2}}\sqrt{(\lambda_1-\lambda_2)^2+(\lambda_1-\lambda_3)^2+(\lambda_2-\lambda_3)^2} \tag{IV.5}$$

Table IV.3 gives the fabric anisotropy magnitude λ_d obtained for all the samples. Beginning with the reference sample made by isotropic compaction, λ_d reached the small value of 0.016 which was expected. The sample with spherical particles and prepared with gravity deposition also exhibited a low anisotropy level, with a value of 0.03.

Then, for the samples generated through gravity deposition, the results indicate that anisotropy rises as irregularity in shape increases. For samples with partially flat, and partially elongated, the fabric anisotropy reached a value between 0.207 to 0.22. However, for the case of flat and elongated particles, the fabric anisotropy values reached 0.384 and 0.319, respectively.

Table IV.3: Fabric anisotropy for the generated samples.

Numerical sample	Fabric anisotropy
Flat	0.384
Partially Flat	0.207
Partially rounded	0.222
Spheres	0.032
Partially elongated	0.211
Elongated	0.319
Isotropic compacted spheres	0.016

2.2. Numerical filtration model

In the past, numerous laboratory filtration tests were executed to investigate the filtration mechanisms in granular materials (Terzaghi et al., 1996; Sherard et al., 1984; Kamruzzaman et al., 2008; Wu et al., 2012). Due to logistical complexities in conducting horizontal filtration tests where the flow direction is perpendicular to gravity, the flow orientation consistently adhered to gravity direction (vertical direction).

An alternative avenue for laboratory tests involves the coupling of the DEM with a flow dynamic model. This substitution for laboratory experiments offers notable advantages, primarily the easy control over the initial boundary conditions, including the flow direction. However, it is well known that the traditional coupling methods such as Computational Fluid Dynamics (CFD) and Lattice Boltzmann Method (LBM) are recognised for their substantial computational requirements, often necessitating super-computing resources to model representative samples containing a high number of particles (Wautier et al., 2019).

An alternative strategy for modelling these filtration tests involves substituting hydraulic forces introduced by flow models with the force of gravity (dry filtration) to move the fine particles within the filter (Reboul et al., 2008; Sjah and Vincens, 2013; Kerimov et al., 2018). This simplified model is universally applicable to particles of all shapes and offers computational affordability. However, this simplification of actual mechanisms has a limitation, as it fails to consider potential lateral movements triggered by hydraulic forces.

To address the limitation of dry models, Abdallah et al. (2023b) introduced an improved dry filtration model denoted as the "Equivalent cyclic wet filtration model".

The underlying concept of this model involves granting fine particles the capacity to explore sideways from along a general pathway, closely emulating the filtration mechanism observed in wet filtration tests. This imposed lateral movement provides fine particles with increased opportunities to migrate further within the filter. This refined approach significantly mitigates the discrepancy in obtained retention coefficients between dry and wet filtration. In particular, the equivalence of minimum particle size for an absolute 100% blockage in the filter between the new model and the wet filtration tests was obtained. Furthermore, the Equivalent cyclic wet filtration model applicability remains unbound by the involved filter particle shapes and just requires the definition for the average distance for exploring sideways. This distance was adjusted to half of the average pore size of the granular filter.

A brief presentation of the Equivalent cyclic wet filtration model is provided in the appendix, while a detailed description can be found in (Abdallah et al., 2023b).

The numerical filters were extracted from the generated samples. The selected volume excluded the zone affected by wall effects which was found equal to D_{100} irrespective of particle shape involved in the samples.

In each filtration test, a class of spherical fine particles with a specific diameter were introduced onto the filter surface. For vertical filtration, these particles are introduced from the top, while for horizontal filtration, they are introduced from one of the sides (Fig. IV.5). A preliminary study showed that the choice of the vertical side between the four is not important and equivalent results for horizontal filtration tests were obtained irrespective of the chosen vertical side, which was expected. To ensure controlled conditions, a total of 200 fine particles are released for each test. This particular quantity was chosen to enable individual particle trajectories, reducing extensive interactions among the fine particles and mitigating the risk of clogging while ensuring that enough different pathways are explored through the sample for representativeness Ghidaglia et al. (1996); Kerimov et al. (2018); Seblany et al. (2021).

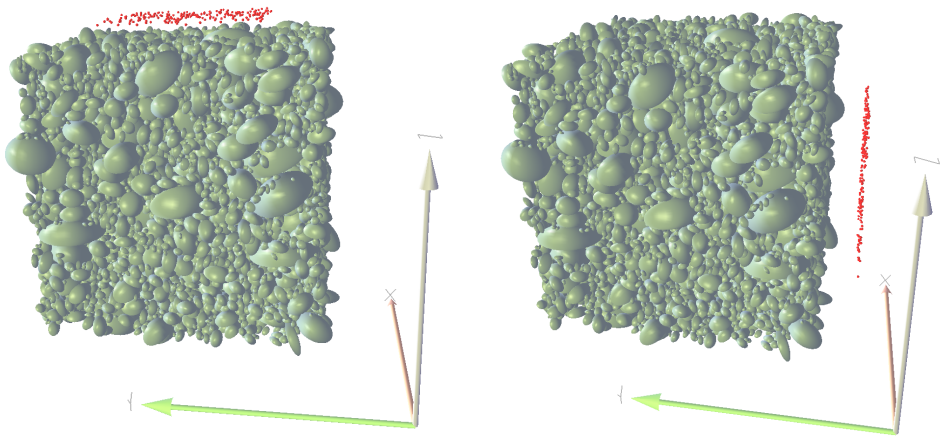

(a) Vertical filtration (b) Horizontal filtration

Fig. IV.5. Position of the fine particles (red colour) with respect to the filter particles

2.3. Pore space extraction

The pore space components (pores and constrictions) were obtained from the generated samples using the Pn-extract extraction algorithm. This algorithm, which is based on the maximum ball method proposed by Dong and Blunt (2009), operates on 3D binary images derived from numerical samples and is applicable irrespective of the particle shapes.

2.3.1. Pn-extract algorithm

A short description of the Pn-extract algorithm is given hereafter. First, the medial axis is defined, serving as a void space skeleton equidistant from the solid boundaries. Subsequently, maximum spheres are generated along the medial axis. These spheres possess a maximum radius that enables them to fit within the pores. Subsequently, a hierarchical arrangement of maximal spheres is deduced, based on a parent-child framework, where larger spheres act as parents to smaller spheres in case of partial overlap. A local pore emerges when a maximum sphere lacks parent neighbours on both sides, which means it is the largest maximum void sphere that can fit in the local pore space. The diameter of the maximal sphere inscribed in this interface defines the constriction size. More comprehensive explanation can be found in (Raeini et al., 2017).

Therefore, by employing the Pn-extract algorithm, the 3D binary image yields an interconnected network of pores and constrictions within the pore space. Figure IV.6 gives an example of pore components (pores and constrictions) extracted using the Pn-extract algorithm including pores in blue, and constrictions in red while filter particles are displayed in grey. Connections between pores and crossing constrictions are displayed in green.

However, it is well known that even with high resolution 3D images, the discretization of complex continuum void spaces using the maximum ball method has some drawbacks, as it generates constrictions that hold no physical meaning in the range of smaller sizes (Shire et al., 2012; Taylor et al., 2015; Abdallah et al., 2023a). Following Abdallah et al. (2023a), a valid constriction able

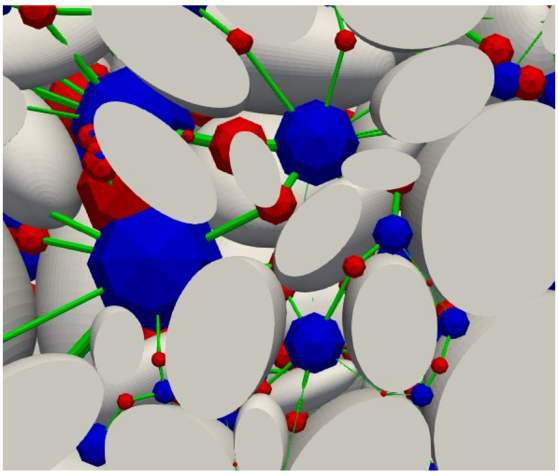

Fig. IV.6. Pore space components extracted from a numerical sample: pores (blue), constrictions (red), filter particles (grey); Connections between pores and crossing constrictions are displayed in green.

to trapped a fine particle was defined as a constriction created by at least three contact points with the filter particles responsible for creating that constriction. To determine the invalid constrictions, first, the position and radius of the constrictions were extracted from the Pn-extract data. Next, in the initially created DEM sample, new spheres with coordinates and radii that correspond to these constrictions were inserted in the sample. The number of contacts with the filter particles for each added sphere was calculated. Any sphere with fewer than three contacts was subsequently removed from the initial statistics.

After removing invalid constrictions, the normal vector for each constriction was calculated. The constriction is defined as the common surface voxels shared by two neighbouring pores; Figure IV.7 gives an example of constriction surface consisting of voxels. A mathematical technique called single-value decomposition (SVD) was employed to obtain the average plane passing through the set of voxels corresponding to the constriction. The normal vector was then derived from this average plane allowing us to determine the orientation of these constrictions.

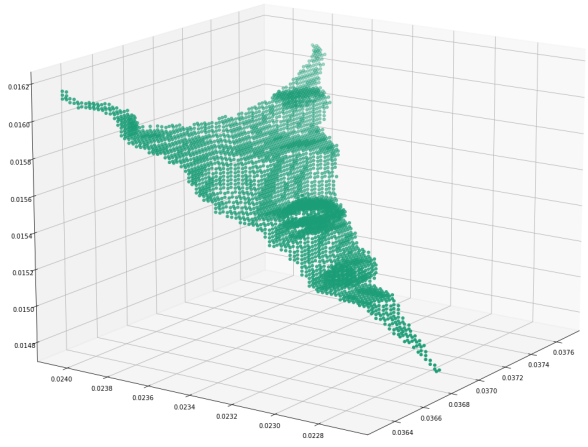

Fig. IV.7. Example of a voxel-based representation of a constriction surface in Pn-extract.

The constrictions were categorised into three groups based on the orientation of the normal vector of their associated average constriction plane. The coordinates of these normal vectors were defined according to a fixed axes system (x, y, z) where z-axis is parallel to gravity direction. If a normal vector had an angle with respect to a given axis (either x,y,z) within the angle range of [-45°, 45°] or [135°, 225°], the orientation of the normal vector was qualified according to this axis. Figure IV.8 gives the three groups of orientations (blue space for x-axis orientation, brown space for y-axis orientation, and red space for z-axis orientation).

Accordingly, in the case of the z-axis, all constrictions belonging to this group are denoted as horizontal constrictions. Fine particles migrating in the vertical direction (parallel to z-axis) are supposed to mainly pass through these "horizontal" constrictions. Moreover, in the case of the x-axis or y-axis, all constrictions belonging to these groups were denoted as "vertical" constrictions. Fine particles migrating in the horizontal direction (perpendicular to z-axis) are supposed to mainly pass through them. However, since the horizontal filtration tests were conducted along the y-axis, only constrictions with normal vectors aligned with the y-axis were used in the statistical analyses. It is important to note that in x and y directions for the normal vectors, the size and number of constrictions were found nearly identical. It arises from the way the samples were created (gravity deposition) leading to an absence of anisotropy along the horizontal axes x and y (Oda and Nakayama, 1989; Masad et al., 2002).

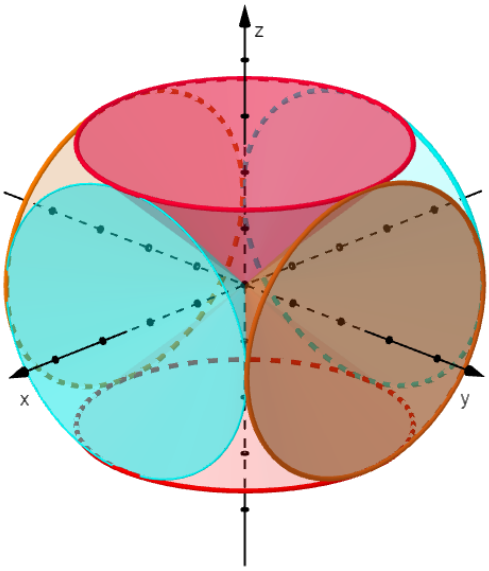

Fig. IV.8. Angle range of the constriction normal vectors belonging to each group of orientation: red for the z-axis, brown for the y-axis and blue for the x-axis.

2.3.2. Representative Elementary Volume and resolution of the 3D image

To ensure an accurate representation of the pore space, it is essential to consider both the volume and resolution of 3D binary images. Starting with the REV, Abdallah et al. (2023a) conducted an investigation to determine the necessary minimum volume needed for having a representative model of the pore space (Fig. IV.9. This investigation involved extracting the constriction size distribution (CSD) from a controlled cubic volume positioned at the centre of the sample. The

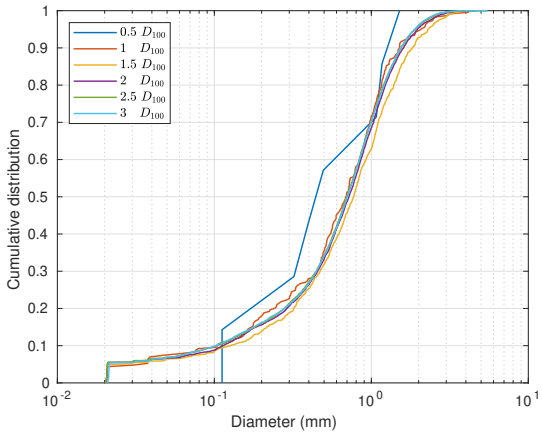

Fig. IV.9. Constriction size distributions computed within a control volume of different sizes. (Abdallah et al., 2023a)

analysis assessed what is the minimum size of the controlled volume in order to find statistics for constriction sizes independent of its size.

The analysis revealed that, to ensure representativeness for all the samples, a volume equivalent to 2.5 times the largest particle diameter ($2.5D_{100}$) is generally necessary. However, in the case of samples with elongated and partially elongated samples, it is necessary to increase the required volume to 3.5 times the largest particle diameter ($3.5D_{100}$) to involve a larger number of particles which, as a consequence will give rise to a larger number of constrictions. Indeed, in the same volume as for the other cases, there are fewer elongated particles able to fit in it, resulting in fewer constrictions (Tab. IV.5).

If a minimum size of the controlled volume is required for the statistics extracted from the pore space to hold a physical meaning for the studied granular material, a minimum resolution for the 3D binary images (herein maximum ratio between the voxel size and the smallest particle size D_0) is also required. As the resolution increases, the level of detail and clarity in the image increases.

Abdallah et al. (2023a) carried out a parametric study to investigate how resolution influences pore space results. They generated multiple 3D binary images having the same volume but with different resolutions and examined their effect on the CSD. The results indicated that for a resolution higher than $D_0/40$ (voxel size smaller than $D_0/40$), the obtained CSD curves were stabilised. In this work, a resolution of $D_0/50$ was selected for all the 3D images. Then, for samples with elongated and partially elongated particles, images with 2800x2800x2800 voxels were used for pore extraction, while for the other samples whose sizes were smaller, images with 2000x2000x2000 voxels were used.

3. Results and discussion

In this section, the effects of sample generation and particle shape on the directional filtration mechanism are analysed based on the results obtained from the filtration tests conducted on all the numerical samples in both vertical and horizontal directions. Additionally, complementary findings obtained from the pore space analysis are provided.

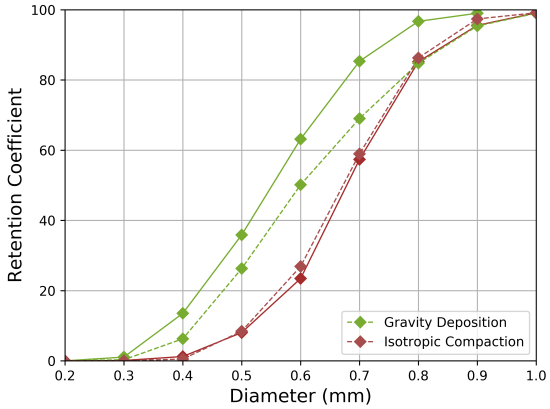

Fig. IV.10. Retention coefficient of samples made of spheres according to the sample creation throughout vertical filtration (solid line) and horizontal filtration (dotted line).

3.1. Vertical and horizontal filtration results

3.1.1. Influence of sample generation: case of spheres

A preliminary study was carried out to exhibit the influence of sample generation on filtration results for the case of samples made of sphere, one with isotropic compaction (reference sample) and the other one by gravity deposition. Figure IV.10 gives the retention coefficient according to the class of diameter of released fines onto the samples. Herein, it was computed by determining the ratio of the number of fine particles retained by the filter to the initial number of fine particles released at the top of the filter.

First, one can note that for the reference sample generated by isotropic compaction, the two retention curves are almost indistinguishable reflecting the isotropic nature of the material, which was expected. The smallest fine size able to be blocked in the filter is 0.4 mm and the 100% blockage is found for a fine of 1 mm. However, in the case of gravity deposition, the retention coefficient curves display an orientation dependency. Overall, the retention coefficient in the vertical direction exceeds that in the horizontal direction, suggesting that fine particles are more likely to be obstructed when passing through the filter vertically rather than horizontally. For both directions, retention appears for fine particles larger than 0.3 mm. For larger fine sizes, the difference between the two curves increases, peaking at a size of 0.7 mm with a difference of almost 15 points. This discrepancy then diminishes until all fine particles are effectively blocked at sizes of 0.9 mm and 1 mm for the vertical and horizontal directions, respectively.

Finally, for a specific size of fine particles, the retention coefficient is higher in the case of gravity deposition sample than in the isotropic compaction case. The maximum departure is obtained for fines of 0.6 mm with a difference of 30 points which is important. Gravity deposition introduces anisotropy of the contact orientation between the filter particles in the generated samples which is reflected throughout the retention curves. However, it is worth noting that the size of fines that experienced a complete blockage within the filter was nearly identical in both samples. Then, in a filter design where a total blockage of fines is expected, the way samples made of spheres are generated does not seem to play any role.

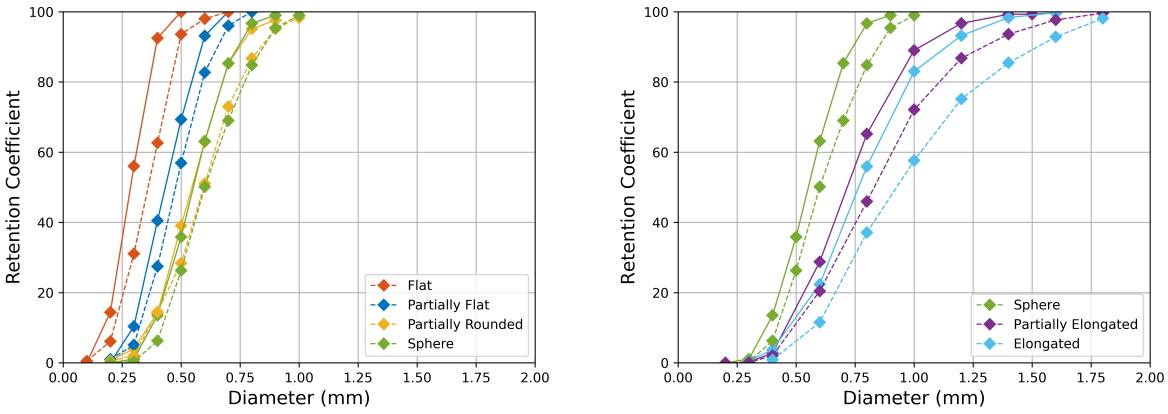

(a) (b)

Fig. IV.11. Retention coefficient of the filters with different particle shapes for vertical filtration (solid line) and horizontal filtration (dotted line); a: case of flat to spherical particles; b: case of spherical to elongated particles.

3.1.2. Influence of particle shape

In the following, only samples (including the sphere case) made with gravity deposition are analysed. Figures IV.11a and IV.11b display the directional filtration results for all the numerical samples.

Abdallah et al. (2023a) had previously explored the influence of particle shape on CSDs and, consequently, on the retention coefficient in the case of vertical filtration. Their work revealed that as the flatness ratio increases, constriction sizes decrease, enhancing the filter's ability to block finer particles. Conversely, as the elongation index increases, constriction sizes increase, leading to reduced filter efficiency.

In this work, filtration tests have been carried out in the vertical direction and in the horizontal direction. Irrespective of particle shapes, the capacity of filters shows distinctive retention capacity according to the direction of filtration. If the minimum fine size able to be blocked in the filters is roughly the same for all cases, the gap between the retention curves corresponding to different directions of filtration progressively widens as released fin sizes increase. However, when the fine size is close to the size of 100% retention, the gap between these curves diminishes again. It is worth noting that the disparity between these two curves reaches its peak for samples with high anisotropy, such as flat and elongated samples, where the difference can be as substantial as 30 points. Conversely, for samples with lower anisotropy, this difference decreases to nearly 15 points.

One interesting observation is that the retention coefficients for samples composed of partially rounded particles and spheres exhibit nearly identical curves in both the vertical and horizontal directions (Fig. IV.11a). This result holds significant implications, highlighting that filter design criteria originally conceived for spherical shapes remain applicable to partially rounded particles, which are commonly found near riverbanks and coastal areas. This result was also obtained by Wu *et al.* in their laboratory experiments (Wu et al., 2012).

3.2. Pore space extraction

To provide a comprehensive explanation of the variation in filtration mechanisms based on the direction of filtration with respect to gravity, an analysis of the void space within these samples was conducted. This analysis specifically examined the size and number of constrictions involved in both vertical and horizontal filtrations.

3.2.1. Influence of sample generation: case of spheres

Figure IV.12 display the cumulative size distribution curves (CSDs) and the underlying probability density functions (PDFs) involved for the samples made of spheres (isotropic compaction and gravity deposition).

When comparing the CSDs in the vertical and the horizontal directions obtained from both the reference sample and that of the sample made of spheres by gravity direction, it becomes clear that the proportion of smaller constrictions is greater for the latter case (Fig. IV.12a). This observation suggests that the gravity deposition method produces in general smaller constrictions. However, the minimum and maximum constriction sizes from Figure IV.12a seem to be similar in both cases. Figure IV.12b giving the underlying probability function (PDF) associated to Figure IV.12a, reveals that the modes of the two PDFs are distinct. While the mode of the PDF for the reference sample is equal to 0.88 mm, the mode of the PDF for the sample made by gravity deposition is equal to 0.61 mm which is 30% smaller than in the former case. It explains why the retention coefficient of the sample made by gravity direction is greater for a given particle size in the sample made by gravity direction than in the sample made by isotropic compaction (Fig. IV.10).

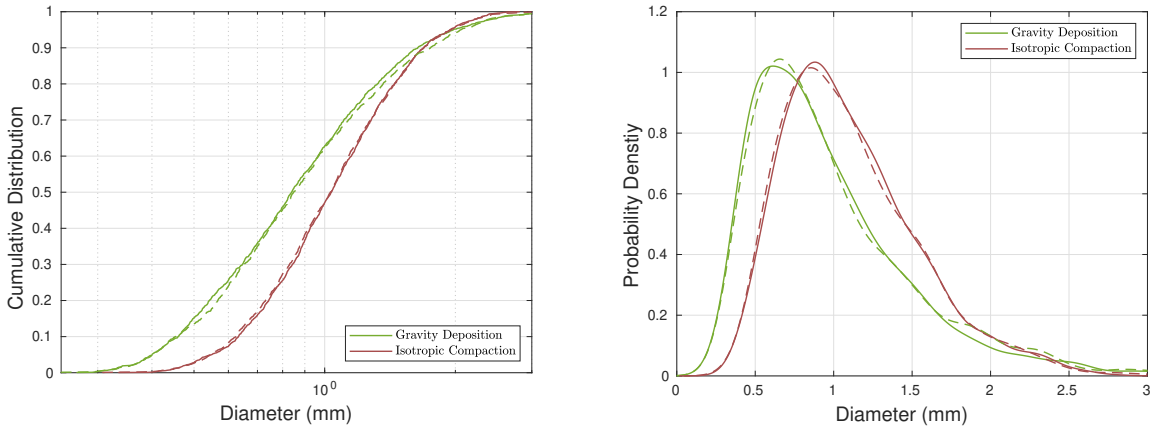

(a) CSD (b) PDF

Fig. IV.12. CSD and associated pdfs of samples made of spheres according to the sample creation for constrictions involved in the vertical filtration (solid line) and in the horizontal filtration (dotted line).

3.2.2. Influence of particle shape

Figure IV.13a and IV.13b display the cumulative size distribution curves (CSDs) found for all the samples created by gravity deposition and different particle shapes. Surprisingly, here again, and contrary to expectations, there is not a substantial difference in CSDs between the two directions for all the samples. The only exception is the sample composed of flat particles, which exhibit a small distinction between the vertical and horizontal directions.

Then, in general, these results fail to provide a conclusive explanation for the directional differences observed in the filtration results.

However, these results do lend support to certain observations made during the filtration tests. Firstly, the pattern of the CSDs for each sample closely mirrors the retention curves: the CSD of flat particles is associated to the smaller constriction sizes, followed by spherical particles, and finally, elongated particles. Additionally, the smallest constriction size from Figure IV.13a closely matches the size of the smallest fine particles that began to be blocked in the filter (Fig.IV.11a). For instance, in the case of the flat sample, the smallest constriction size in both directions is approximately equal to 0.8 mm, and the size of the fine particles that began to be blocked in the filter was around 1 mm. This is consistent across all samples, highlighting the fundamental connection between the smallest constriction size and the size of the smallest fine particle that can be blocked.

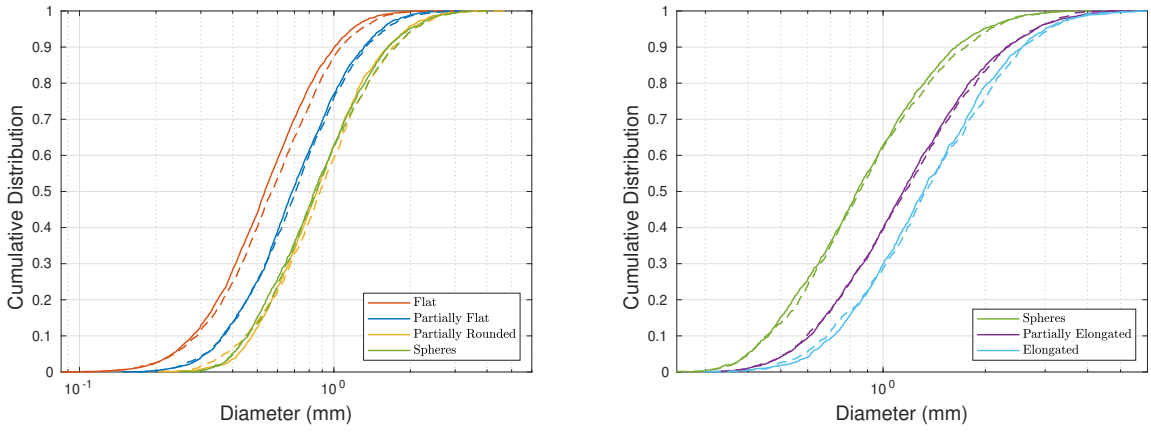

(a) (b)

Fig. IV.13. CSDs for constrictions involved in the vertical filtration (solid line) and in the horizontal filtration (dotted line); a: case of flat to spherical particles ; b: case of spherical to elongated particles.

To have better insight into the distribution of constriction sizes, the PDFs underlying the CSDs are given in Figures IV.14a and IV.14b for flat to spherical particles and spherical to elongated particles respectively.

Once again, the obtained results fall short of providing an explanation for the difference in the observed mechanisms according to filtration direction. Indeed, the PDFs are close to each other when considering a sample with a given particle shape, including the size corresponding to the modes of the PDF which are also close to very close for both directions (Tab. IV.4).

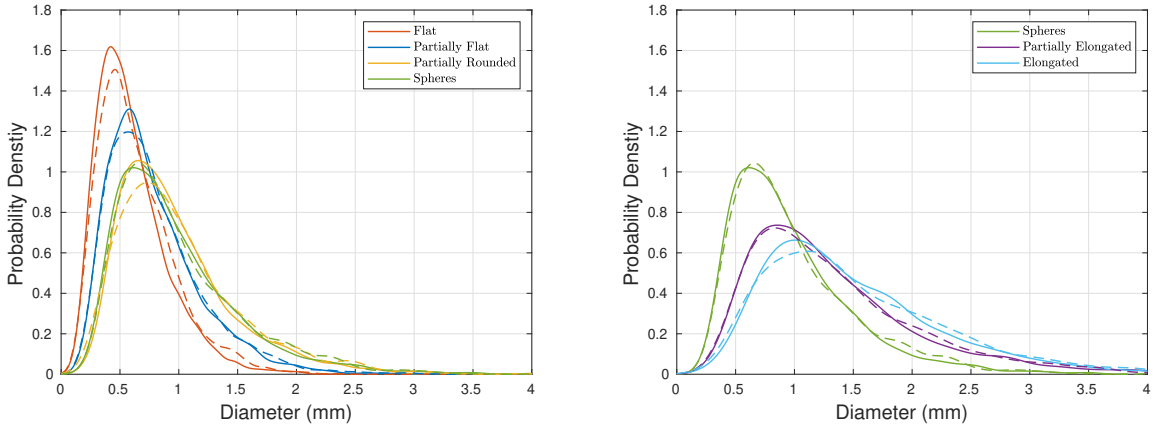

(a) (b)

Fig. IV.14. PDFs associated to CSDs for constrictions involved in the vertical filtration (solid line) and in the horizontal filtration (dotted line); a: case of flat to spherical particles; b: case of spherical to elongated particles.

However, the PDFs hold very different features according to the particle shapes involved in the samples. The PDFs for the case of flat particles are very narrow with a high occurrence for the constriction sizes associated to the mode and a greater uniformity when compared with those of samples made of spherical particles. The spread of the PDFs tends to increase and the occurrence corresponding to the mode decreases when the particles get less flat towards a spherical shape. The same holds true when the particle shape evolves towards elongated particles. The constriction size associated to the mode of the PDFs tends to be the smallest for the case of samples of flat particles and tends to increase when particle shape evolves towards spheres and when they achieve elongated shapes (Tab. IV.4).

Table IV.4: Mode Size of the PDFs underlying the CSDs for constrictions involved in the vertical and horizontal filtrations.

Sample	Dmode (mm)	
	Vertical	Horizontal
Flat	0.42	0.46
Partially Flat	0.57	0.57
Partially Rounded	0.65	0.73
Spheres	0.61	0.66
Partially Elongated	0.94	0.89
Elongated	1.05	1.04
Reference Sample	0.88	0.86

To conclude, the relation of order for the capacity of samples to retain a given class of fines is explained by the diameter of constrictions. In general, a sample with the mode of CSDs smaller than another one will have a greater capacity to retain particles of a given size than this latter. In that sense, the pdfs consistently explain the results found in Figure IV.11a and IV.11b.

Table IV.5: Number of particles and constrictions involved in filtration direction for the different samples and a reference volume of 5 cm^3.

Number of Filtration direction	Particles	Constrictions	
		Vertical	Horizontal
Flat	7200	4740	5323
Partially Flat	4690	2763	2993
Partially rounded	2350	1486	1516
Sphere	2597	1633	1544
Partially elongated	974	697	687
Elongated	549	388	425
Reference sample	2661	1835	1846

3.2.3. Influence of constriction number

The number of constrictions in a filter also influences its filtration mechanism. As the number of constrictions increases, the likelihood of fine particles being blocked somewhere in the filter also increases (Soria et al., 1993). In this study, the number of constrictions in both the vertical and horizontal directions was calculated for all the samples to investigate their impact on directional filtration mechanisms. Table IV.5 displays the number of particles and constrictions (in both directions) for all the samples within a reference volume of 5 cm^3 volume.

Beginning with the samples made of spheres, the number of constrictions in the reference sample is the same in the horizontal and vertical directions, which was expected. However, this number is larger than that of the sample made by gravity deposition. This means that the isotropic compaction can produce more constrictions in the filter while the number of particles in both samples is almost the same.

Table IV.5 indicates that the number of constrictions is higher in the horizontal direction for all samples, except for the sphere sample. The relative difference is approximately 10% for flat and elongated samples, gradually decreasing as the shape aspect ratio diminishes until it switches for the spherical sample, where the number of constrictions in the vertical direction is higher, with a relative difference of 5%.

These results provide a counter-intuitive explanation of the directional filtration mechanisms. While the number of constrictions is generally slightly higher in the horizontal direction, one might expect that fine particles would be more likely to be blocked in this direction, especially since the more represented constriction size is very similar in both directions. However, this was not the observed outcome.

In fact, fine particle retention is not solely determined by the number of constrictions only nor the constriction sizes. It may also depend on the easiness for fine particles to find a enough high succession of constrictions greater than its size in the average direction of movement. This property is partly related to the connectivity of the pore space.

4. Directional size-based pore connectivity

4.1. Definition and methodology

Connectivity is related to the easiness of a fine of a given diameter to find an exit from any accessible pore in the material.

A simple way to quantify this property consists of computing the average count of constrictions (exits) per pore in the sample. The Euler-Poincaré characteristic χ, was also used by Reboul *et al.* Reboul et al. (2008) to analyse the selective connectivity of packing of spheres according to the considered fine size. However, these methods consider that this property is not an oriented one. In this study, we propose a straightforward approach for assessing the directional connectivity of a filter by quantifying the open pores in a specific direction.

The proposed methodology can be summarised as follows: Initially, for a given fine size, a list of constrictions (through the normal vectors of the average constriction plane) that align with the desired filtration direction and larger than this size is computed. Subsequently, for each pore related to these constrictions, the selected constrictions are categorised as either input or output. This determination relies on the position of the constrictions respectively to the pore centre, with consideration of whether the constriction is located upstream (input) or downstream (output) considering the direction of the filtration. To be deemed connected or open, a pore must possess at least one open input and one open output constriction that exceeds the specified size. Figure IV.15 gives an illustration of connected and disconnected pores. This criterion ensures that fine particles have both entry and exit options through the pore. The pores meeting this criterion are counted. Finally, the directional size-based connectivity index is determined by dividing the total count of open pores by the total number of pores present in the filter. As the index value increases, it signifies a greater chance for a fine particle of a considered size to exit a pore (in the considered direction of filtration). This procedure is reiterated throughout the required size range for the fines.

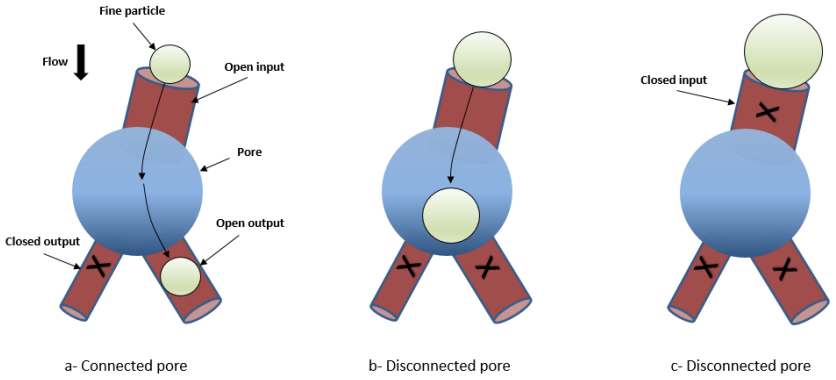

Fig. IV.15. Schematic drawing of a connected pore and examples of disconnected pores.

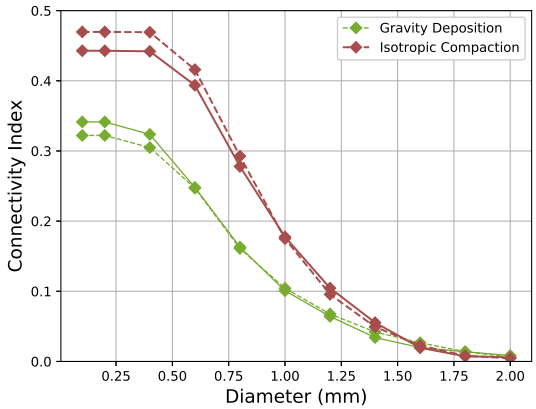

Fig. IV.16. Connectivity index for the samples made of spheres generated with gravity deposition and isotropic compaction in the case of vertical filtration (solid line) and in horizontal filtration (dotted line).

4.2. Influence of sample generation: case of spheres

The directional size-based pore connectivity index for both vertical and horizontal filtration in the case of samples made of spheres is presented in Figure IV.16 according to the sample preparation.

First, one can note that for a given fine size, pores within the sample prepared by isotropic compaction are much more connected than in the case of gravity deposition. It means that for any considered fine size, its chance to find an exit larger than its own size is greater in the former case. In other words, at the pore level, heterogeneity in constriction sizes may be smaller in this case and/or that the number of constrictions per pore with a size greater than the considered size is greater.

The result seems to be consistent with the fact that retention capacity is lower in the case of isotropic compaction. However, connectivity fails to explain the greater retention capacity in the case of vertical filtration with respect to the horizontal direction. It may arise from the fact that the probability of finding a continuous chain of constrictions greater than a given size is larger in this case than in the case of the horizontal direction. In other words, the material is better ordered in that direction than in the horizontal direction.

4.3. Influence of particle shape

The case of samples prepared by gravity deposition and with different particle shapes is given in Figures IV.17a and IV.17b.

Upon examining the connectivity patterns within the samples composed of particles with anisotropic shapes, the connectivity in the horizontal direction is found consistently greater than that in the vertical direction. For a given sample, the fact that connectivity may be larger in a given direction may be an explanation for a higher retention coefficient observed in the vertical direction compared to the horizontal direction (Fig. IV.11a and IV.11b). However, it implies also that in this direction, the probability of finding a continuous chain of constrictions greater than a given size is

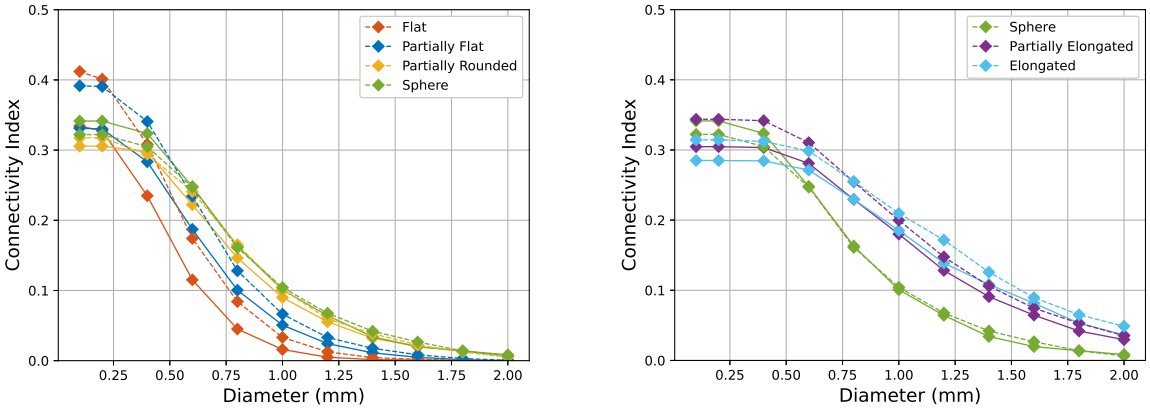

(a) (b)

Fig. IV.17. Connectivity index for the filters with different particle shapes in the case of a vertical filtration (solid line) and of a horizontal filtration (dotted line)

larger in this case than in the case of the horizontal direction.

When comparing samples with different particle shapes, in the range of larger diameters, connectivity is greater for the samples with elongated particles and decreases as flatness increases. This result is consistent with what was obtained in terms of the retention coefficient. In the range of smaller diameters, this correlation is more difficult to find.

5. Conclusion

Granular materials inherently demonstrate anisotropy due to factors such as sample preparation methods and particle shapes, significantly impacting their mechanical and hydraulic properties. The primary goal of this research was to characterise the relationship between fabric anisotropy and its consequent effects on directional filtration mechanisms by performing extensive numerical filtration tests on samples with varying particle shapes.

The filtration tests revealed that the gravity deposition method inherently induces anisotropy in samples due to heterogeneities in particle contact, causing the retention coefficient in the vertical direction to consistently surpass that in the horizontal direction, regardless of particle shape. This anisotropy becomes more pronounced as the irregularity in particle shapes intensifies. However, this differentiation is relatively minor from an engineering perspective, especially in cases of 100% blockage.

Particle shape greatly influences the shape of the constriction size distribution with a greater mode as flatness reduces and elongation ratio increases. The density probability function is more spread with fewer occurrences for the mode. There is no significant difference between the CSDs obtained according to the orientation of the average constriction plane. If the CSDs fail to explain the different values for the retention coefficient according to the direction of filtration, they are strongly correlated to the different retention coefficients found for the different samples according to particle shape.

Generally, the number of particles involved in a sample tends to decrease as flatness decreases and elongation ratio increases. It means that more constrictions can be created in the former than in the latter. The case of spheres is an intermediate case.

The connectivity in the vertical direction for samples with anisotropic particle shapes is systematically smaller in the vertical direction than in the horizontal direction. It seems to explain the greater retention coefficients found in this case. In the range of larger sizes, flatness proves to generate a material that is less connected and elongated particles a material that is more connected. A larger number of greater constriction sizes may explain this aspect. However, in the range of smaller sizes, there is not a clear correlation between connectivity and particle shape.

The case of spheres showed distinct features where no correlation was found between the retention coefficient in a given direction and connectivity. The low level of anisotropy may not make this property relevant for explaining the difference between phenomena in the horizontal and vertical directions.

In conclusion, for a material with the given porosity, particle shapes greatly modify its topological and morphological characteristics. As a consequence, filtration processes are also greatly modified. In particular, the size of fines that are totally blocked by a filter of a given thickness and given porosity greatly depends on the particle geometry. Finally, the role of the direction of filtration with respect to the anisotropy of samples is less prominent than the role of particle shape.

Appendices

Equivalent cyclic wet filtration model

Based on the concept that pore space can be represented as a cubic network of interconnected pores with constrictions (Schuler, 1996), fine particles attempt to exit a pore through five potential pathways: four sideway paths and one direct path aligned with the flow direction. In accordance with this interpretation, the filtration model assumes that applying a lateral displacement equal to half the pore diameter to a fine particle that is blocked in a pore should enable the particle to explore a sideward path (assuming it's initially obstructed at the pore's center). If the fine particle's size is smaller than the constriction along the sideward path, it can successfully exit the pore and potentially migrate further within the filter media.

The filtration test procedure involves a series of cycles, each consisting of two stages. During the first stage, fine particles migrate within the filter under the action of gravity. When all fine particles reach a stable state, either by becoming trapped or by passing through the filter, the second stage begins. In this phase, gravity is deactivated, and the particles trapped within the filter experience a lateral displacement equal to half the average pore diameter. The direction of this displacement is randomly selected in a plane perpendicular to the original flow direction. Once the displacement is complete, gravity returns to its normal direction, and particles that have successfully exited the pore continue migrating within the filter. These cycles are repeated until consistent filtration outcomes are attained, indicating that no more fine particles can effectively traverse the filter, even with the introduction of lateral movement.

The determination of the mean pore diameter is based on the equation (IV.6), initially formulated by Wu *et al.* Wu et al. (2012), and later updated by Seblany *et al.* Seblany et al. (2018b). This equation takes into account both the particle size distribution of the granular material and its density.

$$s = \frac{1}{0.7}\sqrt[3]{\frac{e}{e_{max}}}s_{max} \tag{IV.6}$$

where e,e_{max} and s_{max} are the initial void ratio, maximum void ratio, and mean pore diameter at loose state, respectively. s_{max} can be estimated to be equal to 0.5 times D_{50SA}, where D_{50SA} represents the particle diameter at which 50% of the material holds finer particles, as defined by a particle size distribution based on surface area. Further information regarding the derivation of this estimation can be located in Wu's work (2012) cited as Wu et al. (2012).

Conclusions and perspectives

1. Main conclusions

The conclusions can be divided into three main parts based on the specified objectives:

- The analysis of the filtration mechanisms in granular materials, which utilised both dry and wet filtration models coupled with DEM numerical samples, revealed several key insights. First, wet filtration showed increased tortuosity and a lower retention coefficient of fine particles than dry filtration, due to the role of drag forces in wet conditions. The difference between the results given by the two approaches was found to be influenced by the grading and porosity of the granular filters. This departure was more pronounced in the case of narrowly graded materials than in the case of well-graded materials. Moreover, it was more pronounced in loose samples than in dense samples. Furthermore, cyclic wet filtration analyses indicated that altering the hydraulic head could mobilise fines initially trapped, implying that fines in wet filtration do not consistently follow the path of the highest local flow when exiting a pore. Then, relying solely on dry filtration results introduces inaccuracies when assessing the filter retention capability, particularly for narrowly graded materials. Moreover, performing cyclic tests allowed a more conservative quantification of the retention capability of filters. An enhanced dry filtration model denoted *Equivalent cyclic wet model* was proposed and validated on the basis of cyclic wet filtration tests. The novelty lies in the possibility for fines to explore sideways more easily than in conventional dry filtration. The new model makes computations more efficient and adaptable, making it suitable for various particle shapes.

- The study of the impact of particle shape on pore space geometry highlighted its significant effect on constriction size features. Flatter particles typically had smaller constrictions with tighter distributions, whereas spherical particles displayed larger constrictions with wider ranges. In comparison, elongated particles possessed the largest constriction sizes and broadest distributions. Both partially rounded and spherical particles exhibited similar constriction size distributions, suggesting that the filtration guidelines set for spherical particles might also be suitable for partially rounded particles. The patterns observed for constriction sizes also applied to pore sizes. Moreover, the samples with flat particles demonstrated a higher average number of constrictions per pore, while the sample with elongated particles presented the lowest value. Finally, filtration tests using the equivalent dry filtration model validated the results derived from the pore space analysis, with filters containing flat particles having the highest blockage rate for a specific size of fine particles and those with elongated particles presenting the least blockage.

- The multi-direction filtration tests revealed that sample preparation may have a significant impact on the filtration properties of filters for smaller particles but does not greatly affect the equivalent sieve opening size of samples. In general, gravity deposition led to higher retention coefficients in the vertical direction (parallel to gravity) than in the horizontal direction, regardless of particle shape. This anisotropic behaviour became more pronounced with increasingly irregular particle shapes but remains relatively minor from an engineering perspective. An analysis of the pore space indicated that there is no dependency on the CSD characteristics with respect to the orientation of the average considered plane. As a result, these CSDs could not explain the differences in the retention coefficients observed in different filtration directions. Conversely, there is a direct link between the characteristics of the CSDs and the retention coefficients according to the particle shape. Furthermore, the study found that samples with anisotropic particle shapes have lower connectivity in the vertical direction compared to the horizontal direction, which may explain the higher retention coefficients in the vertical direction. The flatness of the particles results in overall less connectivity in the range of larger sizes, whereas elongated particles lead to greater connectivity, possibly due to a larger number of larger constriction sizes in this latter case.

2. Perspectives

This study has made important advancements in the understanding of filtration mechanisms, particularly in examining the role of particle shape and its intrinsic anisotropy. These insights can be used to improve existing criteria for designing granular filters. However, there remain avenues for further exploration:

- **Particle Shape and Retention Ability**: It is well established that particle shape significantly affects the retention ability of a granular filter. This effect is directly related to the size of the constrictions within the sample. Current filter criteria, based on the controlling constriction size and the analytical methods for determining this size, should be augmented with parameters accounting for particle shape. It has been shown that the controlling size is equal to the mode of the constriction size distribution for spheres under sufficient thickness (Seblany 2021).

  The next step is to verify whether this mode, when obtained for non-spherical shapes, can also be associated to the controlling size. This involves generating numerical samples with appropriate thicknesses and conducting filtration tests using fine particles equal to the obtained modes. The goal is to ensure that the fines are completely blocked. Such tests should use diverse particle shapes and materials with various grades. If validated, a comparative analysis between the modes from non-spherical shapes and those from spheres can lead to the development of a shape-adjusted coefficient. For instance, flat particles present smaller constriction sizes, whereas elongated particles exhibit larger sizes compared to spheres for the same porosity. Integrating this coefficient into the analytical formula ensures that the updated criteria consider the influence of particle shape. However, it seems difficult to retrieve the full CSD with a simple and consistent analytical model.

  Regarding directional filtration, although our findings indicate minimal impact from an engineering standpoint, orientation-based adjustments could still be explored.

- **Particle Angularity**: The investigation exclusively focused on rounded particle shapes and overlooked angular shapes. Given that increased angularity improves retention ability, this aspect warrants further research. With the presence of an enhanced dry filtration model *Equivalent cyclic wet filtration* and a robust algorithm for extracting pore space "Pn-extract", similar methodologies can be applied to samples with angular and anisotropic shapes, thereby refining the filter criteria to include their impact.

In conclusion, while we have made considerable progress in understanding granular filter design, with the necessary tools at our disposal, it is only a matter of time before these additional studies can be undertaken and filter criteria can be further optimised.

References

Abdallah, A., Vincens, E., Magoariec, H., Ardabilian, M., and Picault, C. (2023a). Effect of particle shape on the void space in granular materials: implications for the properties of granular filters (to be submitted). *Granular Matter*.

Abdallah, A., Vincens, E., Magoariec, H., and Picault, C. (2023b). Dem filtration modelling for granular materials: A comparative analysis of dry and wet approaches (submitted). *International Journal for Numerical and Analytical Methods in Geomechanics*.

Abdelhamid, Y. and El Shamy, U. (2016). Pore-scale modeling of fine-particle migration in granular filters. *International Journal of Geomechanics*, 16(3):04015086.

Aboul Hosn, R., Sibille, L., Benahmed, N., and Chareyre, B. (2017). Discrete numerical modeling of loose soil with spherical particles and interparticle rolling friction. *Granular matter*, 19:1–12.

Al-Raoush, R., Thompson, K., and Willson, C. S. (2003). Comparison of network generation techniques for unconsolidated porous media. *Soil Science Society of America Journal*, 67(6):1687–1700.

Ayachit, U. (2015). *The paraview guide: a parallel visualization application*. Kitware, Inc.

Barreto, D., O'Sullivan, C., and Zdravkovic, L. (2009). Quantifying the evolution of soil fabric under different stress paths. In *AIP Conference Proceedings*, volume 1145, pages 181–184. American Institute of Physics.

Barton, J. M. (2004). *Effect of media grain shape on physical capture of particles in a filter bed*. University of Cincinnati.

Barton, J. M. and Buchberger, S. G. (2007). Effect of media grain shape on particle straining during filtration. *Journal of Environmental Engineering*, 133(2):211–219.

BERTRAM, G. (1940). An experimental investigation of protective filters. *Harvard University Soil Mechanics Series*, (7).

Bonelli, S. (2013). Erosion in geomechanics applied to dams and levees.

Boudet, J. (2011). Finite volume methods. *Chapman Hall/CRC numerical analysis and scientific computing*.

Bryant, S. and Blunt, M. (1992). Prediction of relative permeability in simple porous media. *Physical review A*, 46(4):2004.

Bryant, S. L., King, P. R., and Mellor, D. W. (1993). Network model evaluation of permeability and spatial correlation in a real random sphere packing. *Transport in porous media*, 11:53–70.

Catalano, E., Chareyre, B., and Barthélemy, E. (2014). Pore-scale modeling of fluid-particles interaction and emerging poromechanical effects. *International Journal for Numerical and Analytical Methods in Geomechanics*, 38(1):51–71.

Chapuis, R. P., Gill, D. E., and Baass, K. (1989). Laboratory permeability tests on sand: influence of the compaction method on anisotropy. *Canadian Geotechnical Journal*, 26(4):614–622.

Chareyre, B., Cortis, A., Catalano, E., and Barthélemy, E. (2012). Pore-scale modeling of viscous flow and induced forces in dense sphere packings. *Transport in porous media*, 94:595–615.

Chen, F., Liu, H., Yang, Z., and Hu, H. (2017). Tracking characteristics of tracer particles for piv measurements in supersonic flows. *Chinese Journal of Aeronautics*, 30(2):577–585.

Cui, L. and O'sullivan, C. (2006). Exploring the macro-and micro-scale response of an idealised granular material in the direct shear apparatus. *Géotechnique*, 56(7):455–468.

Cundall, P. A. and Strack, O. D. (1979). A discrete numerical model for granular assemblies. *geotechnique*, 29(1):47–65.

Deangeli, C., Giani, G., Chiaia, B., and Fantilli, A. (2009). Dam failures. *WIT Transactions on State-of-the-art in Science and Engineering*, 36.

Deen, N., Annaland, M. V. S., Van der Hoef, M. A., and Kuipers, J. (2007). Review of discrete particle modeling of fluidized beds. *Chemical engineering science*, 62(1-2):28–44.

Delgado-Ramos, F., Escudero-Merino, D., and Olalla, C. (2016). The importance of permeability in granular filter design and control.

Den Boon, J., Sutherland, J., Whitehouse, R., Soulsby, R., Stam, C., Verhoeven, K., Høgedal, M., and Hald, T. (2004). Scour behaviour and scour protection for monopile foundations of offshore wind turbines. In *Proceedings of the European Wind Energy Conference*, volume 14, page 26. EWEC London UK.

Deo, O., Sumanasooriya, M., and Neithalath, N. (2010). Permeability reduction in pervious concretes due to clogging: experiments and modeling. *Journal of Materials in Civil Engineering*, 22(7):741–751.

Dong, H. and Blunt, M. J. (2009). Pore-network extraction from micro-computerized-tomography images. *Physical review E*, 80(3):036307.

Espinoza-Andaluz, M., Velasco-Galarza, V., and Romero-Vera, A. (2020). On hydraulic tortuosity variations due to morphological considerations in 2d porous media by using the lattice boltzmann method. *Mathematics and Computers in Simulation*, 169:74–87.

Evans, G., Dennis, P., Cousins, M., and Campbell, R. (2002). Use of recycled crushed glass as a filtration medium in municipal potable water treatment plants. *Water Science and technology: Water supply*, 2(5-6):9–16.

Fell, R. and Fry, J.-J. (2007). *Internal Erosion of Dams and Their Foundations: Selected and Reviewed Papers from the Workshop on Internal Erosion and Piping of Dams and their Foundations, Aussois, France, 25-27 April 2005*. CRC Press.

Feng, Q., Cha, L., Dai, C., Zhao, G., and Wang, S. (2020). Effect of particle size and concentration on the migration behavior in porous media by coupling computational fluid dynamics and discrete element method. *Powder Technology*, 360:704–714.

Fonseca, J., O'sullivan, C., COOP, M. R., and Lee, P. (2013). Quantifying the evolution of soil fabric during shearing using directional parameters. *Géotechnique*, 63(6):487–499.

Foster, M. A. (1999). *The probability of failure of embankment dams by internal erosion and piping*. PhD thesis, UNSW Sydney.

Fuller, P. (2009). An introduction to high speed photography and photonics.

Gao, K., Naito, C., Suleiman, M. T., Weisman, R., and Carre, T. (2023). Erosion mitigation of bridge abutment backfill during flood events. *Journal of Performance of Constructed Facilities*, 37(6):04023054.

Ghidaglia, C., de Arcangelis, L., Hinch, J., and Guazzelli, E. (1996). Hydrodynamic interactions in deep bed filtration. *Physics of Fluids*, 8(1):6–14.

Hilpert, M., Glantz, R., and Miller, C. T. (2003). Calibration of a pore-network model by a pore-morphological analysis. *Transport in porous media*, 51:267–285.

Ho, L., Grasset, C., Hoefel, D., Dixon, M. B., Leusch, F. D., Newcombe, G., Saint, C. P., and Brookes, J. D. (2011). Assessing granular media filtration for the removal of chemical contaminants from wastewater. *Water research*, 45(11):3461–3472.

Homberg, U., Baum, D., Prohaska, S., Kalbe, U., and Witt, K. J. (2012). Automatic extraction and analysis of realistic pore structures from muct data for pore space characterization of graded soil. In *ICSE6-6th International conference on scour and erosion (Proceedings)*, number ICSE6-181, pages 345–352.

Honjo, Y. and Veneziano, D. (1989). Improved filter criterion for cohesionless soils. *Journal of Geotechnical Engineering*, 115(1):75–94.

Huang, T., Crews, J. B., and Willingham, J. R. (2008). Using nanoparticle technology to control formation fines migration. In *SPE Annual Technical Conference and Exhibition?*, pages SPE–115384. SPE.

Indraratna, B., Dilema, E., and Vafai, F. (1996). An experimental study of the filtration of a lateritic clay slurry by sand filters. *Proceedings of the Institution of Civil Engineers-Geotechnical Engineering*, 119(2):75–83.

Indraratna, B. and Raut, A. K. (2006). Enhanced criterion for base soil retention in embankment dam filters. *Journal of Geotechnical and Geoenvironmental Engineering*, 132(12):1621–1627.

Indraratna, B., Raut, A. K., and Khabbaz, H. (2007). Constriction-based retention criterion for granular filter design. *Journal of Geotechnical and Geoenvironmental Engineering*, 133(3):266–276.

Iritani, E. (2013). A review on modeling of pore-blocking behaviors of membranes during pressurized membrane filtration. *Drying technology*, 31(2):146–162.

Jackson, G. and Letterman, R. (1980). Granular media filtration in water and wastewater treatment: Part 2. *Critical Reviews in Environmental Science and Technology*, 11(1):1–36.

Jung, J., Cao, S. C., Shin, Y.-H., Al-Raoush, R. I., Alshibli, K., and Choi, J.-W. (2018). A microfluidic pore model to study the migration of fine particles in single-phase and multi-phase flows in porous media. *Microsystem Technologies*, 24:1071–1080.

Kamalov, R., Ghataora, G., Burrow, M., Musgrave, P., et al. (2017). Migration of fine particles from subgrade soil to the overlying ballast. In *Railway Engineering 2017: 14th International Conference & Exhibition*.

Kamruzzaman, A., Haque, A., and Bouazza, A. (2008). Filtration behaviour of granular soils under cyclic load. *Geotechnique*, 58(6):517–522.

Karpoff, K. P. (1955). The use of laboratory test to develop design criteria for protective filters. In *Proc. ASTM*, volume 55, page 1183.

Kenney, T., Chahal, R., Chiu, E., Ofoegbu, G., Omange, G., and Ume, C. (1985). Controlling constriction sizes of granular filters. *Canadian Geotechnical Journal*, 22(1):32–43.

Kenney, T. and Lau, D. (1985). Internal stability of granular filters. *Canadian geotechnical journal*, 22(2):215–225.

Kerimov, A., Mavko, G., Mukerji, T., and Al Ibrahim, M. A. (2018). Mechanical trapping of particles in granular media. *Physical Review E*, 97(2):022907.

Kézdi, A. (1979). Soil physics-selected topics-developments in geotechnical engineering-25. Technical report.

Khilar, K. C. and Fogler, H. S. (1987). Colloidally induced fines migration in porous media. *Reviews in chemical engineering*, 4(1-2):41–108.

Khilar, K. C. and Fogler, H. S. (1998). *Migrations of fines in porous media*, volume 12. Springer Science & Business Media.

Krumbein, W. C. (1941). Measurement and geological significance of shape and roundness of sedimentary particles. *Journal of Sedimentary Research*, 11(2):64–72.

Kuhn, M. R., Sun, W., and Wang, Q. (2015). Stress-induced anisotropy in granular materials: fabric, stiffness, and permeability. *Acta Geotechnica*, 10:399–419.

Kwan, A. K., Mora, C., and Chan, H. (1999). Particle shape analysis of coarse aggregate using digital image processing. *Cement and Concrete Research*, 29(9):1403–1410.

Ladd, A. J. and Verberg, R. (2001). Lattice-boltzmann simulations of particle-fluid suspensions. *Journal of statistical physics*, 104:1191–1251.

Lallemand, P. and Luo, L.-S. (2000). Theory of the lattice boltzmann method: Dispersion, dissipation, isotropy, galilean invariance, and stability. *Physical review E*, 61(6):6546.

Li, F., Zhang, Q., Klumpp, E., Bol, R., Nischwitz, V., Ge, Z., and Liang, X. (2021a). Organic carbon linkage with soil colloidal phosphorus at regional and field scales: insights from size fractionation of fine particles. *Environmental science & technology*, 55(9):5815–5825.

Li, G.-y., Zhan, L.-t., Hu, Z., and Chen, Y.-m. (2021b). Effects of particle gradation and geometry on the pore characteristics and water retention curves of granular soils: a combined dem and pnm investigation. *Granular Matter*, 23:1–16.

Li, W., Vincens, E., Reboul, N., and Chareyre, B. (2014). Constrictions and filtration of fine particles in numerical granular filters: Influence of the fabric within the material. In *Proceedings of the 7th International Conference on Scour and Erosion, Perth, Australia, 2-4 December 2014*, page 241. CRC Press.

Lindow, N., Baum, D., and Hege, H.-C. (2011). Voronoi-based extraction and visualization of molecular paths. *IEEE Transactions on Visualization and Computer Graphics*, 17(12):2025–2034.

Lindquist, W. B., Venkatarangan, A., Dunsmuir, J., and Wong, T.-f. (2000). Pore and throat size distributions measured from synchrotron x-ray tomographic images of fontainebleau sandstones. *Journal of Geophysical Research: Solid Earth*, 105(B9):21509–21527.

Liu, Y., Wang, L., Yin, Z.-Y., and Hong, Y. (2022). A coupled cfd-dem investigation into suffusion of gap-graded soil considering anisotropic stress conditions and flow directions. *Acta Geotechnica*, pages 1–22.

Locke, M., Indraratna, B., and Adikari, G. (2001). Time-dependent particle transport through granular filters. *Journal of geotechnical and geoenvironmental engineering*, 127(6):521–529.

Lominé, F. and Oger, L. (2009). Dispersion of particles by spontaneous interparticle percolation through unconsolidated porous media. *Physical Review E*, 79(5):051307.

Ma, H., Zhou, L., Liu, Z., Chen, M., Xia, X., and Zhao, Y. (2022). A review of recent development for the cfd-dem investigations of non-spherical particles. *Powder Technology*, page 117972.

Ma, Q., Wautier, A., and Zhou, W. (2021). Microscopic mechanism of particle detachment in granular materials subjected to suffusion in anisotropic stress states. *Acta Geotechnica*, 16:2575–2591.

Mansouri, M., Delenne, J.-Y., El Youssoufi, M. S., and Séridi, A. (2009). A 3d dem-lbm approach for the assessment of the quick condition for sands. *Comptes Rendus Mécanique*, 337(9-10):675–681.

Mansur, C. I. and Dietrich, R. J. (1965). Pumping test to determine permeability ratio. *Journal of the Soil Mechanics and Foundations Division*, 91(4):151–183.

Maroof, M. A., Mahboubi, A., Vincens, E., and Noorzad, A. (2022). Effects of particle morphology on the minimum and maximum void ratios of granular materials. *Granular Matter*, 24(1):41.

Martin, R. (2013). Clogging issues associated with managed aquifer recharge methods. *IAH Commission on Managing Aquifer Recharge, Australia*, pages 26–33.

Masad, E., Muhunthan, B., and Crowe, C. (2002). Numerical modelling of fluid flow in microscopic images of granular materials. *International journal for numerical and analytical methods in geomechanics*, 26(1):53–74.

Morgan, K. and Peraire, J. (1998). Unstructured grid finite-element methods for fluid mechanics. *Reports on Progress in Physics*, 61(6):569.

Muresan, B., Saiyouri, N., and Hicher, P.-Y. (2013). Dynamic behavior of straining in randomly packed beads: experimental study. *Journal of Environmental Engineering*, 139(5):692–702.

Nguyen, T. T. and Indraratna, B. (2020). The role of particle shape on hydraulic conductivity of granular soils captured through kozeny–carman approach. *Géotechnique Letters*, 10(3):398–403.

Nouguier-Lehon, C., Cambou, B., and Vincens, E. (2003). Influence of particle shape and angularity on the behaviour of granular materials: a numerical analysis. *International journal for numerical and analytical methods in geomechanics*, 27(14):1207–1226.

Novak, P., Moffat, A., Nalluri, C., and Narayanan, R. (2017). *Hydraulic structures*. CRC Press.

NRCS (1994). *Natural Resources Conservation Services "Gradation design of sand and gravel filters." Part 633 national engineering handbook, Chap. 26,*. U.S. Dept. of Agriculture, Washington, D.C.

Oda, M. (1972). Initial fabrics and their relations to mechanical properties of granular material. *Soils and foundations*, 12(1):17–36.

Oda, M. and Nakayama, H. (1989). Yield function for soil with anisotropic fabric. *Journal of Engineering Mechanics*, 115(1):89–104.

Oda, M., Nemat-Nasser, S., and Konishi, J. (1985). Stress-induced anisotropy in granular masses. *Soils and foundations*, 25(3):85–97.

O'Sullivan, C., Bluthé, J., Sejpar, K., Shire, T., and Cheung, L. (2015). Contact based void partitioning to assess filtration properties in dem simulations. *Computers and Geotechnics*, 64:120–131.

Popescu, I. (2014). *Computational hydraulics*. IWA Publishing.

Raeini, A. Q., Bijeljic, B., and Blunt, M. J. (2017). Generalized network modeling: Network extraction as a coarse-scale discretization of the void space of porous media. *Physical Review E*, 96(1):013312.

Raut, A. K. and Indraratna, B. (2008). Further advancement in filtration criteria through constriction-based techniques. *Journal of Geotechnical and Geoenvironmental Engineering*, 134(6):883–887.

Reboul, N., Vincens, E., and Cambou, B. (2008). A statistical analysis of void size distribution in a simulated narrowly graded packing of spheres. *Granular Matter*, 10(6):457–468.

Reboul, N., Vincens, E., and Cambou, B. (2010). A computational procedure to assess the distribution of constriction sizes for an assembly of spheres. *Computers and Geotechnics*, 37(1):195–206.

Reddi, L. N., Ming, X., Hajra, M. G., and Lee, I. M. (2000). Permeability reduction of soil filters due to physical clogging. *Journal of geotechnical and geoenvironmental engineering*, 126(3):236–246.

Ren, B., Zhong, W., Chen, Y., Chen, X., Jin, B., Yuan, Z., and Lu, Y. (2012). Cfd-dem simulation of spouting of corn-shaped particles. *Particuology*, 10(5):562–572.

Ren, X. and Santamarina, J. (2018). The hydraulic conductivity of sediments: A pore size perspective. *Engineering Geology*, 233:48–54.

Rong, L., Zhou, Z., and Yu, A. (2015). Lattice–boltzmann simulation of fluid flow through packed beds of uniform ellipsoids. *Powder technology*, 285:146–156.

Sari, H., Chareyre, B., Catalano, E., Philippe, P., and Vincens, E. (2011). Investigation of internal erosion processes using a coupled dem-fluid method. In *PARTICLES II: proceedings of the II International Conference on Particle-Based Methods: fundamentals and applications*, pages 820–830. CIMNE.

Satake, M. (1982). Fabric tensor in granular materials. In *IUTAM-Conference on Deformation and Failure of Granular Materials, 1982*, pages 63–68.

Schaller, F. (2017). *The Structure of Random Particle Packings: Die Struktur Ungeordneter Packungen*. PhD thesis, Friedrich-Alexander-Universität Erlangen-Nürnberg.

Schuler, U. (1996). Scattering of the composition of soils. an aspect for the stability of granular filters. In *Proceedings of Geofilters*, volume 96, pages 21–34.

Sciacchitano, A. (2019). Uncertainty quantification in particle image velocimetry. *Measurement Science and Technology*, 30(9):092001.

Seblany, F. (2018). *Filter criterion for granular soils based on the constriction size distribution*. PhD thesis, Université de Lyon.

Seblany, F., Homberg, U., Vincens, E., Winkler, P., and Josef Witt, K. (2018a). Merging criteria for defining pores and constrictions in numerical packing of spheres. *Granular Matter*, 20:1–14.

Seblany, F., Vincens, E., and Picault, C. (2018b). Simplified estimation of some main characteristics of pores and constrictions in granular materials. In *European Working Group on Internal Erosion*, pages 189–199. Springer.

Seblany, F., Vincens, E., and Picault, C. (2021). Determination of the opening size of granular filters. *International Journal for Numerical and Analytical Methods in Geomechanics*, 45(9):1195–1211.

Sen, T. K. and Khilar, K. C. (2006). Review on subsurface colloids and colloid-associated contaminant transport in saturated porous media. *Advances in colloid and interface science*, 119(2-3):71–96.

Sherard, J. L., Dunnigan, L. P., and Talbot, J. R. (1984). Basic properties of sand and gravel filters. *Journal of Geotechnical Engineering*, 110(6):684–700.

Shire, T., O'SULLIVAN, C., Barreto, D., and Gaudray, G. (2013). Quantifying stress-induced anisotropy using inter-void constrictions. *Géotechnique*, 63(1):85–91.

Shire, T., O'Sullivan, C., and Gaudray, G. (2012). Comparison of two methods for measurement of soil constriction size distribution. In *International Conference on Scour and Erosion, Paris*, pages 249–256.

Sibille, L., Villard, P., Darve, F., and Aboul Hosn, R. (2019). Quantitative prediction of discrete element models on complex loading paths. *International Journal for Numerical and Analytical Methods in Geomechanics*, 43(5):858–887.

Silin, D. and Patzek, T. (2006). Pore space morphology analysis using maximal inscribed spheres. *Physica A: Statistical mechanics and its applications*, 371(2):336–360.

Silveira, A. (1965). An analysis of the problem of washing through in protective filters. In *Proceedings of the 6th International Conference on Soil Mechanics and Foundation Engineering, Montréal, Que*, pages 551–555.

Silveira, A., de Lorena Peixoto, T., and Nogueira, J. (1975). On void size distribution of granular materials. In *Proceedings of the 5th Pan American Conference on Soil Mechanics and Foundation Engineering, Buenos Aires*, pages 161–177.

Siriwardene, N. R., Deletic, A., and Fletcher, T. (2007). Clogging of stormwater gravel infiltration systems and filters: Insights from a laboratory study. *Water research*, 41(7):1433–1440.

Sjah, J. and Vincens, E. (2013). Determination of the constriction size distribution of granular filters by filtration tests. *International Journal for Numerical and Analytical Methods in Geomechanics*, 37(10):1231–1246.

Skouras, E., Burganos, V., Paraskeva, C., and Payatakes, A. (2011). Phenomenological description and network simulation of horizontal filtration dynamics. *Separation and purification technology*, 80(1):105–118.

Šmilauer, V., Catalano, E., Chareyre, B., Dorofeenko, S., Duriez, J., Gladky, A., Kozicki, J., Modenese, C., Scholtès, L., Sibille, L., et al. (2010). Yade reference documentation. *Yade Documentation*, 474(1).

Song, S., Le-Clech, P., and Shen, Y. (2023). Microscale fluid and particle dynamics in filtration processes in water treatment: A review. *Water Research*, 233:119746.

Song, S., Rong, L., Dong, K., Liu, X., Le Clech, P., and Shen, Y. (2020). Particle-scale modelling of fluid velocity distribution near the particles surface in sand filtration. *Water research*, 177:115758.

Song, S., Rong, L., Dong, K., and Shen, Y. (2021). Numerical investigation of drag property for fluid flow through random arrays of elliptical cylinders. *Powder Technology*, 380:539–552.

Soria, M., Aramaki, R., and Viviani, E. (1993). Experimental determination of void size curves. In *Brauns, J and Heibaum, M and Schuler, U, (eds.) Filters in Geotechnical and Hydraulic Engineering*, pages 43–48. Balkema, Rotterdam, The Netherlands.

Suthaker, S., Smith, D. W., and Stanley, S. J. (1995). Evaluation of filter media for upgrading existing filter performance. *Environmental technology*, 16(7):625–643.

Taylor, H., O'Sullivan, C., Shire, T., and Moinet, W. (2019). Influence of the coefficient of uniformity on the size and frequency of constrictions in sand filters. *Géotechnique*, 69(3):274–282.

Taylor, H., O'Sullivan, C., and Sim, W. (2015). A new method to identify void constrictions in micro-ct images of sand. *Computers and Geotechnics*, 69:279–290.

Terzaghi, K. (1922). The failure of dams by piping and its prevention. *Die Wasserkraft*, 17:445–449.

Terzaghi, K., Peck, R. B., and Mesri, G. (1996). *Soil mechanics in engineering practice*. John wiley & sons.

Thornton, C. (2000). Numerical simulations of deviatoric shear deformation of granular media. *Géotechnique*, 50(1):43–53.

Torskaya, T., Shabro, V., Torres-Verdín, C., Salazar-Tio, R., and Revil, A. (2014). Grain shape effects on permeability, formation factor, and capillary pressure from pore-scale modeling. *Transport in porous media*, 102:71–90.

Trussell, R. R., Trussell, A. R., Lang, J. S., and Tate, C. H. (1980). Recent developments in filtration system design. *Journal-American Water Works Association*, 72(12):705–710.

Tsuji, Y., Kawaguchi, T., and Tanaka, T. (1993). Discrete particle simulation of two-dimensional fluidized bed. *Powder technology*, 77(1):79–87.

Versluis, M. (2013). High-speed imaging in fluids. *Experiments in fluids*, 54:1–35.

Vincens, E., Witt, K. J., and Homberg, U. (2015). Approaches to determine the constriction size distribution for understanding filtration phenomena in granular materials. *Acta Geotechnica*, 10(3):291–303.

Vogel, H.-J. and Roth, K. (2001). Quantitative morphology and network representation of soil pore structure. *Advances in Water Resources*, 24(3):233–242. Pore Scale Modeling.

Wan, C. F. and Fell, R. (2008). Assessing the potential of internal instability and suffusion in embankment dams and their foundations. *Journal of geotechnical and geoenvironmental engineering*, 134(3):401–407.

Wautier, A., Bonelli, S., and Nicot, F. (2019). Dem investigations of internal erosion: Grain transport in the light of micromechanics. *International Journal for Numerical and Analytical Methods in Geomechanics*, 43(1):339–352.

Wellmann, C., Lillie, C., and Wriggers, P. (2008). A contact detection algorithm for superellipsoids based on the common-normal concept. *Engineering Computations*, 25(5):432–442.

Wereley, S. T. and Meinhart, C. D. (2010). Recent advances in micro-particle image velocimetry. *Annual review of fluid mechanics*, 42:557–576.

Witt, K. J. (1986). *Filtrationsverhalten und bemessung von erdstoff-filtern*, volume 104. Institut für Bodenmechanik und Felsmechanik der Universität Fridericiana, Karlsruhe.

Witt, K. J. (1993). Reliability study of granular filters. *Filters in Geotechnical and Hydraulic Engineering*, pages 35–42.

Wu, L., Nzouapet, B. N., Vincens, E., and Bernat-Minana, S. (2012). Laboratory experiments for the determination of the constriction size distribution of granular filters. In *Proceedings of 6th International Conference on Scour and Erosion (ICSE-6)*.

Xie, Z., Wang, S., and Shen, Y. (2021). Cfd-dem modelling of the migration of fines in suspension flow through a solid packed bed. *Chemical Engineering Science*, 231:116261.

Xing, H., Zhang, Q., Braithwaite, C., Pan, B., and Zhao, J. (2017). High-speed photography and digital optical measurement techniques for geomaterials: fundamentals and applications. *Rock Mechanics and Rock Engineering*, 50:1611–1659.

Xiong, H., Zhang, Z., Yang, J., Yin, Z.-y., and Chen, X. (2023). Role of inherent anisotropy in infiltration mechanism of suffusion with irregular granular skeletons. *Computers and Geotechnics*, 162:105692.

Yan, X., Zhan, W., Hu, Z., Wang, L., Yu, Y., and Xiao, D. (2022). Experimental study on the anti-clogging ability of siphon drainage and engineering application. *Soils and Foundations*, 62(6):101221.

Yang, R., Zou, R., and Yu, A. (2002). Voronoi tessellation of the packing of fine uniform spheres. *Physical Review E*, 65(4):041302.

Younes, N., Benseghier, Z., Millet, O., Wautier, A., Nicot, F., and Wan, R. (2022). Phase-field lattice boltzmann model for liquid bridges and coalescence in wet granular media. *Powder Technology*, 411:117942.

Zhao, B. and O'Sullivan, C. (2022). Fluid particle interaction in packings of monodisperse angular particles. *Powder Technology*, 395:133–148.

Zhao, B. and Wang, J. (2016). 3d quantitative shape analysis on form, roundness, and compactness with μct. *Powder technology*, 291:262–275.

Zhao, J. and Shan, T. (2013). Coupled cfd–dem simulation of fluid–particle interaction in geomechanics. *Powder technology*, 239:248–258.

Zhao, S., Evans, T. M., and Zhou, X. (2018). Effects of curvature-related dem contact model on the macro-and micro-mechanical behaviours of granular soils. *Géotechnique*, 68(12):1085–1098.

Zhao, S., Zhang, N., Zhou, X., and Zhang, L. (2017). Particle shape effects on fabric of granular random packing. *Powder technology*, 310:175–186.

Zhao, S. and Zhao, J. (2019). A poly-superellipsoid-based approach on particle morphology for dem modeling of granular media. *International Journal for Numerical and Analytical Methods in Geomechanics*, 43(13):2147–2169.

Zhao, S. and Zhao, J. (2021). Sudodem: Unleashing the predictive power of the discrete element method on simulation for non-spherical granular particles. *Computer Physics Communications*, 259:107670.

Zheng, W., Hu, X., Tannant, D. D., and Zhou, B. (2021). Quantifying the influence of grain morphology on sand hydraulic conductivity: A detailed pore-scale study. *Computers and Geotechnics*, 135:104147.

dernière page de la thèse

AUTORISATION DE SOUTENANCE

Vu les dispositions de l'arrêté du 25 mai 2016 modifié par l'arrêté du 26 août 2022,

Vu la demande du directeur de thèse

Monsieur E. VINCENS

et les rapports de

Mme C. O'SULLIVAN
Professeure - Department of Civil and Environmental Engineering, Imperial College London, London, UK

et de

M. L. SIBILLE
Maître de conférences (HDR) - Univ. Grenoble Alpes, CNRS, Grenoble INP, 3SR, F-38000 Grenoble

Monsieur ABDALLAH Ali

est autorisé à soutenir une thèse pour l'obtention du grade de **DOCTEUR**

Ecole doctorale Mécanique, Energétique, Génie Civil, Acoustique

Fait à Ecully, le 27 novembre 2023

Pour le directeur de l'École Centrale de Lyon
Le directeur de la recherche

Christophe CORRE